Metallic glasses

D. V. Louzguine
WPI-AIMR, Tohoku University, Japan

Metals and Alloys are very important but the research field saturation

Steels, Al-, Ti-, Cu- based alloys

Glassy/amorphous alloys have **high tensile strength** and **low Young's modulus**.

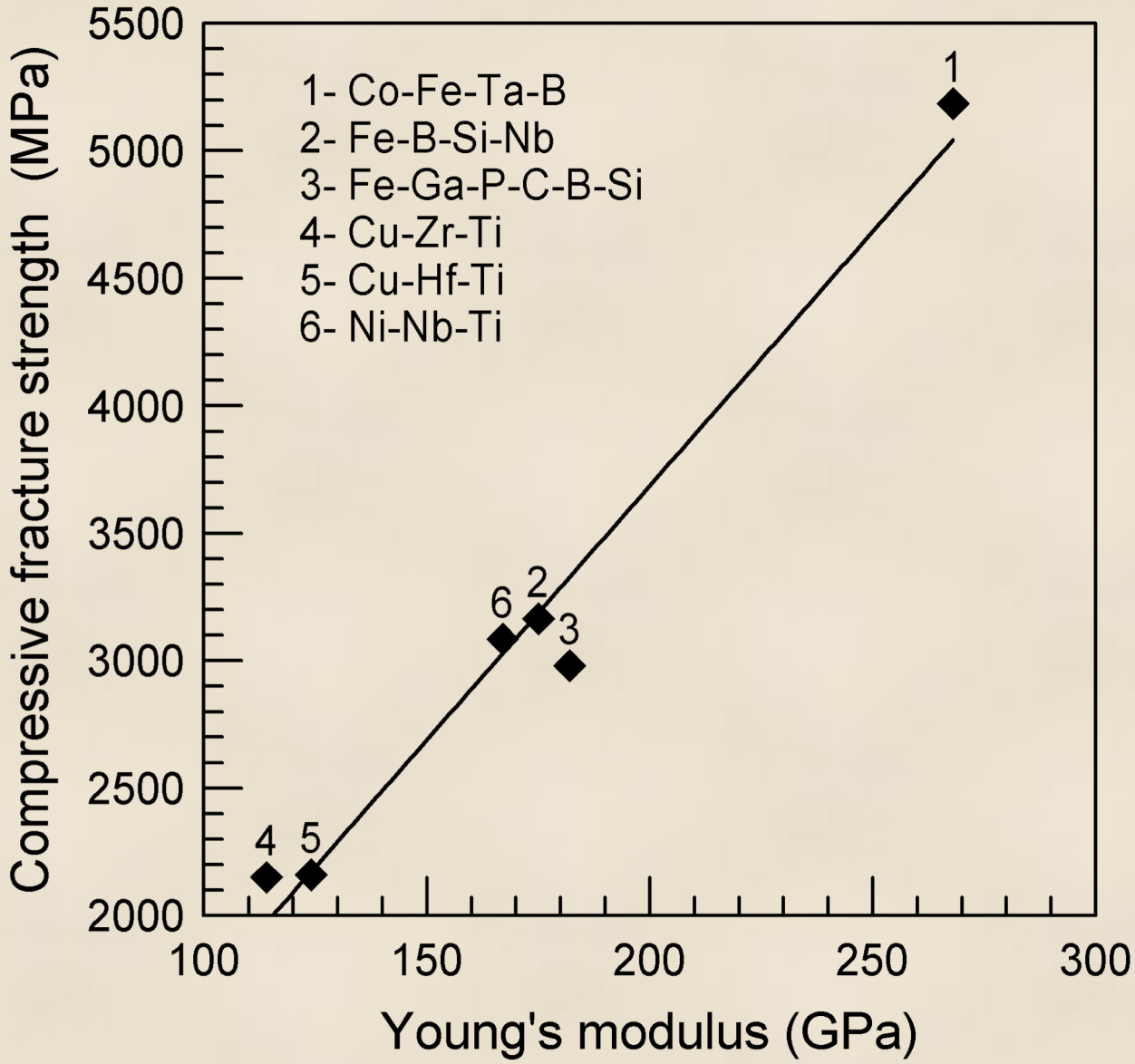

Mechanical Properties

Some BMGs: High Specific Strength (σ/ρ)

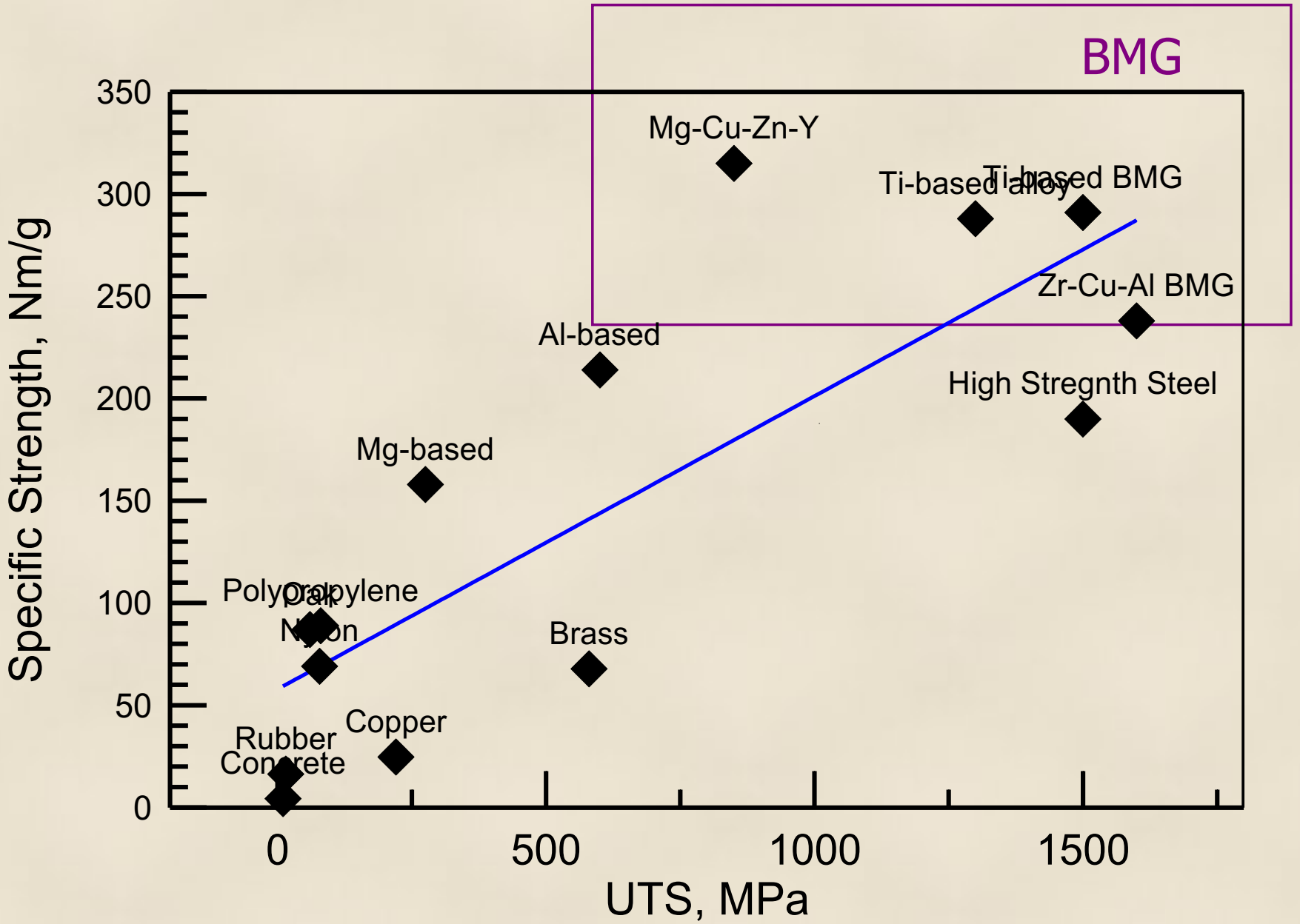

Glassy samples preparation techniques

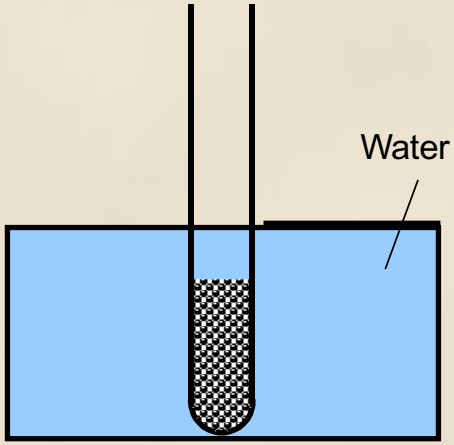

Water cooling of the melt

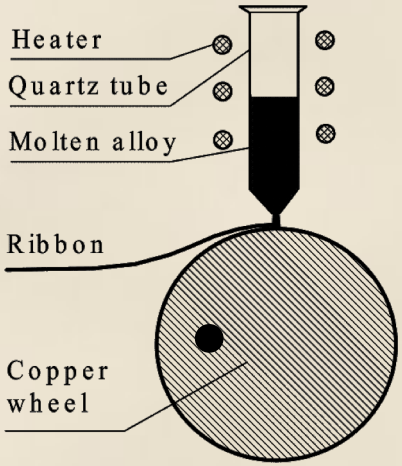

Melt spinning

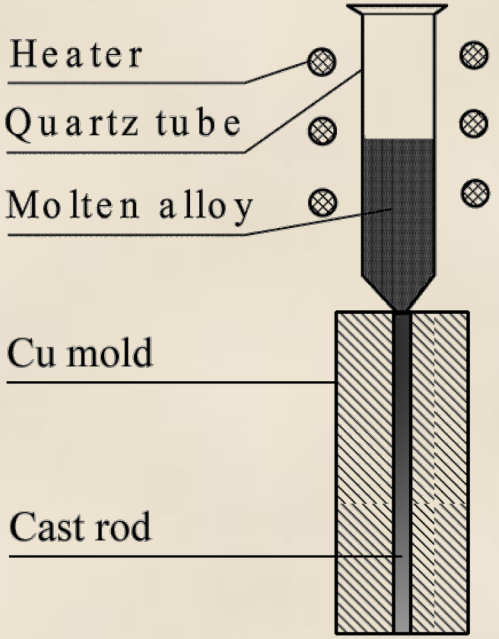

Melt casting

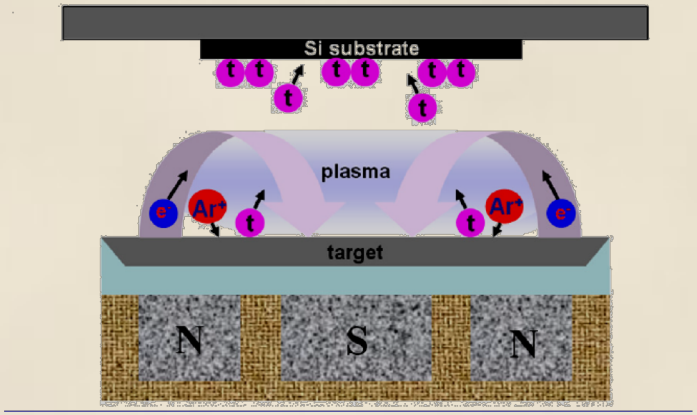

Magnetron sputtering

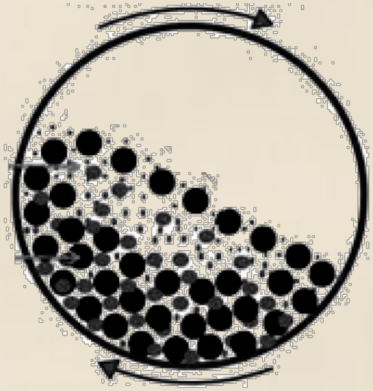

Ball milling

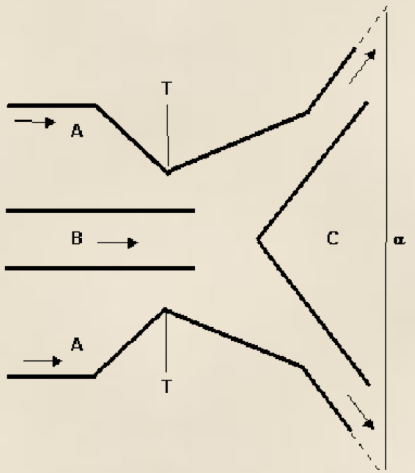

Gas atomization

Bulk Metallic Glass (BMG) – high strength functional material

- Casting: Ar pressure, gravity, suction
- Water cooling

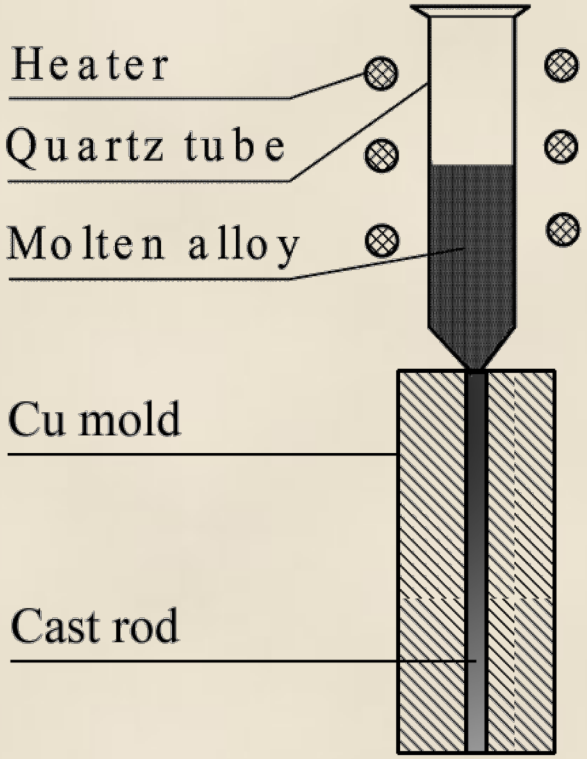

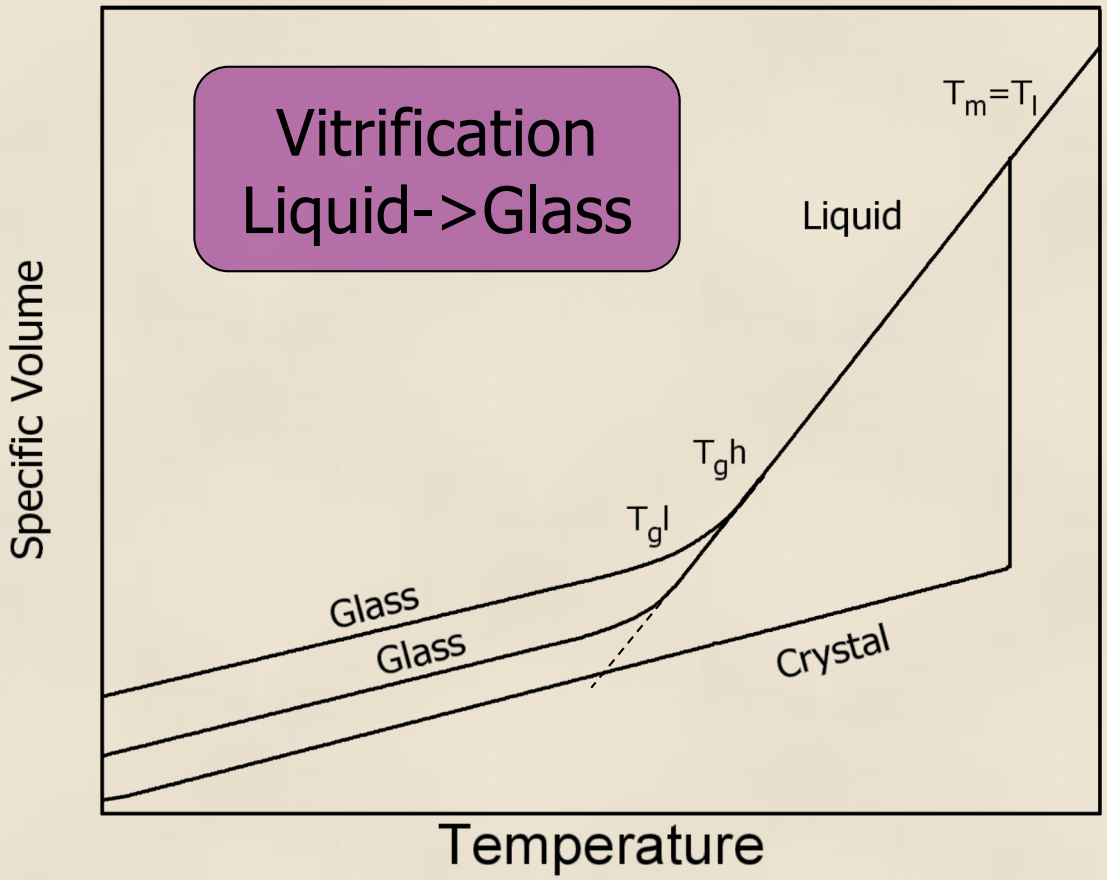

2. Devitrification

Glass->Liquid transition

Glass->Crystal or QC

Crystalline structure

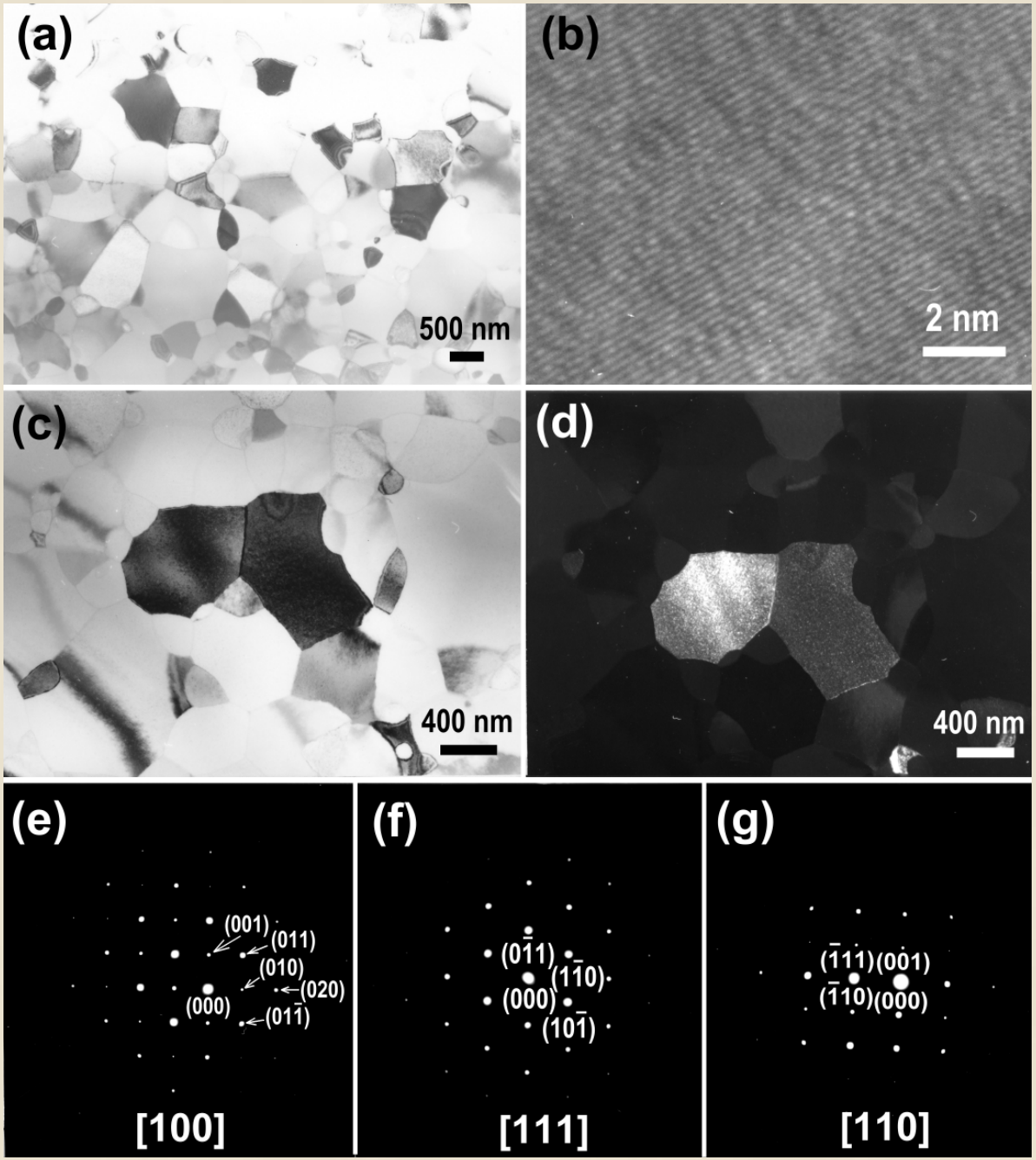

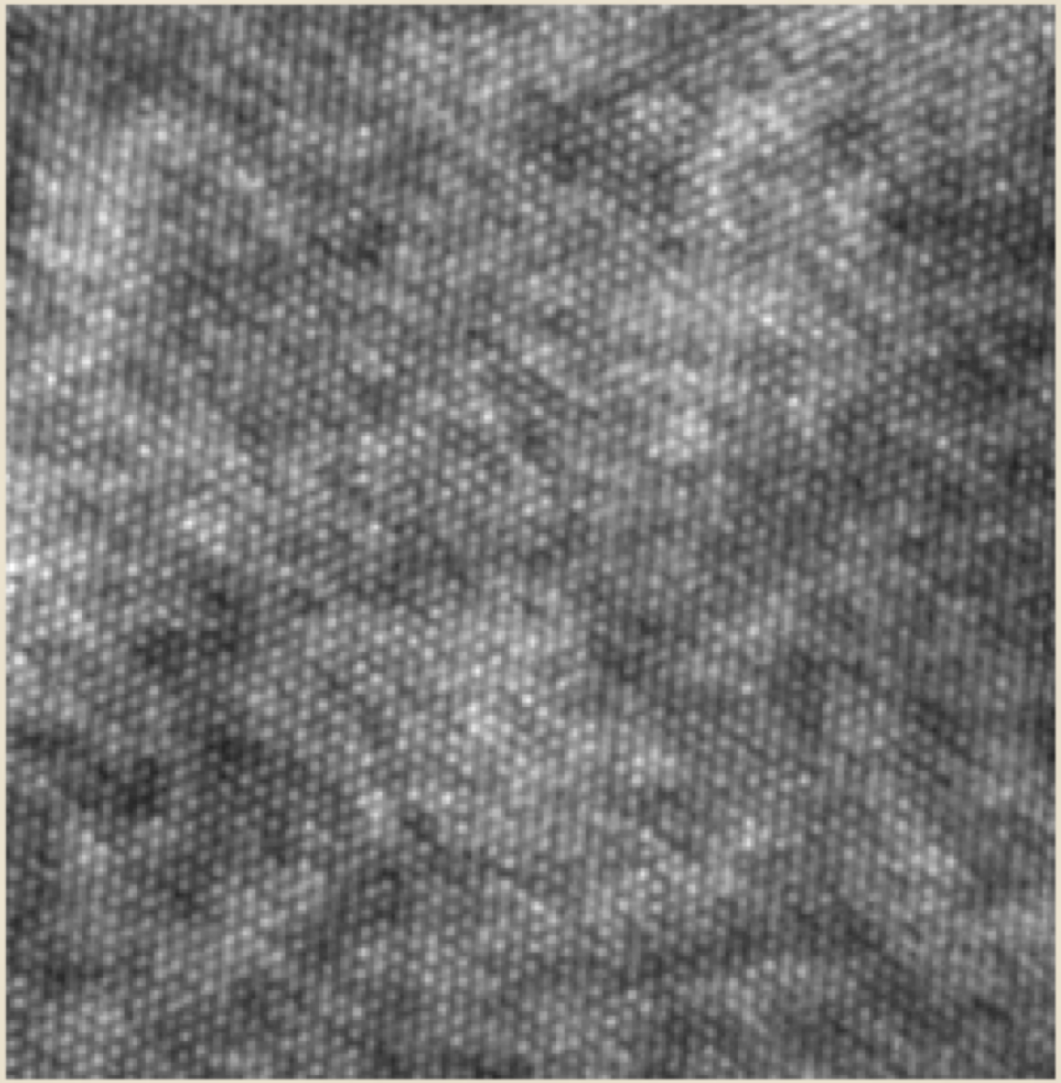

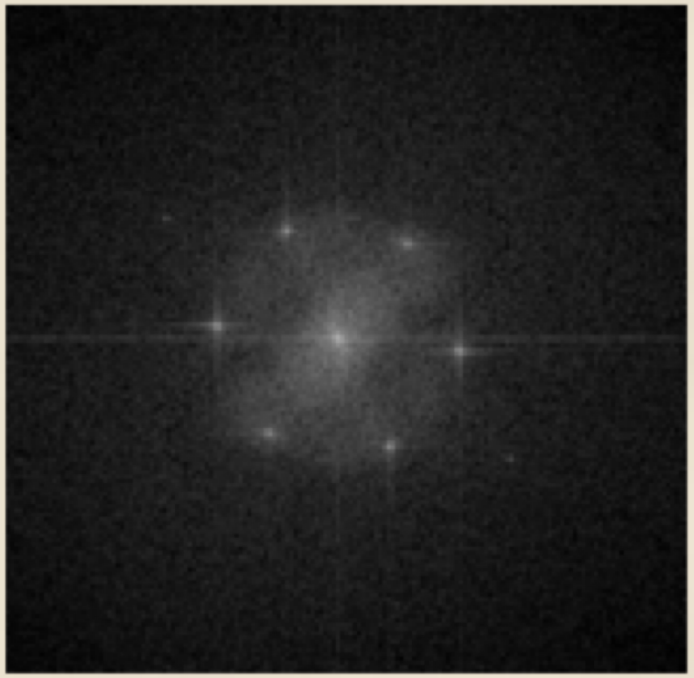

Amorphous/Glassy structure

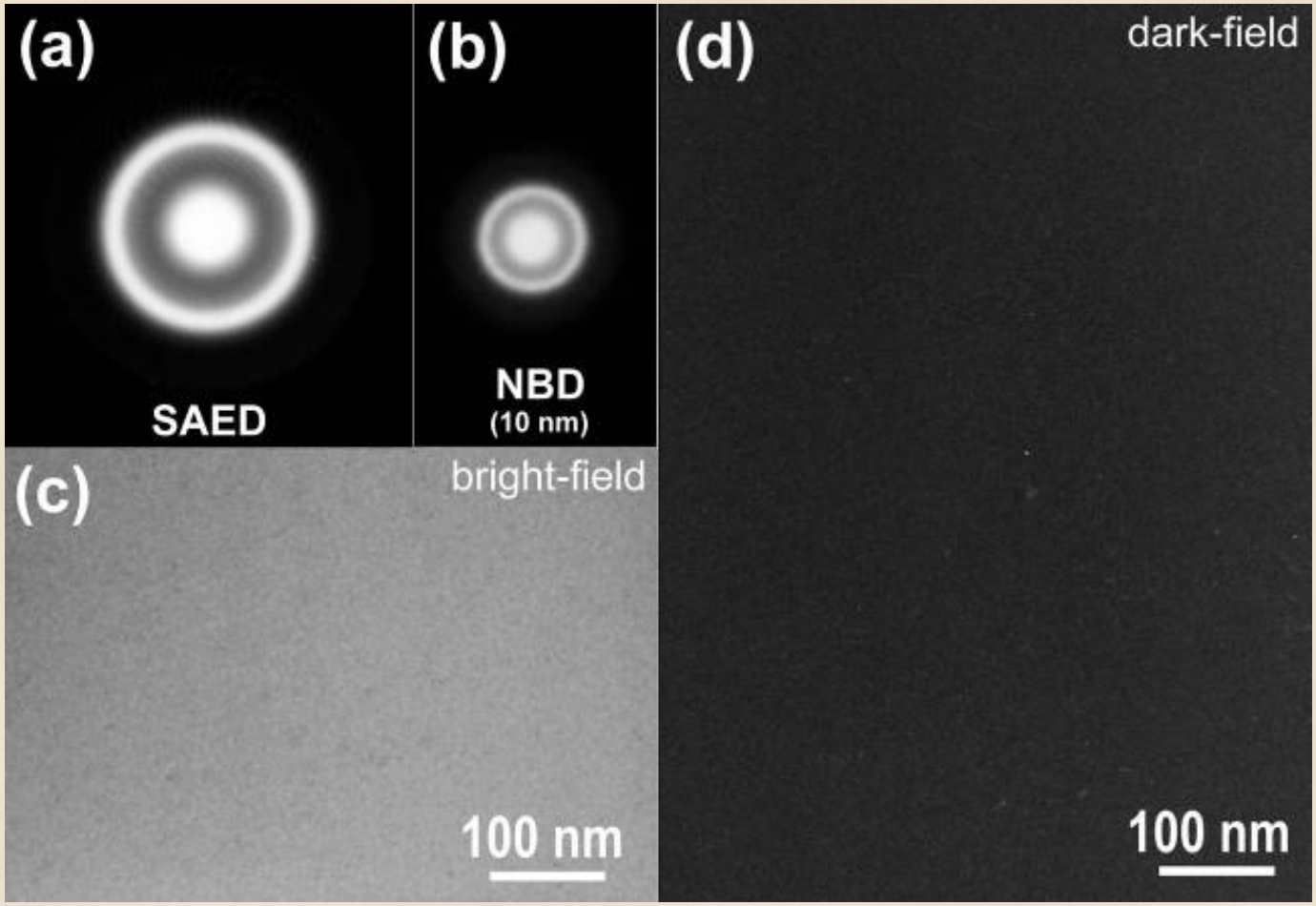

$Cu_{55}Zr_{30}Ti_{10}Pd_5$ (as-solidified, ion polishing)

Bulk Metallic Glasses

Disordered structure, no dislocations - large flow stress

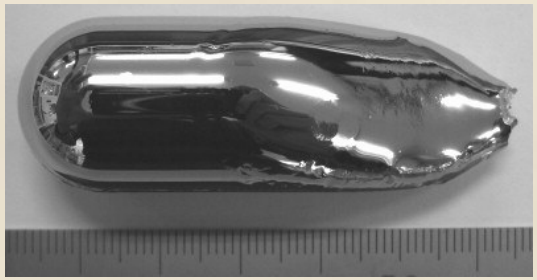

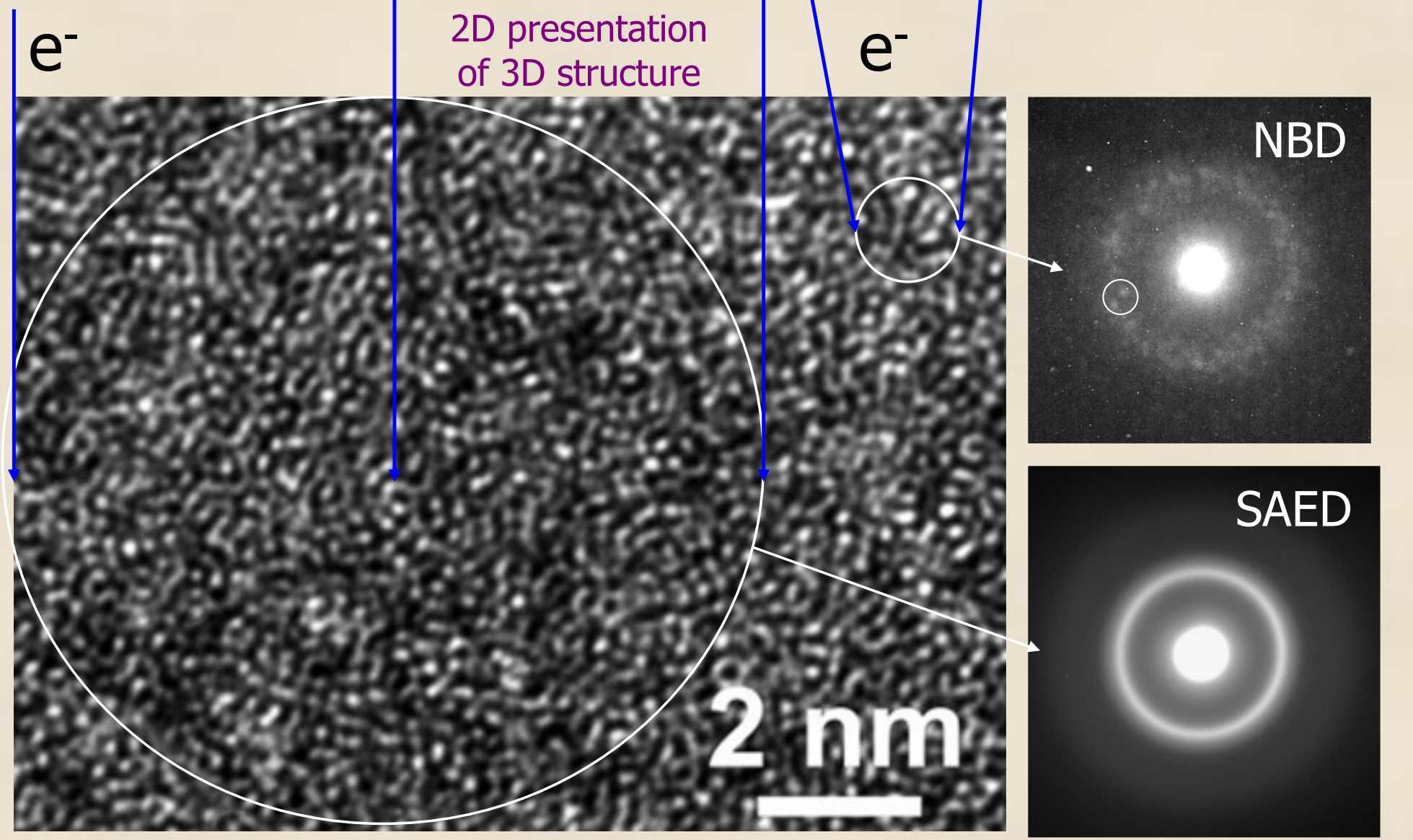

$$4\pi r^2 \rho(r) = 4\pi r^2 \rho_0 + 2r/\pi \int_0^{kmax} Qi(k)\sin(kr)dk$$

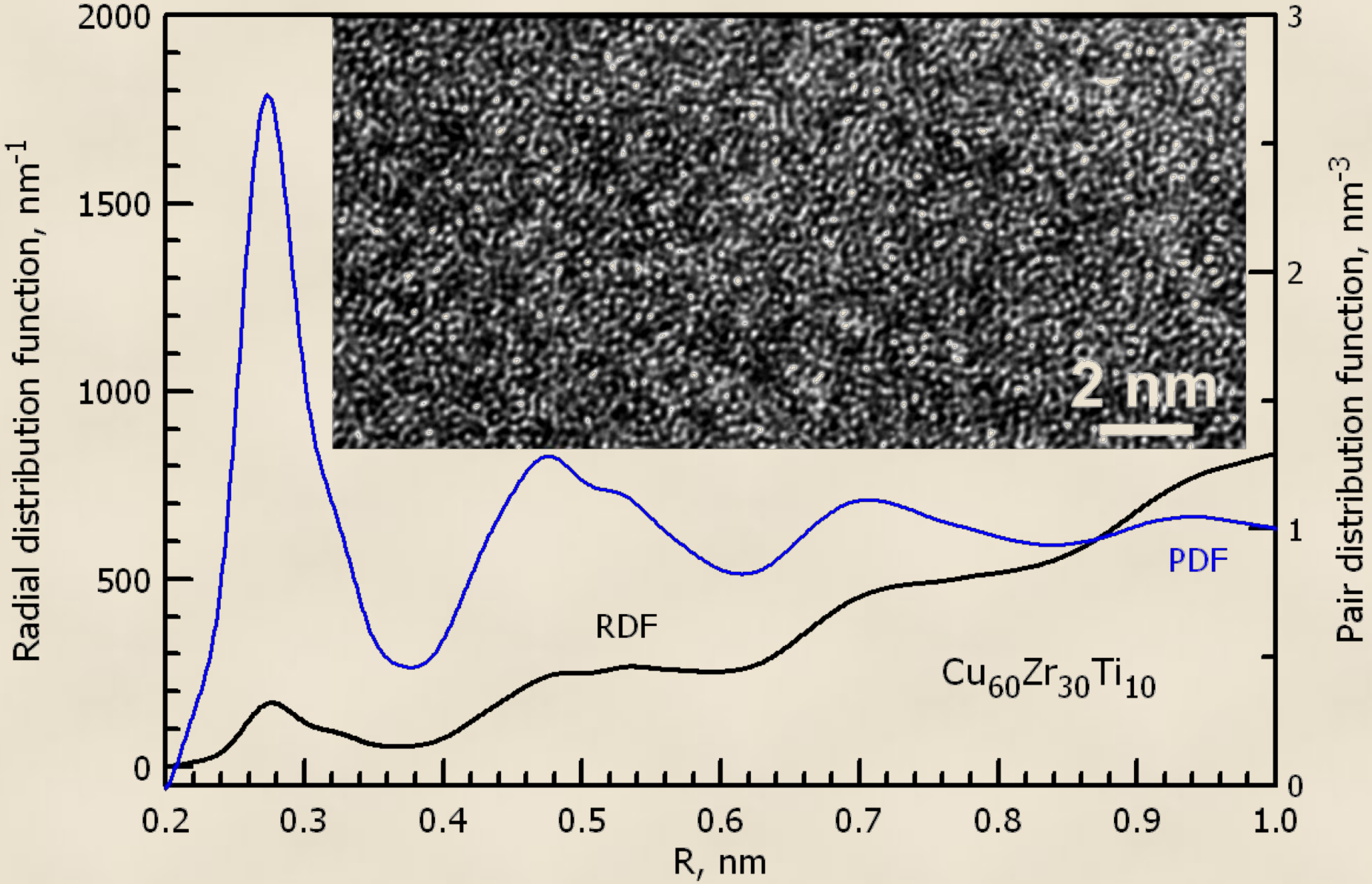

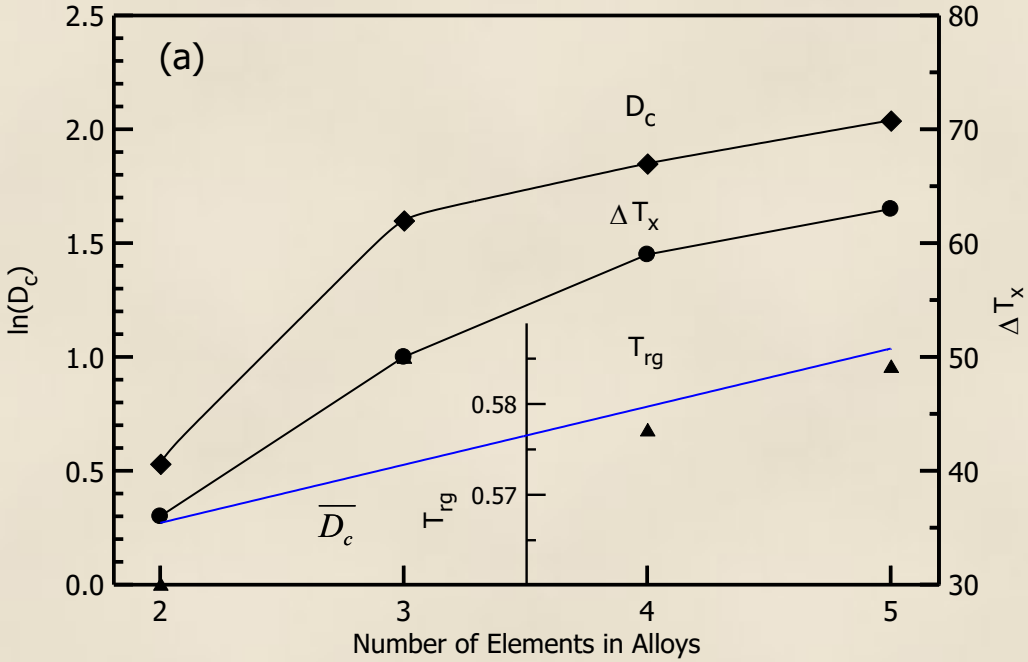

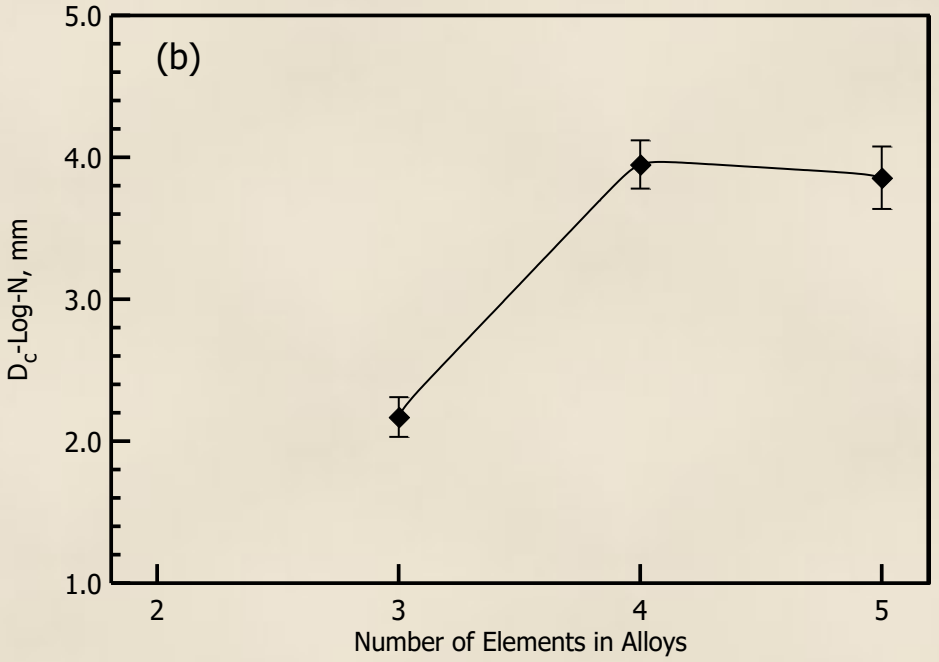

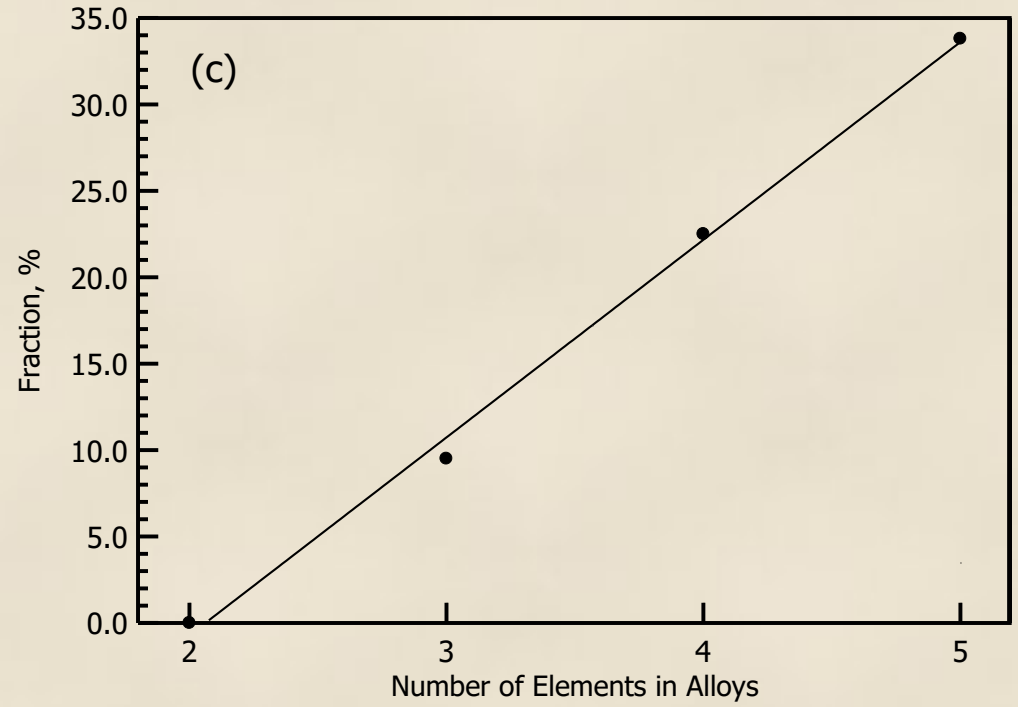

(a) Natural logarithm of simple average critical diameter ln(Dc), average ΔT_x and T_{rg} as a function of alloy system complexity. (b) Average critical diameter $D_{c\text{-}Log\text{-}N}$ obtained using log-normal distribution and the confidence interval (P=0.95). (c) the fraction of alloys having critical diameter larger than 7 mm.

D. V. Louzguine-Luzgin, D. B. Miracle, L. Louzguina-Luzgina, and A. Inoue "Comparative analysis of glass-formation in binary, ternary, and multicomponent alloys" Journal of Applied Physics 108, (2010) 103511.

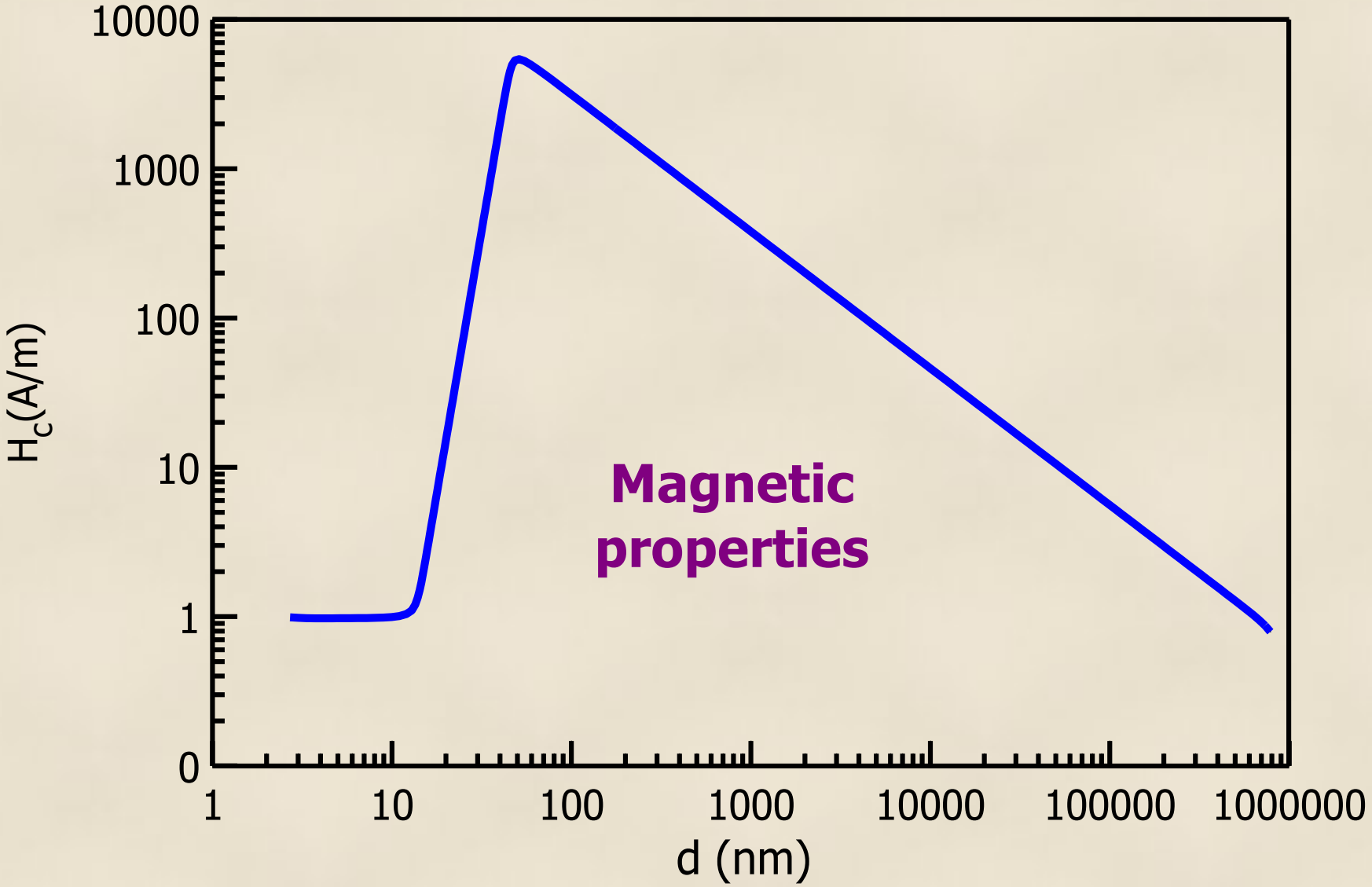
10000
1000
100
10
1
0
H_c(A/m)
Magnetic properties
1
10
100
1000
10000
100000
1000000
d (nm)

Nr	Alloy	D_{cr} (mm)	B_s (T)	H_c (A/m)	Ref.
5	$Fe_{70}Mo_5P_{10}C_{10}B_5$	3	0.93	2.36	[i]
6	$Fe_{74}Nb_6Y_3B_{17}$	2	0.81	15	[ii]
10	$(Fe_{0.75}B_{0.15}Si_{0.1})_{96}Nb_4$	1.5	1.2	3.7	[iii]
11	$[(Fe_{0.8}Co_{0.1}Ni_{0.1})_{0.75}B_{0.2}Si_{0.05}]_{96}Nb_4$	2.5	1.1	3	iii
12	$Co_{43}Fe_{20}Ta_{5.5}B_{31.5}$	3	0.49	0.25	[iv]

[[i]] W. Zhang, C.F. Fang, Y.H. Li, Ferromagnetic Fe-based bulk metallic glasses with high thermoplastic formability, Scripta Materialia 69 (2013) 77–80.
[[ii]] D.S. Song, J.H. Kim, E. Fleury, W.T. Kim, D.H. Kim, Synthesis of ferromagnetic Fe-based bulk glassy alloys in the Fe–Nb–B–Y system, J. Alloys Compd., 389 (2005) 159.
[[iii]] A. Inoue and B.L. Shen, Soft magnetic bulk glassy Fe–B–Si–Nb alloys with high saturation magnetization above 1.5 T, Materials Transactions, 43, (2002) 766.
[[iv]] A. Inoue, B. Shen, H. Koshiba, H. Kato and. A. R. Yavari, Cobalt-based bulk glassy alloy with ultrahigh strength and soft magnetic properties, Nature Materials 2 (2003) 661 - 663.

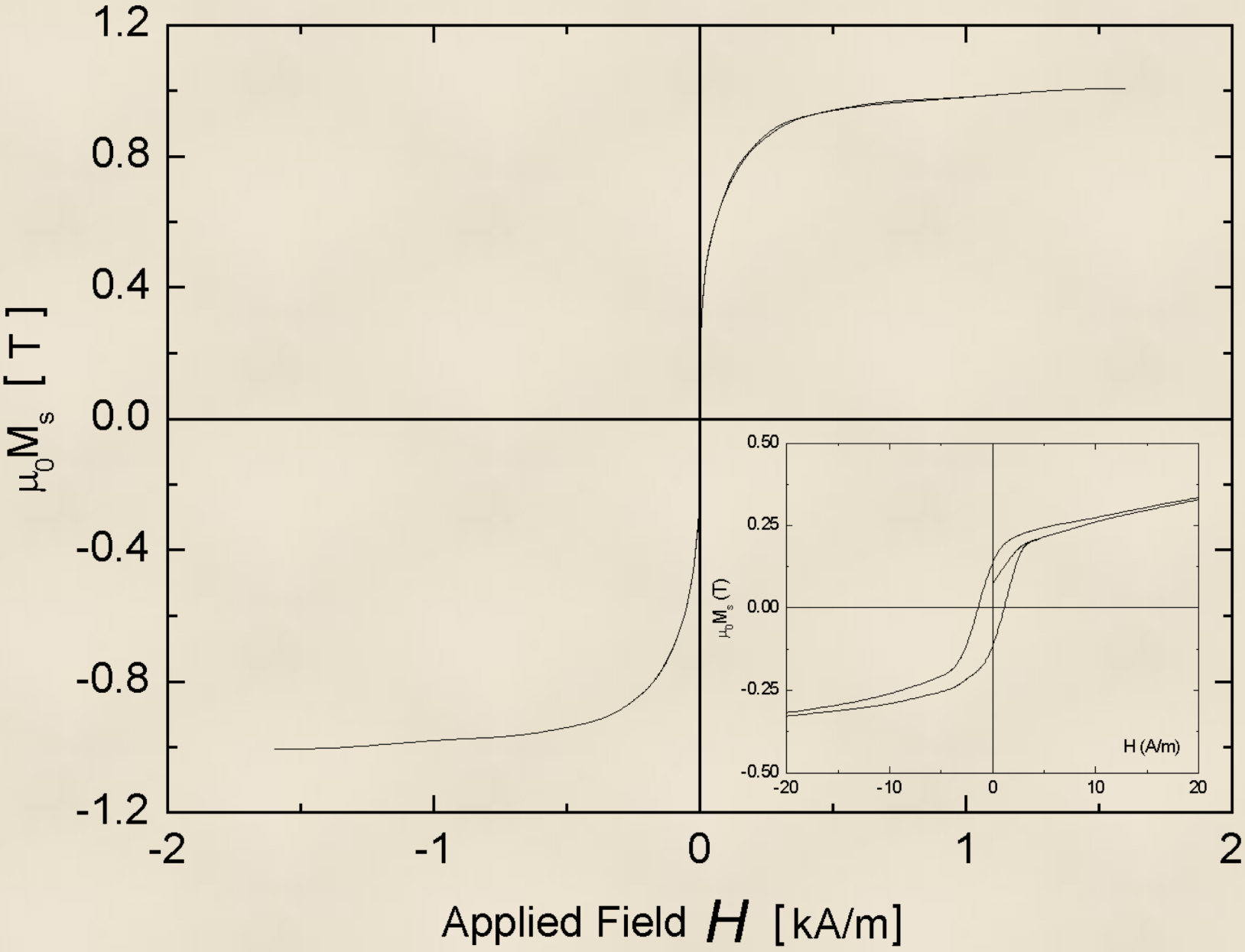
1.2
0.8
0.4
0.0
-0.4
-0.8
-1.2
$\mu_0 M_s$ [T]
-2
-1
0
1
2
Applied Field H [kA/m]
0.50
0.25
0.00
-0.25
-0.50
$\mu_0 M_s$ (T)
-20
-10
0
10
20
H (A/m)

By proper alloying – relatively ductile bulk metallic glasses

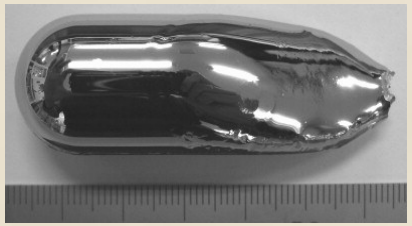

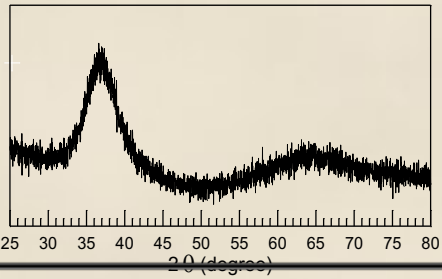

$Zr_{60+x}Cu_{25-x}Fe_5Al_{10}$ x = 0 (a), 2.5 (b)

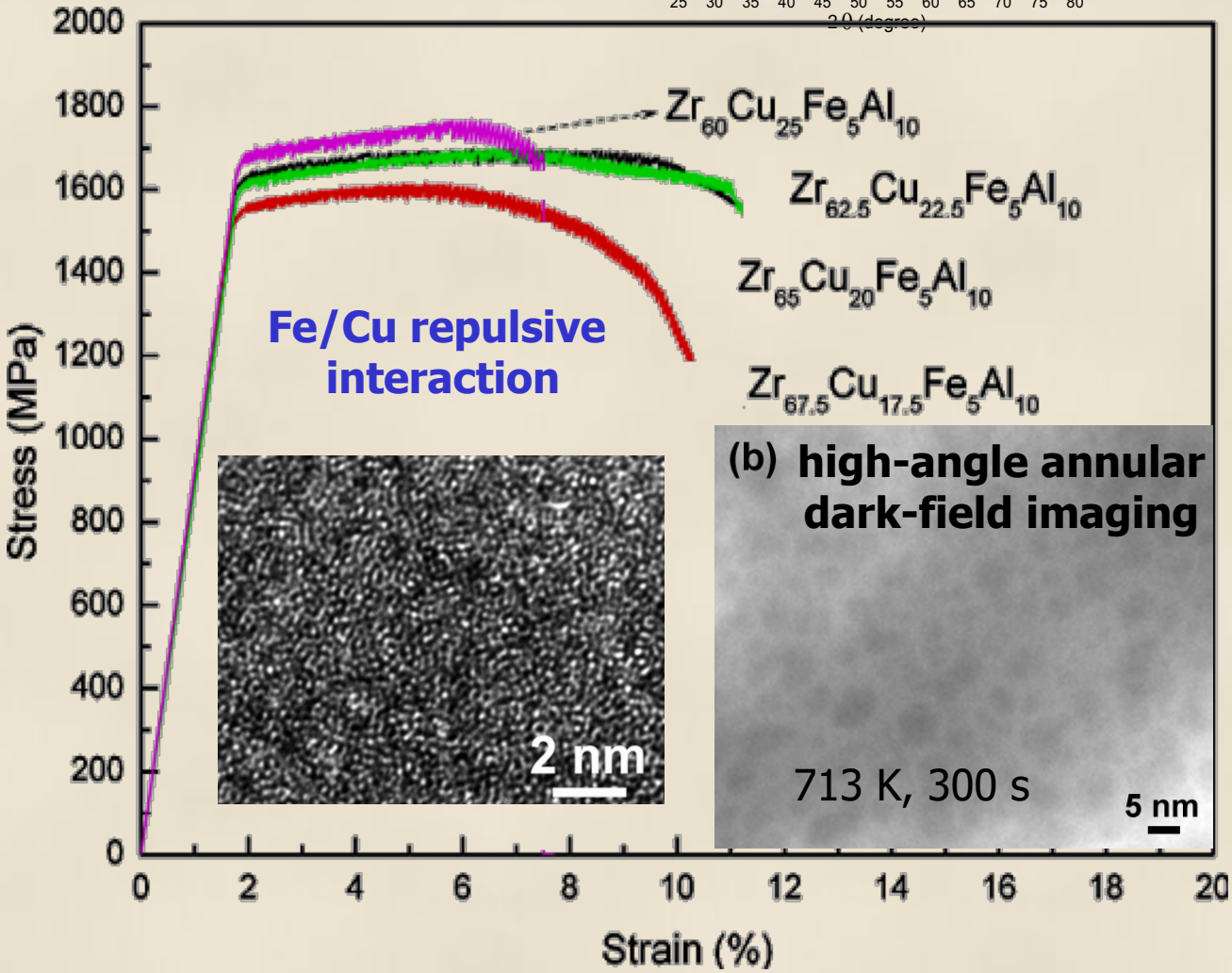

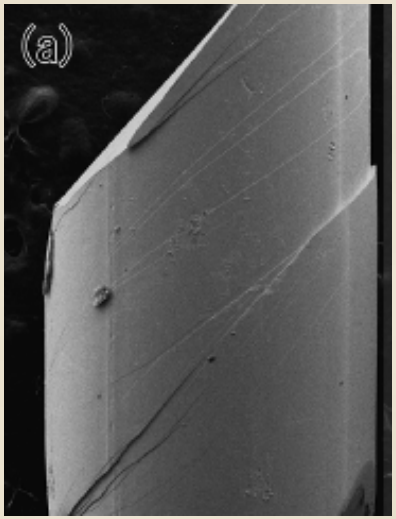

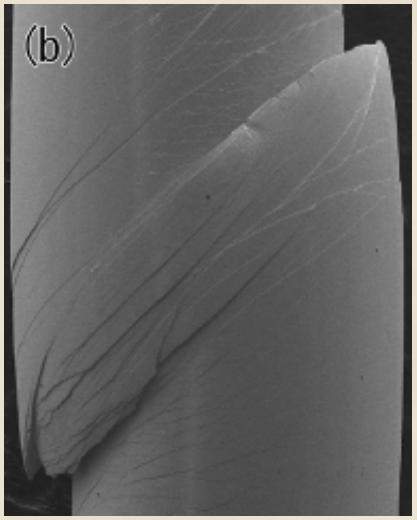

Q. S. Zhang, W. Zhang, G. Q. Xie, D. V. Louzguine-Luzgin, A. Inoue "Stable flowing of localized shear bands in soft bulk metallic glasses" Acta Materialia, Vol. 58, (2010), pp. 904-909.

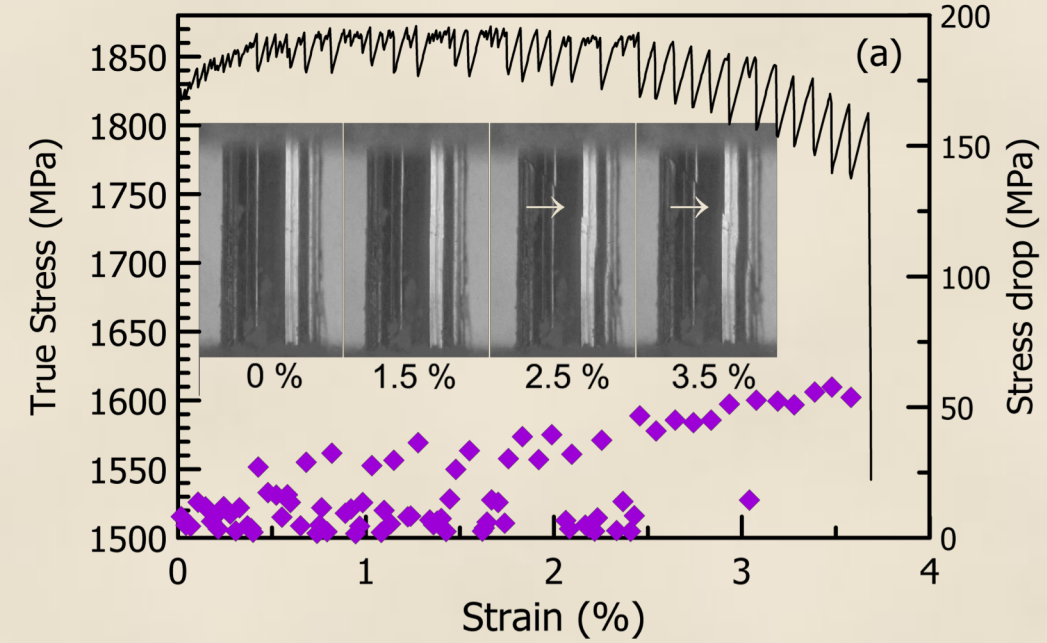

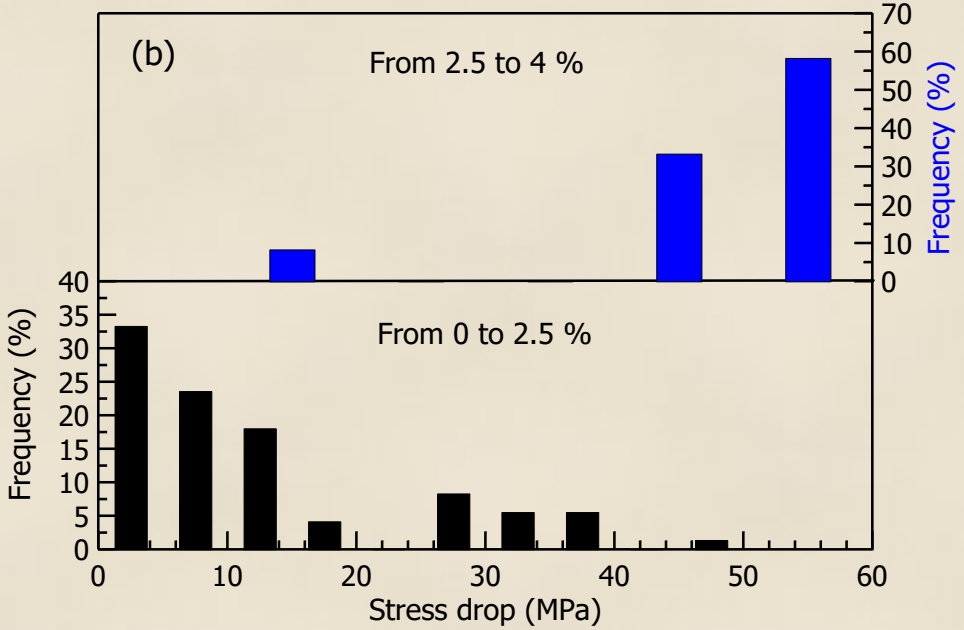

D.V. Louzguine-Luzgin, V.Yu. Zadorozhnyy, N. Chen, and S.V. Ketov Journal of Non-Crystalline Solids, Vol. 396–397 (2014) pp. 20–24.

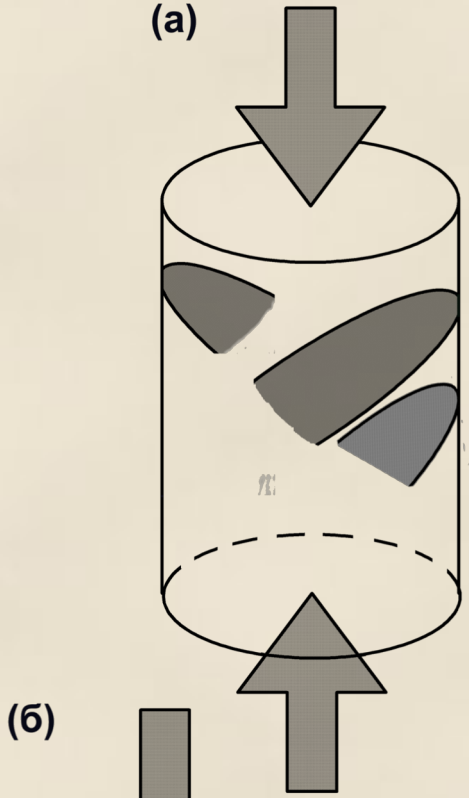

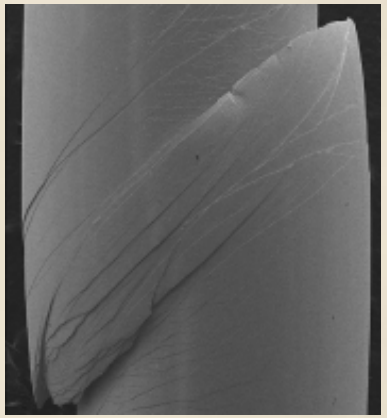

$Zr_{62.5}Cu_{22.5}Fe_5Al_{10}$
2:1 aspect ratio

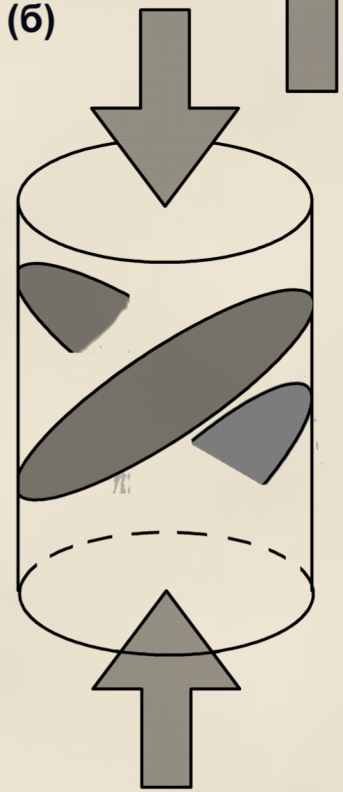

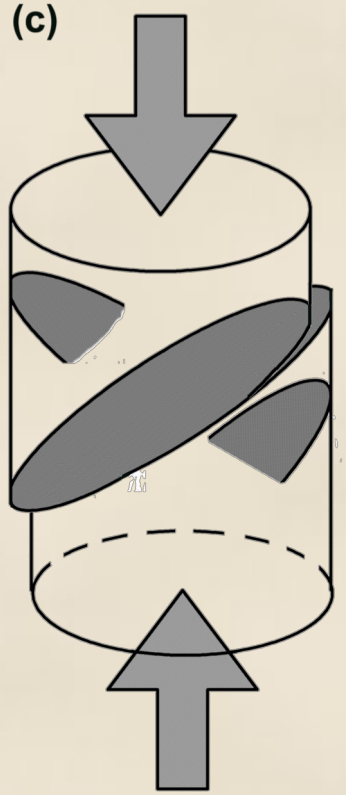

Porous $Pd_{42.5}Cu_{30}Ni_{7.5}P_{20}$ Alloy

Preparation condition : hydrogen absorption at 15 MPa
foaming and water cooling at 13.5 MPa

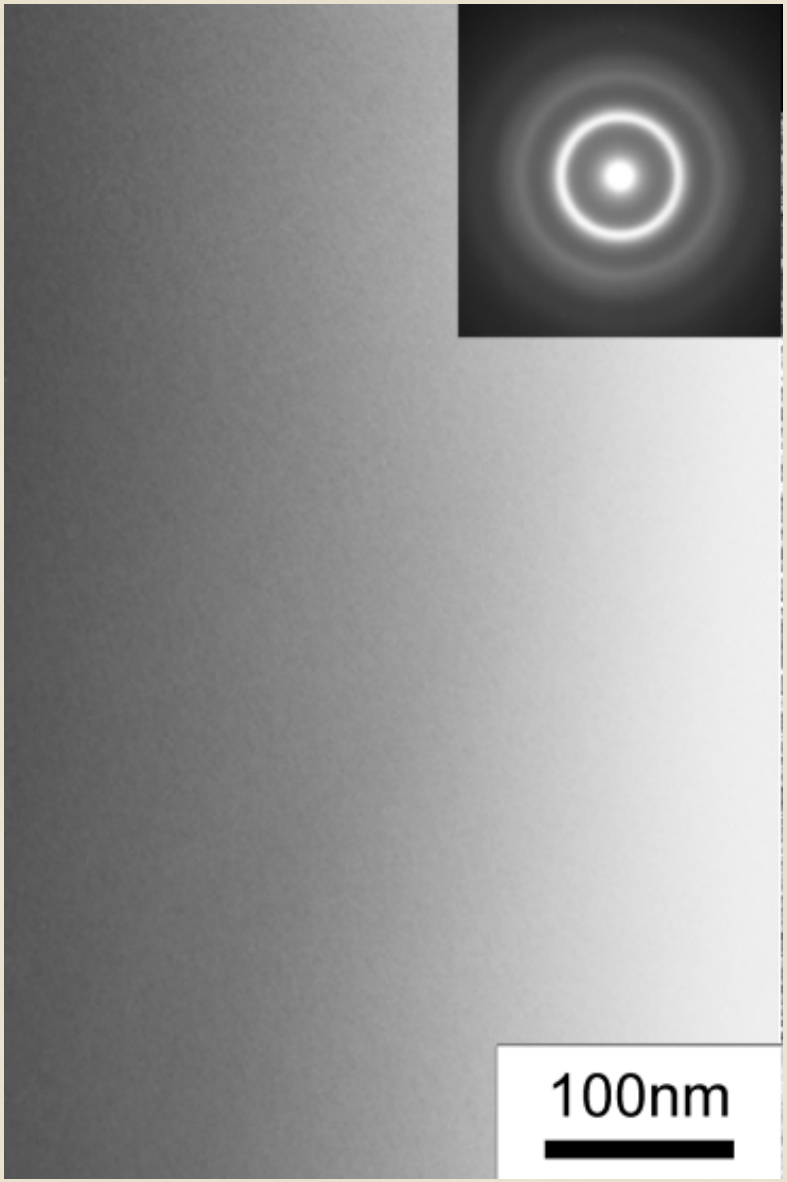

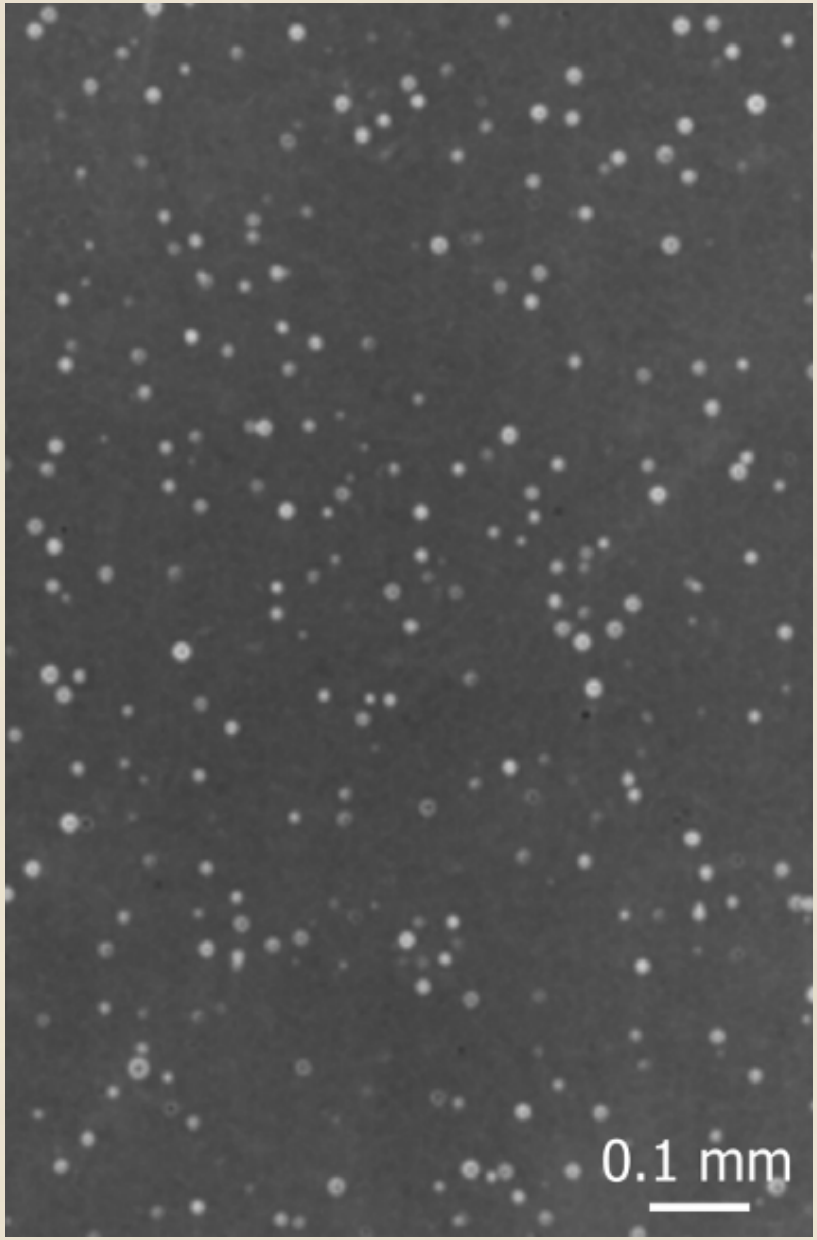

Compressive Stress-Strain Traces

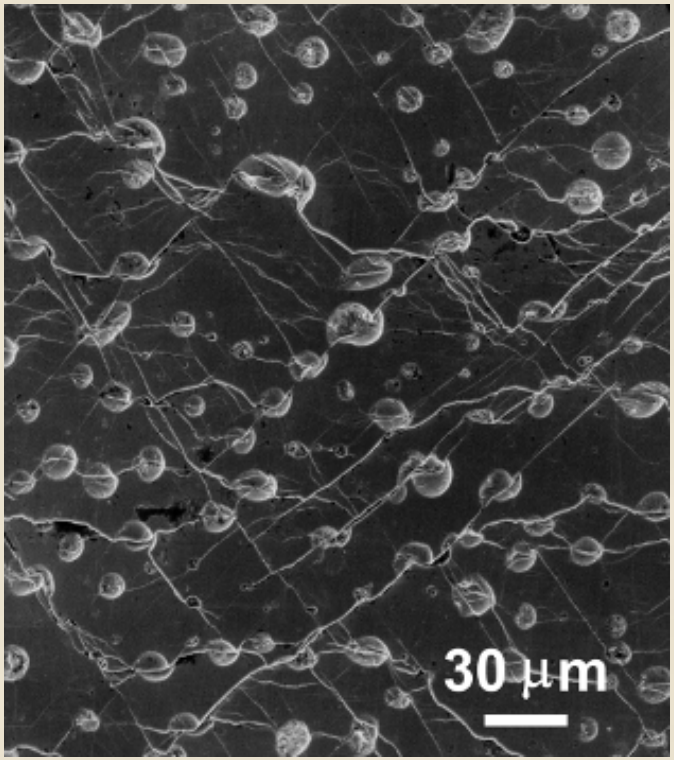

$Pd_{42.5}Cu_{30}Ni_{7.5}P_{20}$

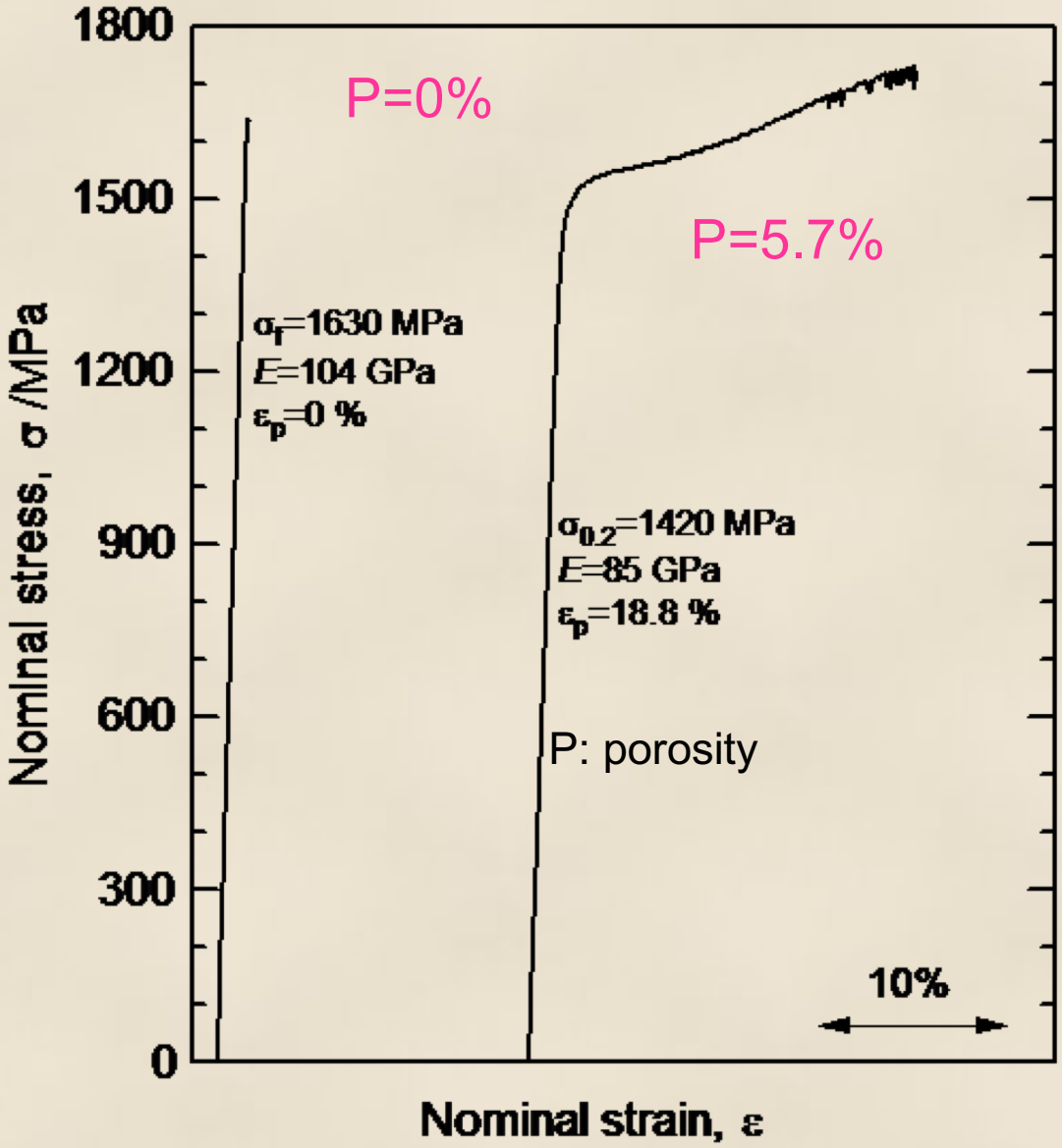

Composites

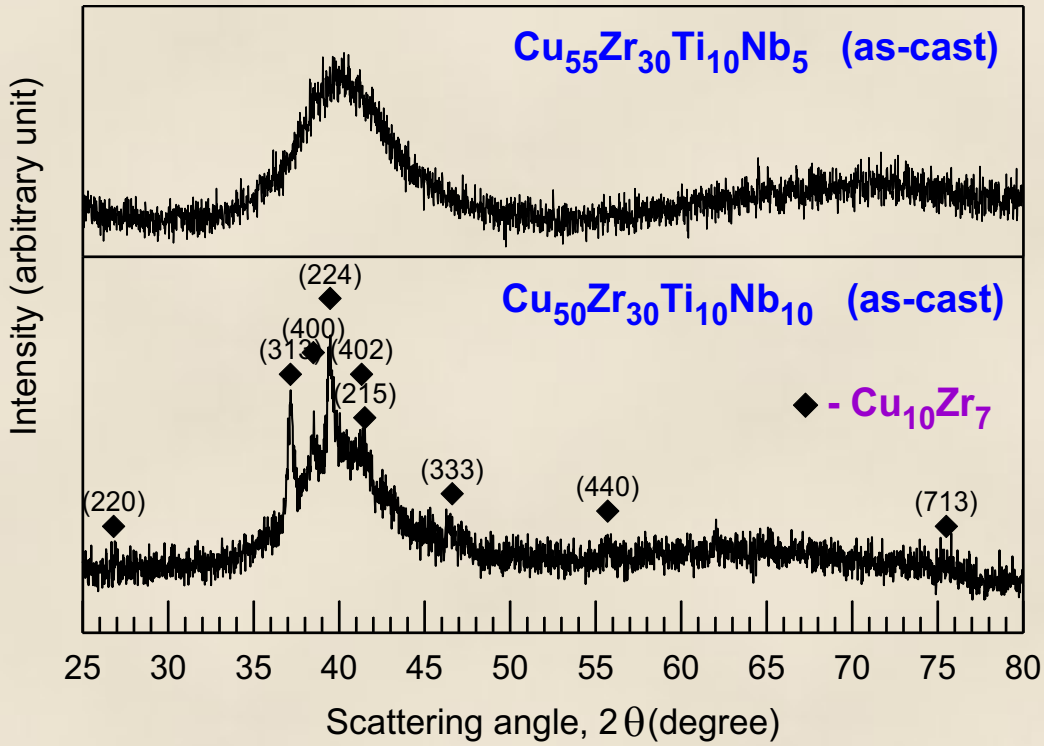

D. V. Louzguine, H. Kato, and A. Inoue "High-strength Cu-based crystal-glassy composite with enhanced ductility" Applied Physics Letters, Vol. 84, N: 7, (2004) pp. 1088-1089.

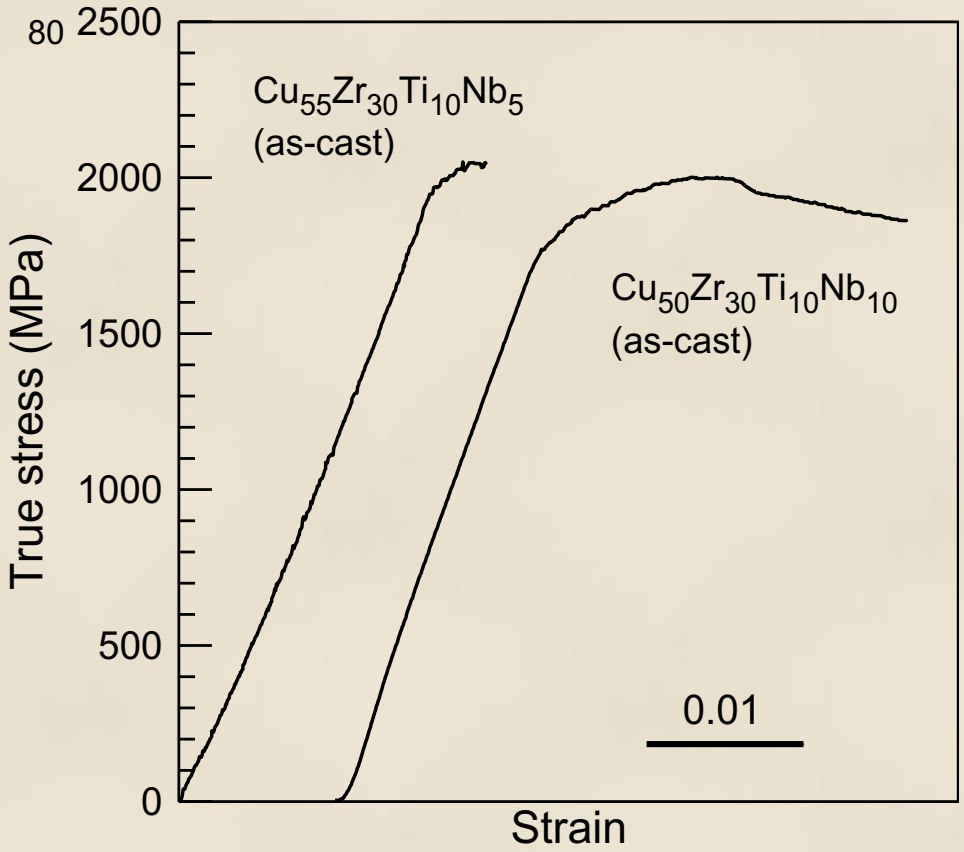

Deformation-induced martensite in $Ni_{40}Ti_{33}Zr_{17}Cu_{10}$ Glassy-Crystal Alloy

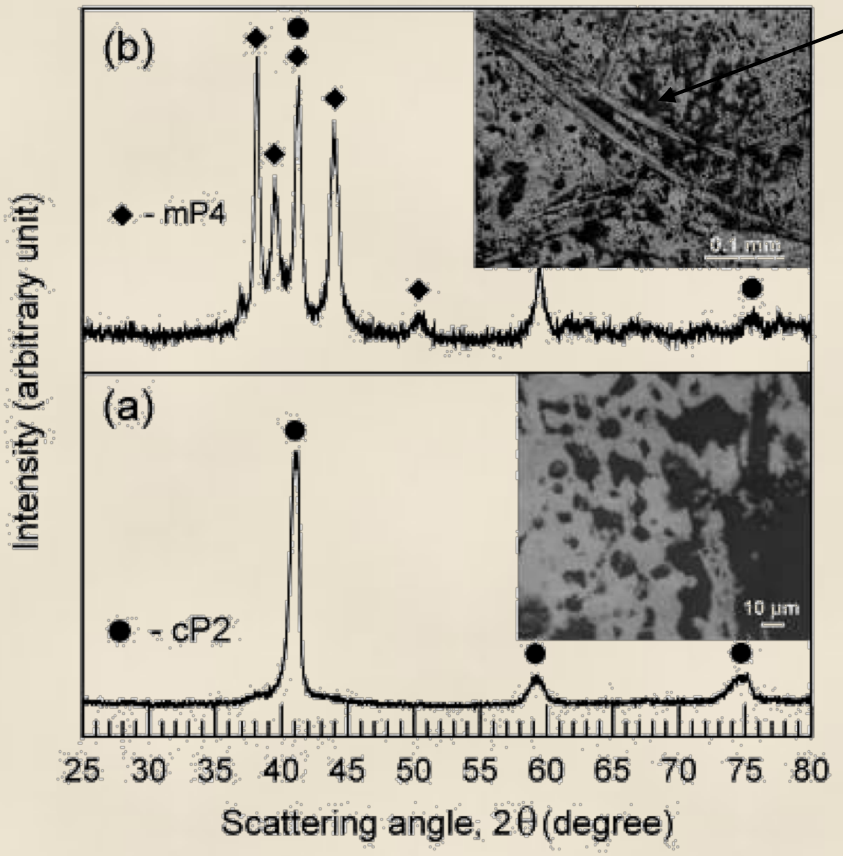

X-ray diffraction pattern of the **$Ni_{40}Ti_{33}Zr_{17}Cu_{10}$ alloy** (a) in the as-solidified state and (b) deformed to about 5 % total strain.

lateral surface after deformation to 5 %

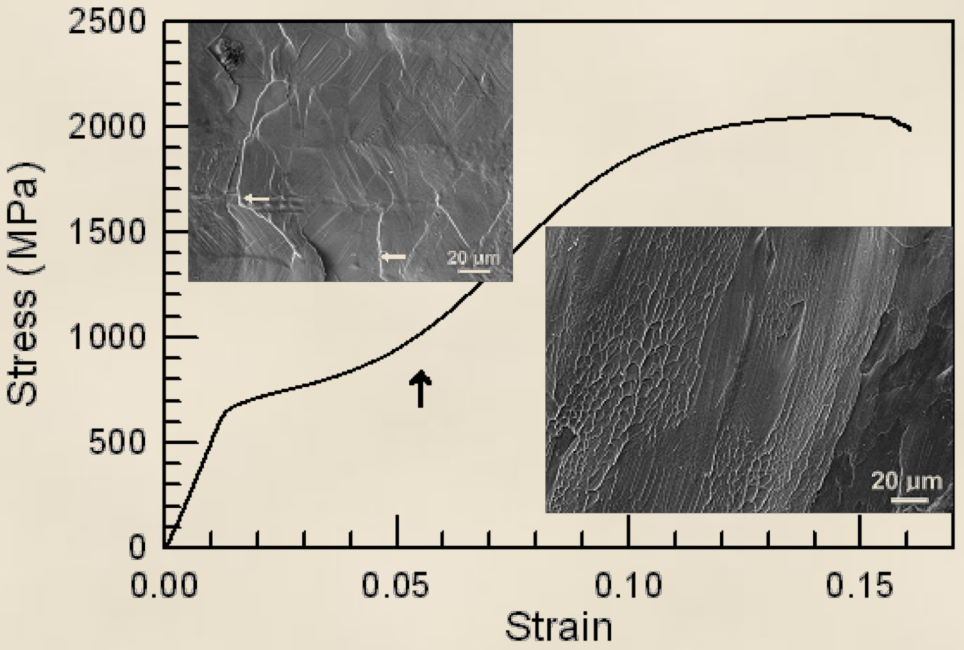

Typical compressive true stress-strain curve of the **$Ni_{40}Ti_{33}Zr_{17}Cu_{10}$ alloy**. Upper corner insert shows the lateral surface of the sample deformed to fracture, SEM.

D. V. Louzguine-Luzgin, et al. Philosophical Magazine, 89, 2009, 2887.

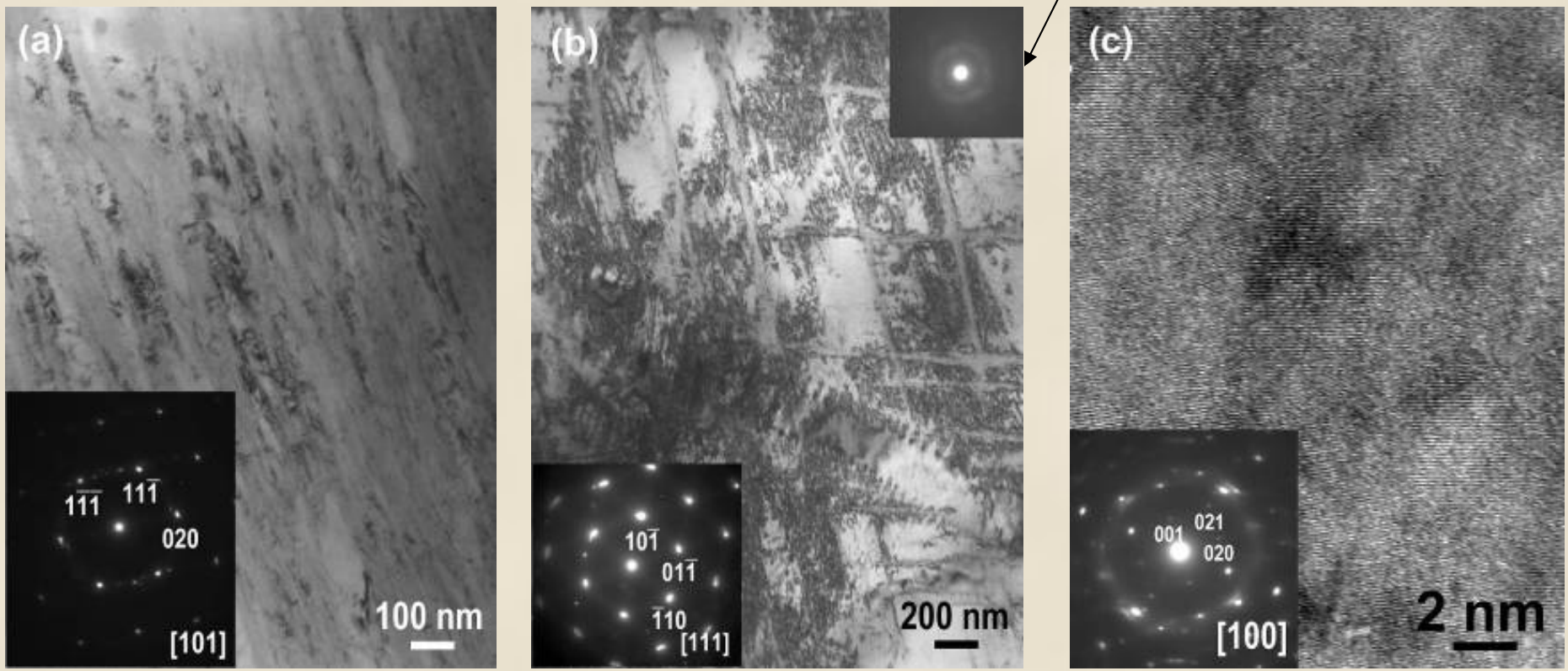

mP4 martensite

cP2 austenite

Nanoscale
CuZr superstructure

	Ni	**Cu**	**Ti**	**Zr**
cP2 austenite	39.4±1.2	11.1±1.1	31.6±0.8	17.9±0.9
glassy matrix	38.4±1.2	12.1±0.7	30.1±0.9	19.3±1.5
mP4 martensite	41.0±0.4	10.4±0.1	31.6±0.5	16.9±0.7

Deformed to about 5 %

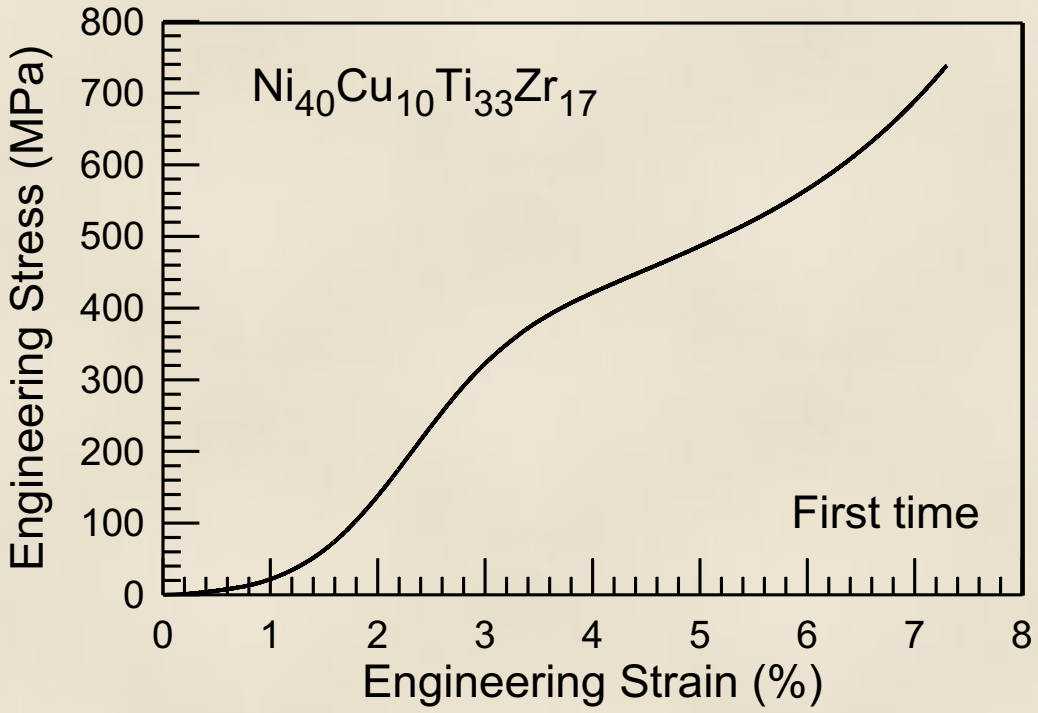

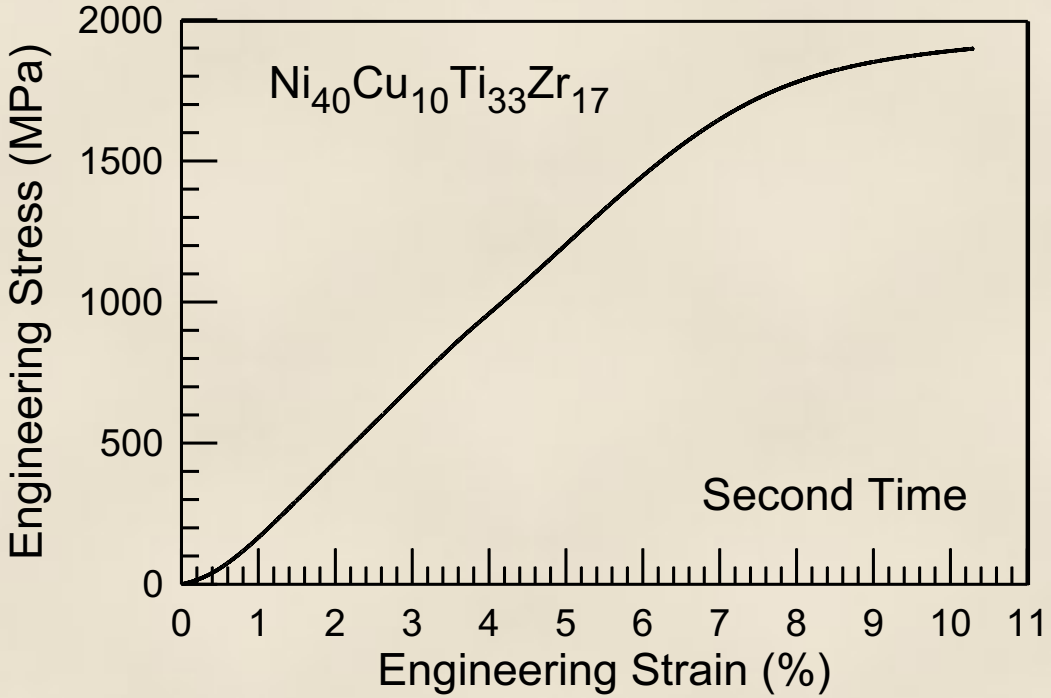

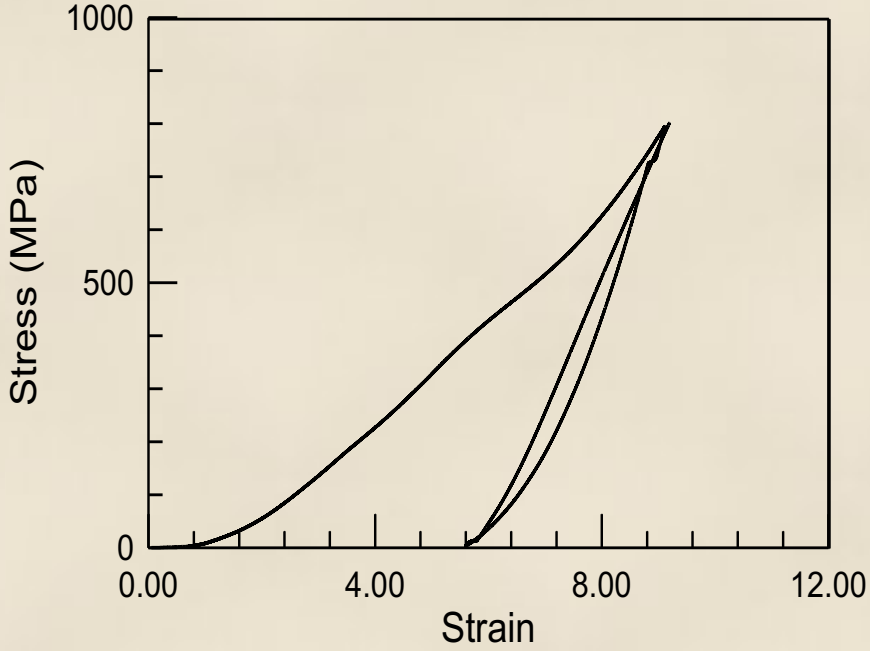

3 mm diameter
cast sample

Micro plastic forming in the supercooled liquid 643 K

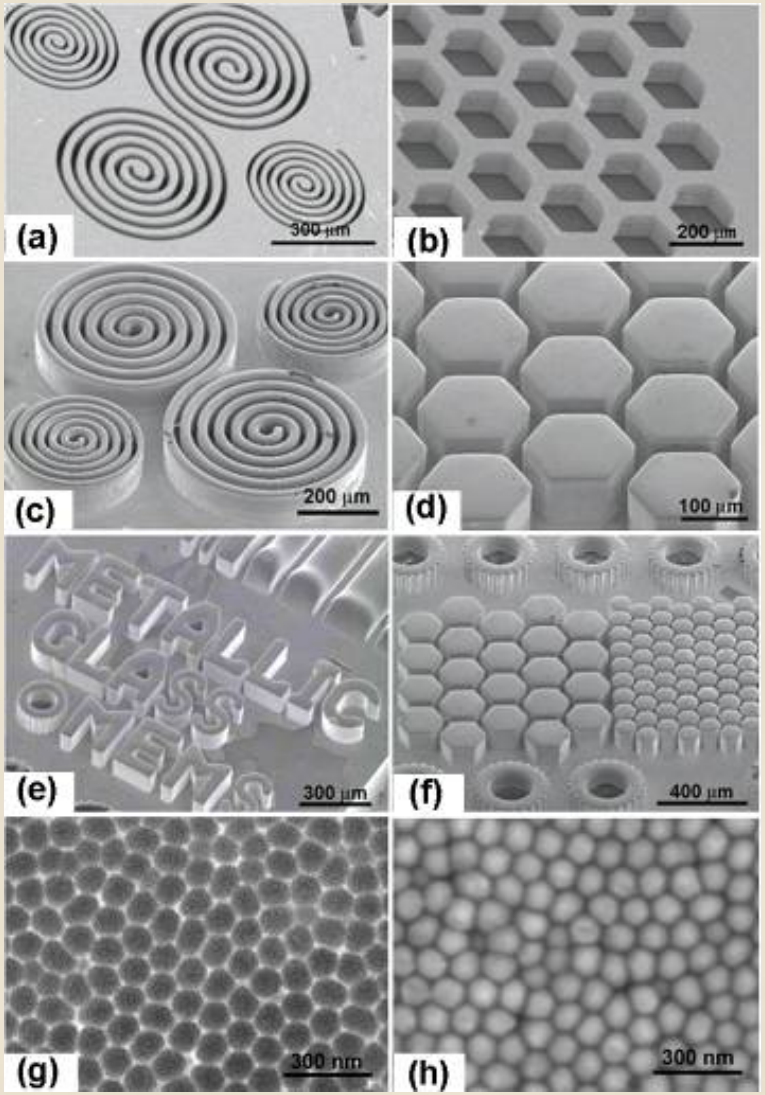

$Pd_{40}Ni_{40}Si_4P_{16}$

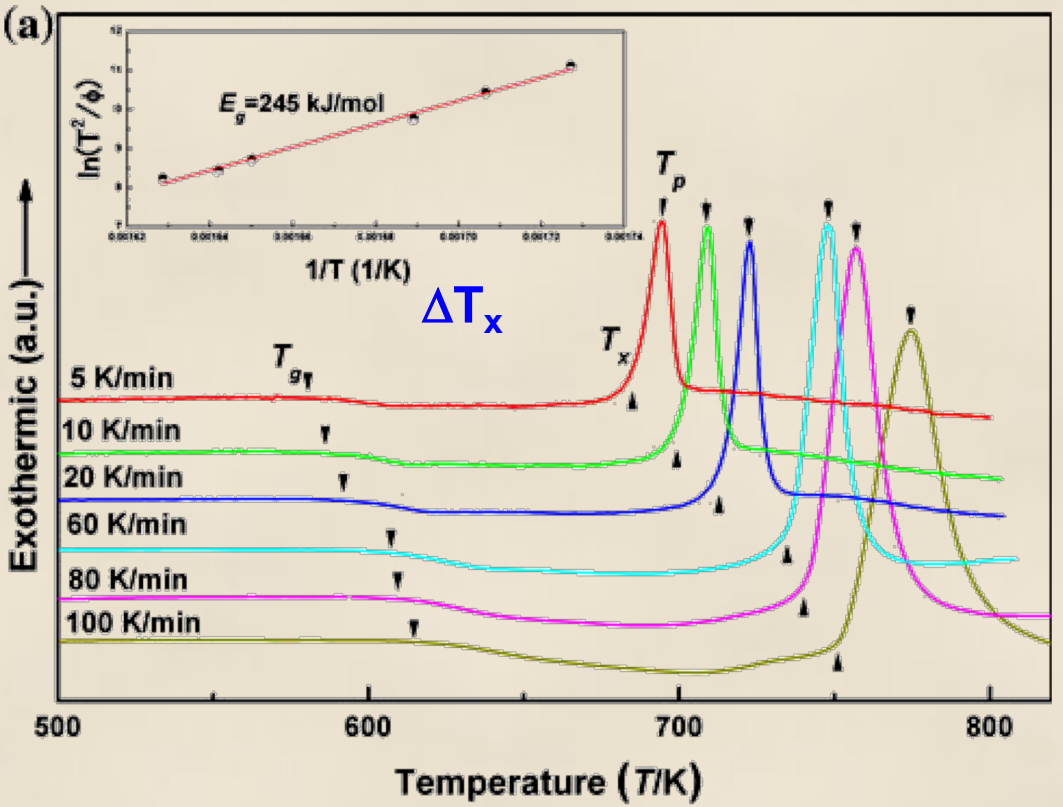

N. Chen, H. A. Yang, A. Caron, P. C. Chen, Y. C. Lin, D. V. Louzguine-Luzgin, K. F. Yao, M. Esashi, A. Inoue, Glass-forming ability and thermoplastic formability of a Pd40Ni40Si4P16 glassy alloy, Journal of Materials Science 46 (2011) 2091-2096.

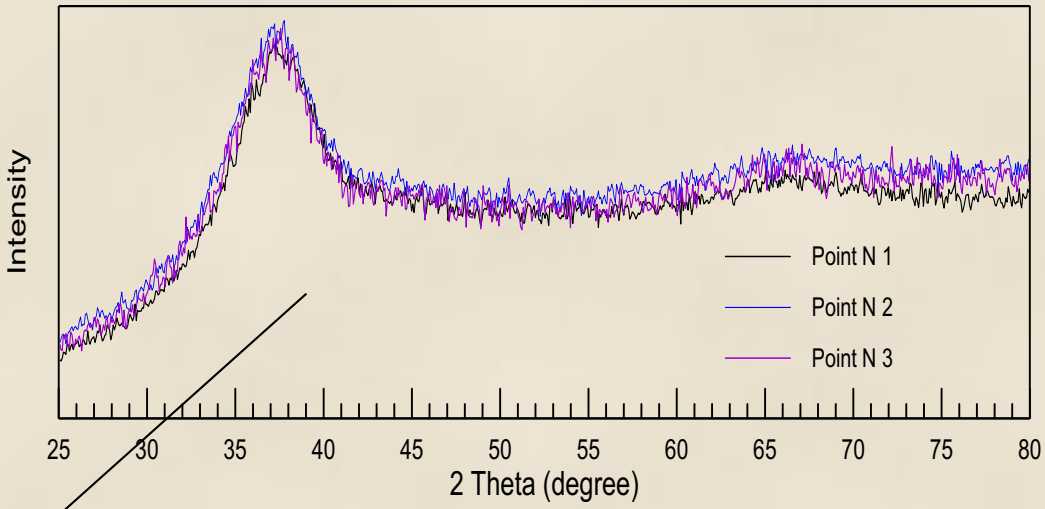

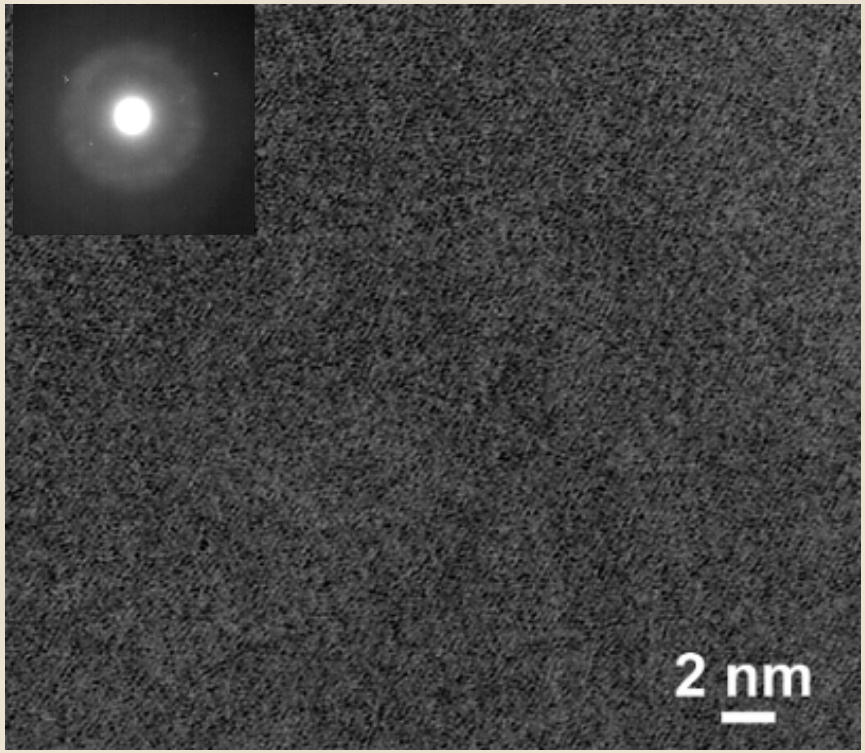

Composition: $Ni_{53}Nb_{20}Ti_{10}Zr_8Co_6Cu_3$
Welding conditions:
(**Fiber laser welding in the atmosphere**)
laser power: 120 W
wave length of the laser: 1070 nm
spot diameter: 0.3 mm
slit width of the cover plate: 0.6 mm
welding speeds: 6 m/min

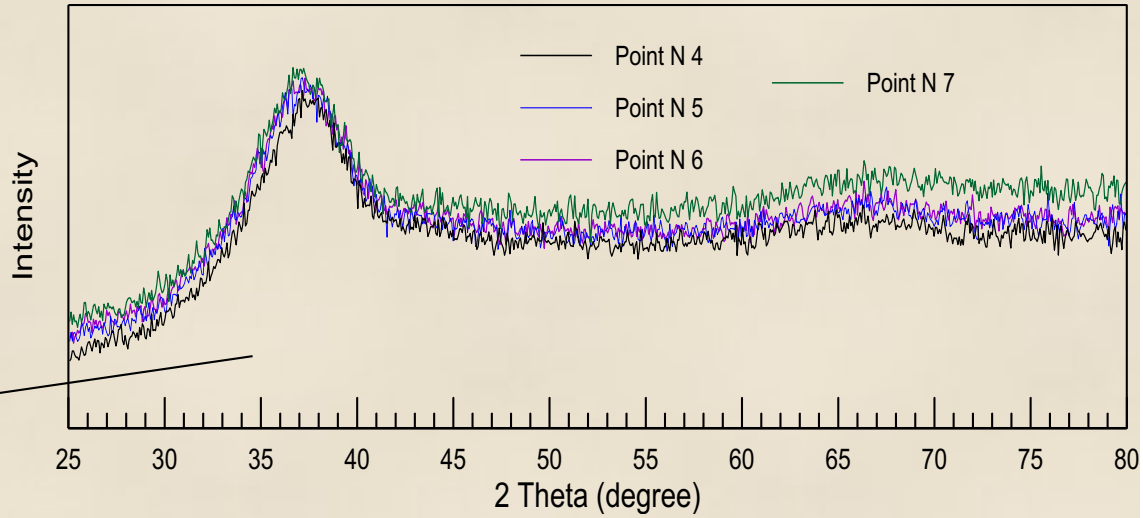

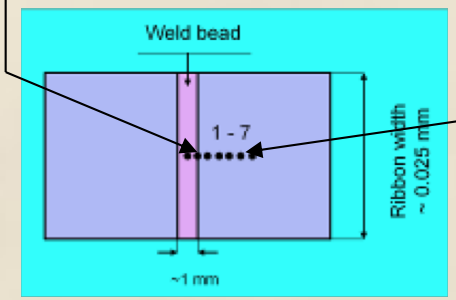

D. V. Louzguine-Luzgin, G. Q. Xie, T. Tsumura, K. Nakata, Y. Murakami, H. M. Kimura, A. Inoue, Ceramic Transactions, Vol. 198 (2007) pp. 3-8.

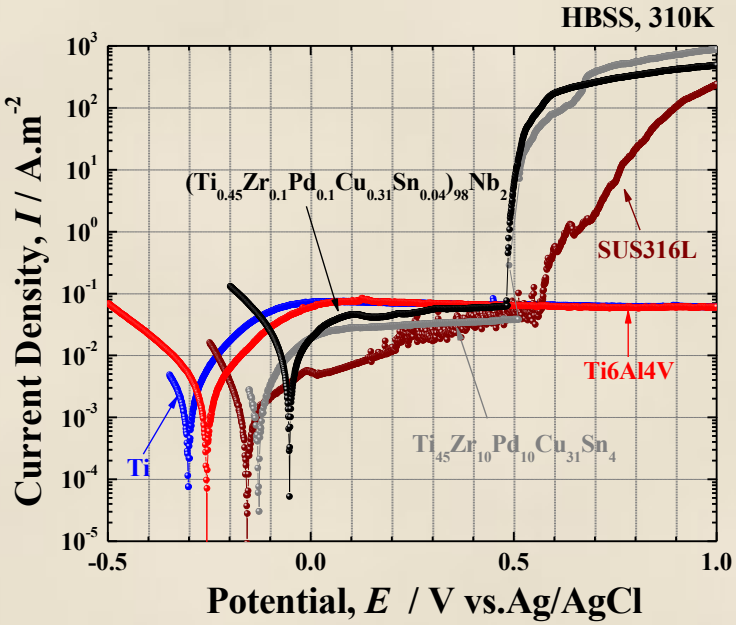

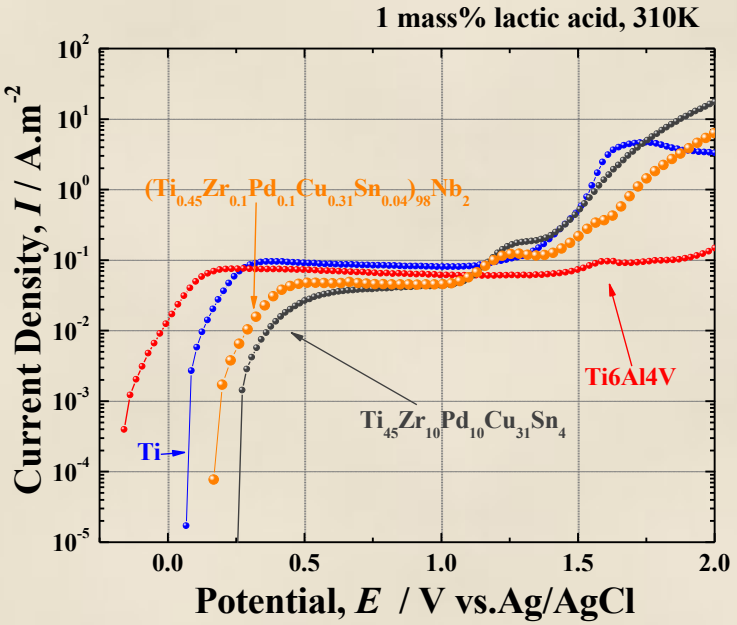

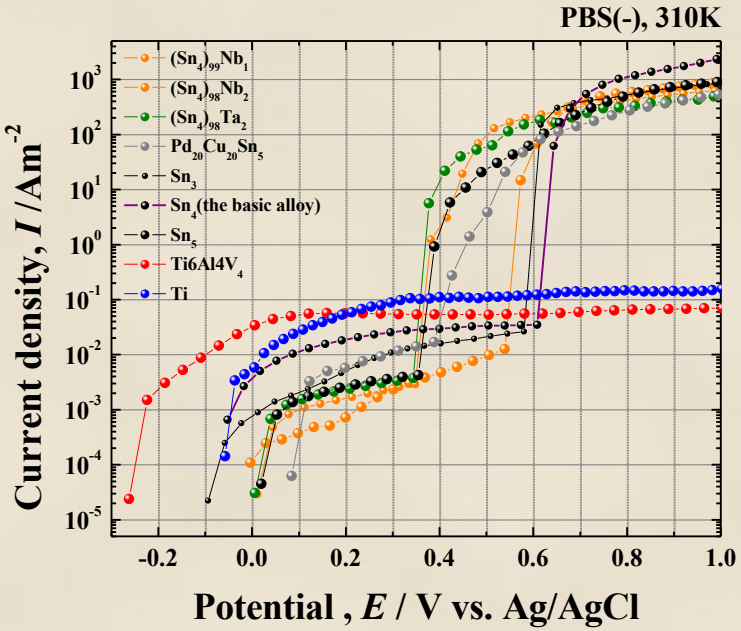

1 mass.% lactic acid, PBS (8 g/l NaCl, 0.2 g/l KCl, 1.15 g/l Na_2HPO_4, 0.2 g/l KH_2PO_4) and HBSS (8 g/l NaCl, 0.4 g/l KCl, 0.09 g/l $Na_2HPO_4 \cdot 7H_2O$, 0.06 g/l KH_2PO_4, 0.35 g/l $NaHCO_3$, 1.0 g/l glucose) at 310 K in atmosphere

Anodic polarization curves **$(Ti_{0.45}Zr_{0.1}Pd_{0.1}Cu_{0.31}Sn_{0.4})_{98}Nb_2$.**

J. J. Oak, D. V. Louzguine-Luzgin and A. Inoue "Fabrication of Ni-free Ti-based bulk-metallic glassy alloy having potential for application as biomaterial, and investigation of its mechanical properties, corrosion, and crystallization behavior" Journal of Materials Research, 22, (2007) 1346

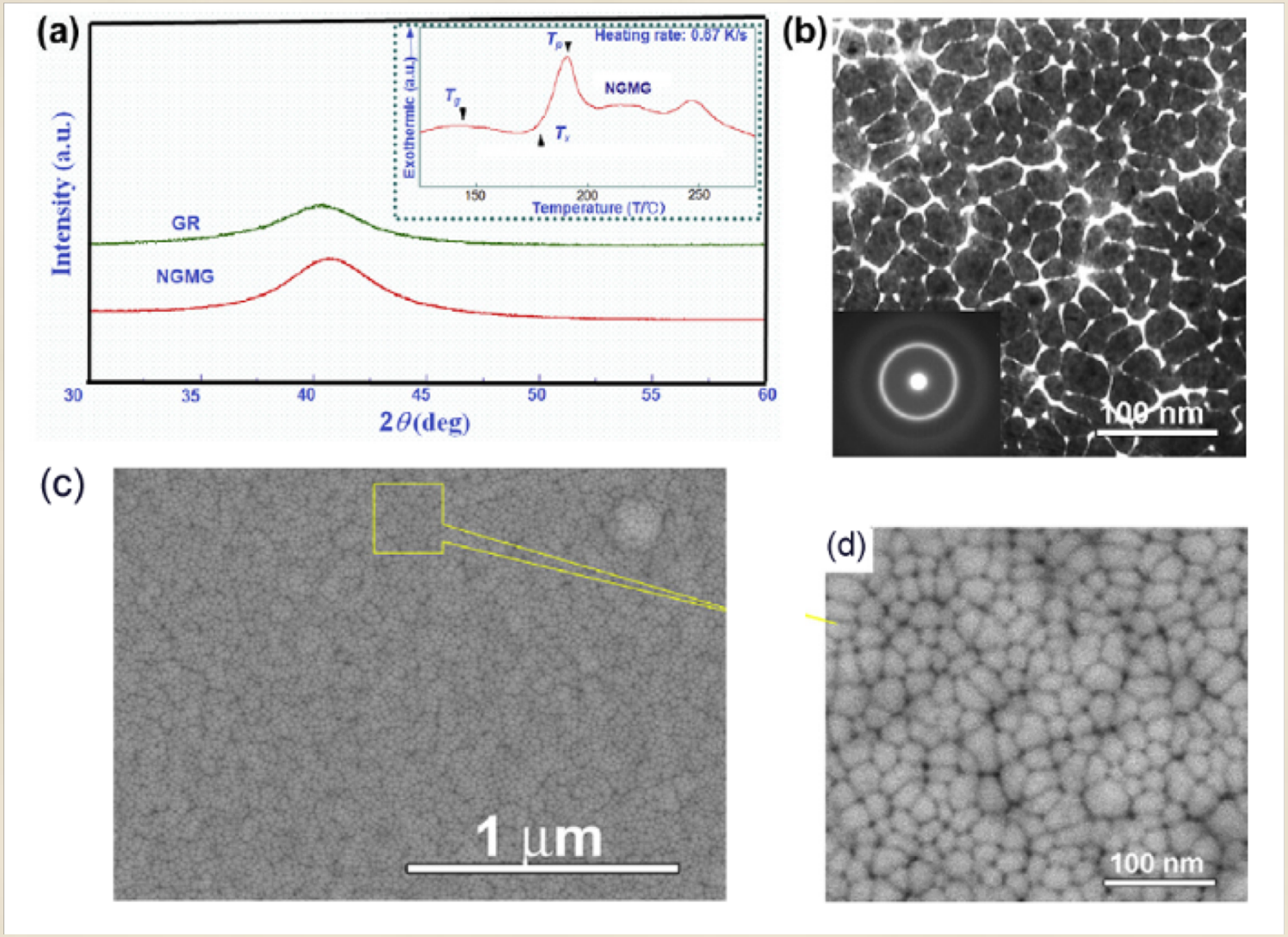

(a)XRD patterns of the $Au_{49}Ag_{5.5}Pd_{2.3}Cu_{26.9}Si_{16.3}$ glassy ribbons (GR) and **$Au_{52}Ag_5Pd_2Cu_{25}Si_{10}Al_6$ nano-grained metallic glass (NGMG)** prepared by **magnetron sputtering**. The inset of (a**)** is the DSC curve of NGMG sample. (b) Bright-field TEM image. The inset of (b) is SAED pattern. (c) SEM images of the surface morphology of NGMG.

N. Chen, R. Frank, N. Asao, D. V. Louzguine-Luzgin, P. Sharma, J. Q. Wang, G. Q. Xie, Y. Ishikawa, N. Hatakeyama, Y. C. Lin, M. Esashi, Y. Yamamoto, A. Inoue, Acta Materialia 59, (2011) pp. 6433–6440.

$Ti_{34}Zr_{14}Cu_{22}Pd_{30}$ nanograined metallic glass (NGMG)

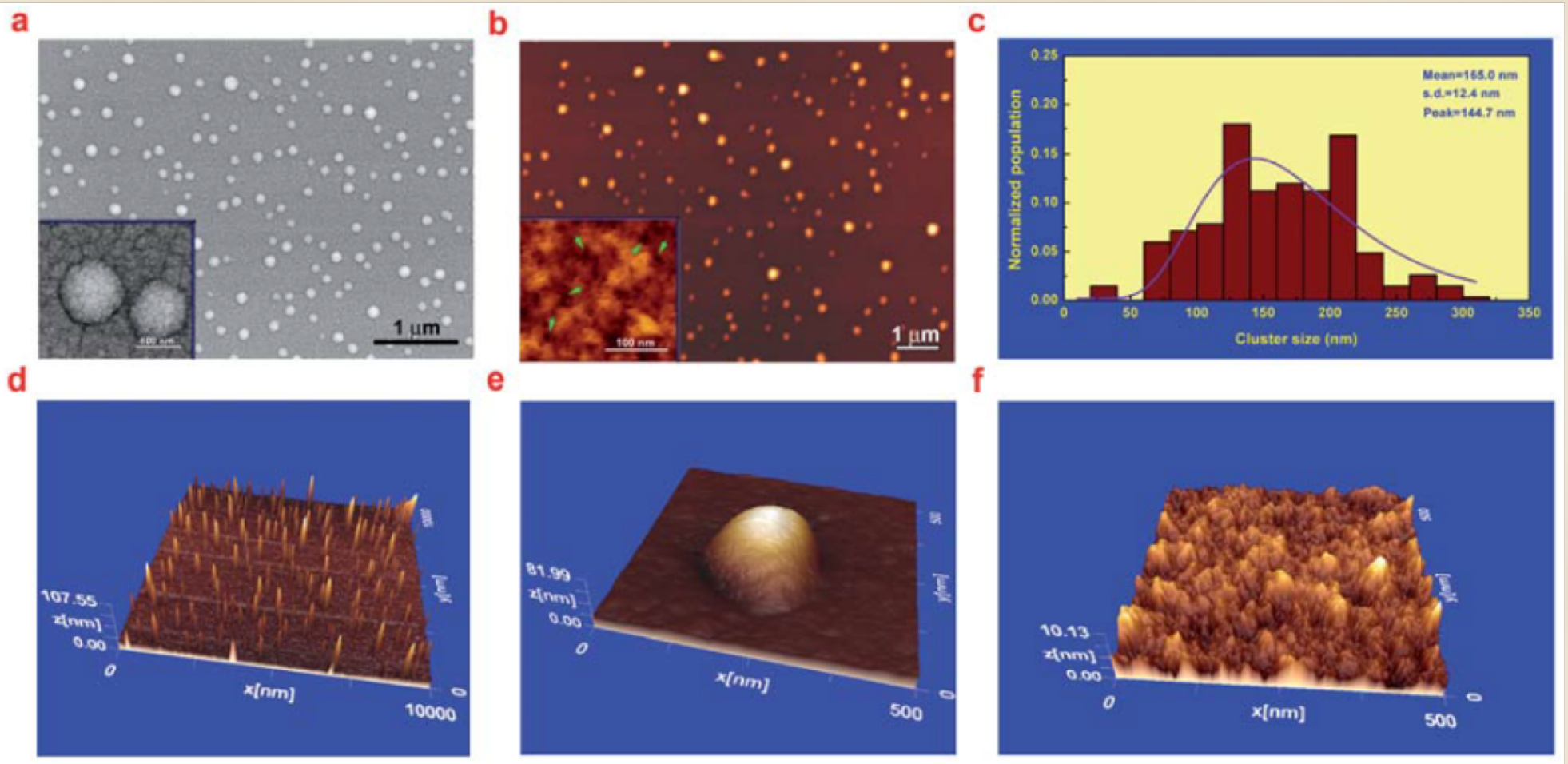

Surface topography of the Ti34Zr14Cu22Pd30 NMG: (a) SEM image; (b) 2D AFM image; the insets in (a) and (b) are enlarged images. (c) Size distribution of the glassy clusters; (d) 3D AFM image corresponding to (b); (e) 3D AFM image of one submicron cluster shown in (b); and (f) 3D AFM image of the nanostructured matrix shown in (b).

N. Chen, X. Shi, R. Witte, K. S. Nakayama, K. Ohmura, H. K. Wu, A. Takeuchi, H. Hahn, M. Esashi, H. Gleiter, A. Inoue and D. V. Louzguine "A novel Ti-based nanoglass composite with submicron–nanometer-sized hierarchical structures to modulate osteoblast behaviors" J. Mater. Chem. B, Vol. 1, N: 20 (2013), pp. 2568–2574.

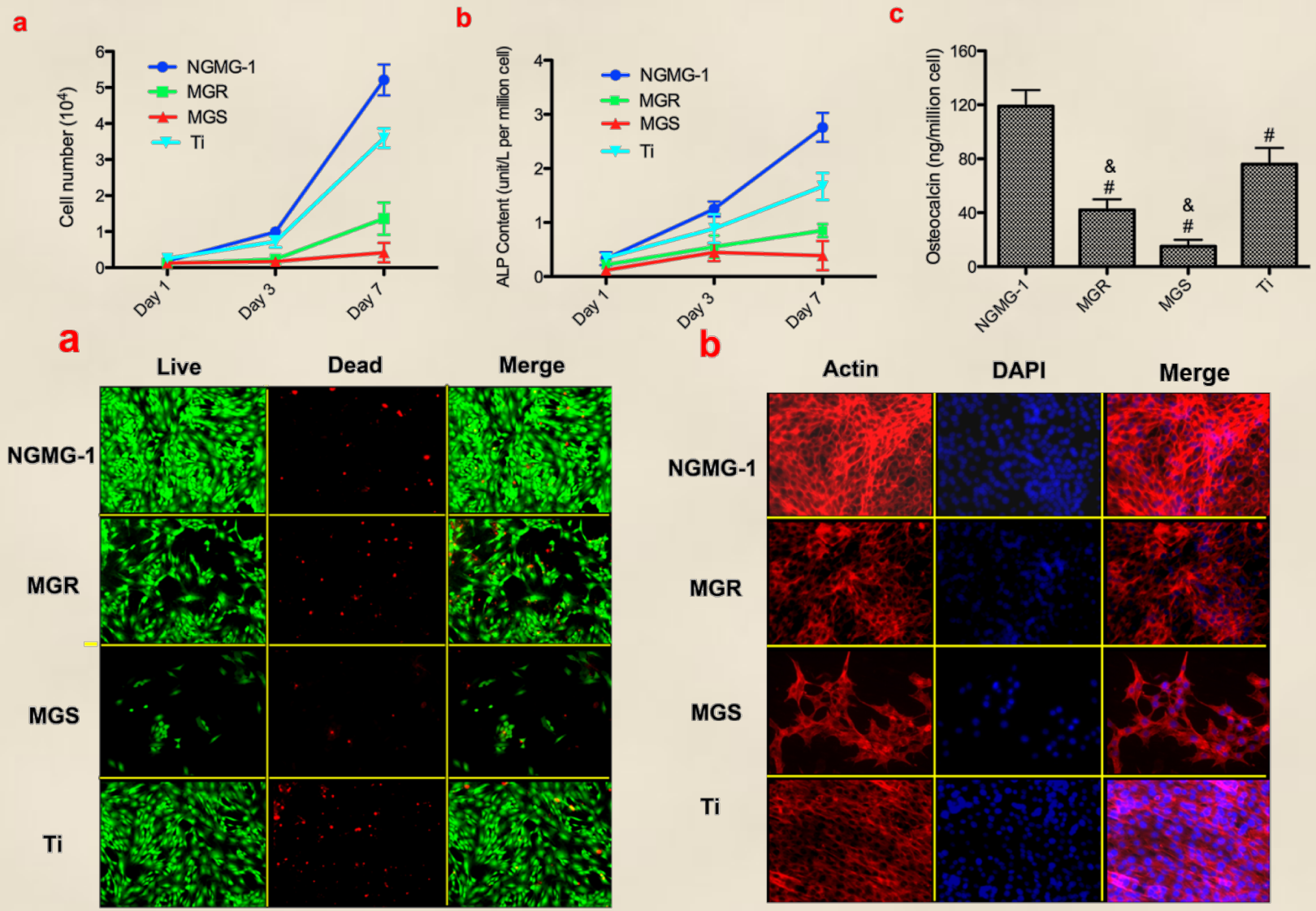

Cell proliferation and phenotypes on NGMG, MGRib, MGSurf, and Ti surfaces: (a) cell number; (b) activity of alkaline phosphatase (ALP) content; (c) osteocalcin secretion after 7 days of culture; (d) live/dead cell staining, magnification: 10; and (e) TRITC–phalloidin for F-actin staining and 4',6-diamidino-2-phenylindole (DAPI) for cell nucleus staining, magnification: 20. Ampersand (&) and pound sign (#) indicate statistical significance when compared with NGMG and Ti, and NGMG ($n = 6$ for all the conditions). Significant differences (unpaired Student's t-test): $P < 0.05$.

The history of weight change during exposure of the Zr-BMG to ions of deuterium plasma of 60 eV/ion, ion current density 2.1 mA/cm^2.

№ of exposure	Ion fluence, 10^{25} ions/m^2	Weight gain for BMG, μg	Weight gain for BMG-C, μg
1	0.47	30	40
2	2.4	620	0
3	2.4	920	640
4	2.4	820	Destroyed
5	1.6	375	
6	2.4	825	
7	2.4	870	

Voitsenya VS, Bakai AS, Bardamid AF, Konovalov VG, Kovtun KV, Naidenkova DI, Ryzhkov IV, Shtan' AF, Solodovchenko SI, Trembach OV, Vasil'ev AA. Mint: J. Plasma Fusion Res. SERIES. 2009;8:1379-1384.

(a) The Zr-based BMG-C crystallized sample after the fourth exposure to 60 eV ions of deuterium plasma and (b) its amorphous counterpart (BMG) after the seventh exposure to 60 eV ions of deuterium plasma.

V. S. Voitsenya, et al. On the Prospects of Using Metallic Glasses for In-vessel Mirrors for Plasma Diagnostics in ITER, Metallic Glasses - Formation and Properties, Edited by Behrooz Movahedi, DOI: 10.5772/63885

Factors influencing GFA

Intrinsic (belonging to a glass itself)

Extrinsic (depending upon external conditions)

Homogeneous nucleation (intrinsic)

- Equilibrium phase diagram
  $T_l(\beta->0)$; Kauzmann T_g

- Non-equilibrium solidification
  $T_l(\beta)\downarrow$ $T_g(\beta)\uparrow$

a) Supercooling
b) Shift of the eutectic point and widening
c) Appearance of the competitive non-equilibrium phases

Heterogeneous nucleation (extrinsic)

Glass-forming ability criteria

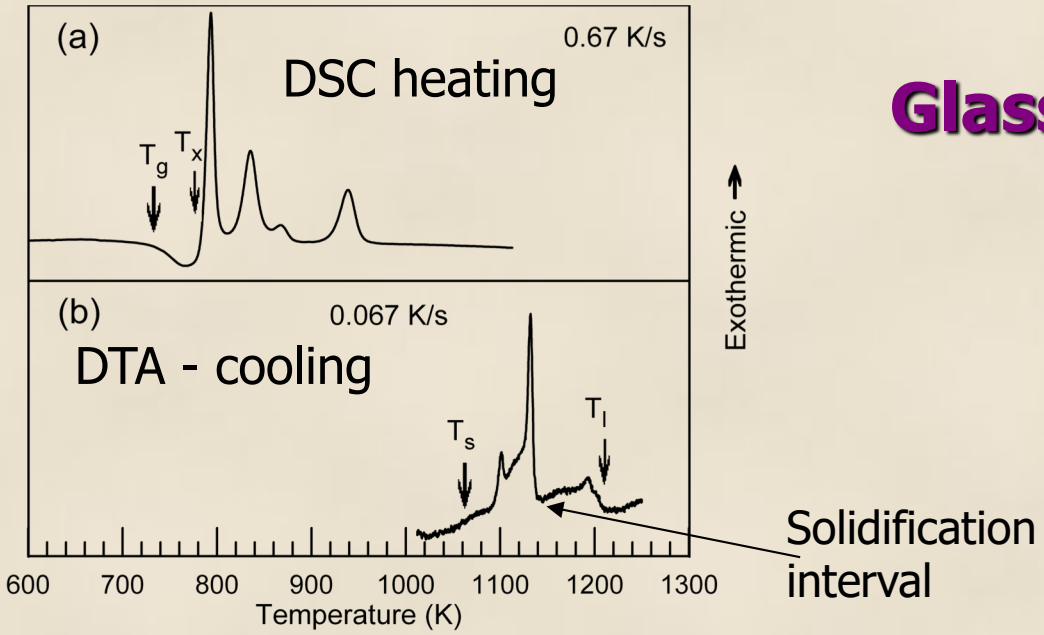

1. T_g/T_l
2. $\Delta T_x=T_x-T_g$
3. $\gamma=T_x/(T_g+T_l)$
4. $\alpha*T_g/T_l$

   $\alpha=(T_e-T_g)/(T_l-T_g)$

   and many others…

β_c critical cooling rate concept

Analysis of the database of binary (glassy), ternary, quaternary and quinary bulk glassy alloys.

In collaboration with D. B. Miracle, Air Force Research Laboratory, Materials and Manufacturing Directorate, Dayton, OH, USA

M196 1165

	System	EL1	EL2	EL3	AT% 1	AT% 2	At% 3	Critical Diam	Diam,	Density	T_g, K	T_x, K	T_l, K	Tm, K	ΔT_x
675	Zr-Ni-Al	Zr	Ni	Al	60	21	19	8	8		723	766.4	1295	1185	43.4
676	Zr-Ni-Al	Zr	Ni	Al	65	20	15	2	2		695.3	741.7	1306	1179	46.4
677	Zr-Ni-Al	Zr	Ni	Al	61	20	19	2	2		717.1	758.7	1304	1176	41.6
678	Zr-Ni-Al	Zr	Ni	Al	63	19	18	2	2		706	745.2	1314	1179	39.2
679	Zr-Ni-Al	Zr	Ni	Al	61.5	19	18.5	2	2		721	756.3	1318	1187	35.3
680	Zr-Ni-Al	Zr	Ni	Al	60	20	20	2	2		730	768.9	1354	1179	38.6
681	Zr-Ni-Al	Zr	Ni	Al	60	19	21	2	2		731.6	763.8	1300	1185	32.2
682	Zr-Ni-Al	Zr	Ni	Al	60	22	18	2	2		720.1	766.6	1290	1182	46.5
683	Zr-Ni-Al	Zr	Ni	Al	58	21	21	2	2		744.3	779.1	1337	1174	34.8
684	Zr-Ni-Al	Zr	Ni	Al	52	26	22								
685	Zr-Ni-Al	Zr	Ni	Al	55	25	20				757	803			
686	Zr-Ni-Al	Zr	Ni	Al	57	27	16								
687	Zr-Ni-Al	Zr	Ni	Al	60	25	15				670				
688	Zr-Ni-Al	Zr	Ni	Al	55	25	20				725				
689	Zr-Ni-Al	Zr	Ni	Al	65	25	10				640				
690	Zr-Ni-Al	Zr	Ni	Al	60	25	15				696	787	1230		
691	Zr-Ni-Al	Zr	Ni	Al	65	20	15				671	741	1234		
692	Zr-Ni-Al	Zr													
693	Zr-Ni-Al	Zr													
694	Zr-Ni-Al	Zr													
695		Zr													
696	Zr-Ni-Al	Zr													

G1100 =IF(D1100<>D1099,VLOOKUP(ELEM2mar,RadiiIB$2:G$78,6,FALSE),VLOOKUP(ELEM1mar,R

	System	EL1	EL2	AT% 1	AT% 2	System Radius Ratio	Alloy Radius Ratio	GL/AM	FORM	Thick, mm	T_g, K	T_x, K	T_l, K	ΔT_x	T_{rg}
1067	Zr-Pd	Zr	Pd	65	35		0.882	AM	flake						
1068	Zr-Pd	Zr	Pd	65	35										
1069	Zr-Pd	Zr	Pd	65	35										
1070	Zr-Pd	Zr	Pd	66.7	33.3										
1071	Zr-Pd	Zr	Pd	67	33										
1072	Zr-Pd	Zr	Pd	67	33										
1073	Zr-Pd	Zr	Pd	70	30										
1074	Zr-Pd	Zr	Pd	70	30										
1075	Zr-Pd	Zr	Pd	70	30										
1076	Zr-Pd	Zr	Pd	80	20										
1077	Zr-Rh	Zr	Rh	72	28										
1078	Zr-Rh	Zr	Rh	74	26										
1079	Zr-Rh	Zr	Rh	82	18										
1080	Zr-Rh	Zr	Rh	83	17										
1081	Zr-Si	Zr	Si	77	23										
1082	Zr-Si	Zr	Si	78	22										
1083	Zr-Si	Zr	Si	80	20										
1084	Zr-Si	Zr	Si	80	20										
1085	Zr-Si	Zr	Si	81	19										
1086	Zr-Si	Zr	Si	83	17										
1087	Zr-Si	Zr	Si	83	17										
1088	Zr-Si	Zr	Si	83	17										
1089	Zr-Si	Zr	Si	83	17										
1090	Zr-Si	Zr	Si	84	16										
1091	Zr-Si	Zr	Si	85	15										
1092	Zr-Si	Zr	Si	85	15										
1093	Zr-Si	Zr	Si	85	15										
1094	Zr-Si	Zr	Si	85	15										
1095	Zr-Si	Zr	Si	87	13										
1096	Zr-Si	Zr	Si	87	13										
1097	Zr-Si	Zr	Si	87	13										
1098	Zr-Si	Zr	Si	78	22										
1099		Zr	Si	80	20										
1100	Ti-Si	Ti	Si	85	15										

R412C19

	System	EL1	EL2	EL3	El4	AT% 1	AT% 2	At% 3	At% 4	Ref
391	Zr-Cu-Fe-Al	Zr	Cu	Fe	Al	59.2	24.8	8.9	6.9	55LIU
392	Zr-Cu-Fe-Al	Zr	Cu	Fe	Al	59.2	25.4	9.1	6.3	55LIU
393	Zr-Cu-Fe-Al	Zr	Cu	Fe	Al	59.2	23.6	8.4	8.1	55LIU
394	Zr-Cu-Fe-Al	Zr	Cu	Fe	Al	59.2	22.9	8.2	8.7	55LIU
395	Zr-Cu-Fe-Al	Zr	Cu	Fe	Al	58	22	8	12	55HONG
396	Zr-Cu-Fe-Al	Zr	Cu	Fe	Al	59.2	24.2	8.6	7.5	55LIU
397	Zr-Cu-Fe-Al	Zr	Cu	Fe	Al	55.2	25.4	9.11	10.3	55LIU
398	Zr-Cu-Ni-Al	Zr	Cu	Ni	Al	65	17.5	10	7.5	48PERE
399	Zr-Cu-Ni-Al	Zr	Cu	Ni	Al	62	17	13	8	51PARK
400	Zr-Cu-Ni-Al	Zr	Cu	Ni	Al	52	32	4	12	23INOUE
401	Zr-Cu-Ni-Al	Zr	Cu	Ni	Al	52	30	6	12	23INOUE
402	Zr-Cu-Ni-Al	Zr	Cu	Ni	Al	50	26	12	12	23INOUE
403	Zr-Cu-Ni-Al	Zr	Cu	Ni	Al	50	34	4	12	23INOUE
404	Zr-Cu-Ni-Al	Zr	Cu	Ni	Al	48	32	8	12	23INOUE
405	Zr-Cu-Ni-Al	Zr	Cu	Ni	Al	50	32	6	12	23INOUE
406	Zr-Cu-Ni-Al	Zr	Cu	Ni	Al	52	28	8	12	23INOUE
407	Zr-Cu-Ni-Al	Zr	Cu	Ni	Al	50	30	8	12	23INOUE
408	Zr-Cu-Ni-Al	Zr	Cu	Ni	Al	46	34	8	12	23INOUE
409	Zr-Cu-Ni-Al	Zr	Cu	Ni	Al	48	28	12	12	23INOUE
410	Zr-Cu-Ni-Al	Zr	Cu	Ni	Al	48	34	6	12	23INOUE
411	Zr-Cu-Ni-Al	Zr	Cu	Ni	Al	50	28	10	12	23INOUE
412	Zr-Cu-Ni-Al	Zr	Cu	Ni	Al	48	30	10	12	23INOUE
413	Zr-Cu-Ni-Al	Zr	Cu	Ni	Al	48	30	10	12	23INOUE
414	Zr-Cu-Ni-Al	Zr	Cu	Ni	Al	52	26	10	12	23INOUE
415	Zr-Cu-Ni-Al	Zr	Cu	Ni	Al	44	34	10	12	23INOUE
416	Zr-Cu-Ni-Al	Zr	Cu	Ni	Al	46	30	12	12	23INOUE
417	Zr-Cu-Ni-Al	Zr	Cu	Ni	Al	44	32	12	12	23INOUE
418	Zr-Cu-Ni-Al	Zr	Cu	Ni	Al	55	30	5	10	90Inoue

R2C1 Ca-Mg-Al-Zn-Cu

	System	EL1	EL2	EL3	El4	El5	AT% 1	AT% 2	At% 3	At% 4	At% 5	Ref	Critical Diam
87	Zr-Cu-Co-Ag-Al	Zr	Cu	Co	Ag	Al	58	22	2	6	12	37Mondal	5.0
88	Zr-Cu-Co-Fe-Al	Zr	Cu	Co	Fe	Al	58	22	4	4	12	37Mondal	5.0
89	Zr-Cu-Ni-Al-Nb	Zr	Cu	Ni	Al	Nb	55	25	5	10	5	36 Wang	2.0
90	Zr-Cu-Ni-Al-Ti	Zr	Cu	Ni	Al	Ti	52.5	17.9	14.6	10	5	14 WANG	5.0
91	Zr-Nb-Cu-Ni-Al	Zr	Nb	Cu	Ni	Al	59.5	2.5	15.4	12.6	10	25 Dong	6.0
92	Zr-Nb-Cu-Ni-Al	Zr	Nb	Cu	Ni	Al	59.2	2.8	15.4	12.6	10	25 Dong	8.0
93	Zr-Nb-Cu-Ni-Al	Zr	Nb	Cu	Ni	Al	57	5	15.4	12.6	10	25 Dong	12.0
94	Zr-Nb-Cu-Ni-Al	Zr	Nb	Cu	Ni	Al	54.5	7.5	15.4	12.6	10	25 Dong	5.0
95	Zr-Nb-Cu-Ni-Al	Zr	Nb	Cu	Ni	Al	52	10	15.4	12.6	10	25 Dong	
96	Zr-Ni-Cu-Al-Ag	Zr	Ni	Cu	Al	Ag	65	10	7.5	7.5	10	15Pang	2.0
97	Zr-Ti-Al-Cu-Ni	Zr	Ti	Al	Cu	Ni	57	5	10	20	8	12LU	
98	Zr-Ti-Al-Cu-Ni	Zr	Ti	Al	Cu	Ni	57	5	10	20	8	13LU	
99	Zr-Ti-Al-Cu-Ni	Zr	Ti	Al	Cu	Ni	57	5	10	20	8	19LU	
100	Zr-Ti-Al-Cu-Ni	Zr	Ti	Al	Cu	Ni	57	5	10	20	8	19 LU	
101	Zr-Ti-Al-Cu-Ni	Zr	Ti	Al	Cu	Ni	55	5	10	20	10	83 INOUE	30.0
102	Zr-Ti-Al-Cu-Ni	Zr	Ti	Al	Cu	Ni	52.5	5	12.5	20	10	83 INOUE	30.0
103	Zr-Ti-Cu-Al-Ni	Zr	Ti	Cu	Al	Ni	57	5	20	10	8	16Revesz	8.0
104	Zr-Ti-Cu-Al-Ni	Zr	Ti	Cu	Al	Ni	60	2	20	10	8	20Gebert	
105	Zr-Ti-Cu-Ni-Be	Zr	Ti	Cu	Ni	Be	41.2	13.8	12.5	10	22.5	11KIM	
106	Zr-Ti-Cu-Ni-Be	Zr	Ti	Cu	Ni	Be	42.6	12.4	11.3	10	23.8	11KIM	
107	Zr-Ti-Cu-Ni-Be	Zr	Ti	Cu	Ni	Be	41.2	13.8	12.5	10	22.5	12LU	
108	Zr-Ti-Cu-Ni-Be	Zr	Ti	Cu	Ni	Be	42.63	12.37	11.25	10	23.75	12LU	
109	Zr-Ti-Cu-Ni-Be	Zr	Ti	Cu	Ni	Be	44	11	10	10	25	12LU	
110	Zr-Ti-Cu-Ni-Be	Zr	Ti	Cu	Ni	Be	45.38	9.62	8.75	10	26.25	12LU	
111	Zr-Ti-Cu-Ni-Be	Zr	Ti	Cu	Ni	Be	46.25	8.25	7.5	10	27.5	12LU	
112	Zr-Ti-Cu-Ni-Be	Zr	Ti	Cu	Ni	Be	41.2	13.8	12.5	10	22.5	13LU	
113	Zr-Ti-Cu-Ni-Be	Zr	Ti	Cu	Ni	Be	41.2	13.8	12.5	10	22.5	2LI	
114	Zr-Ti-Cu-Ni-Be	Zr	Ti	Cu	Ni	Be	42.6	12.4	11.3	10	23.8	11KIM	
115	Zr-Ti-Cu-Ni-Be	Zr	Ti	Cu	Ni	Be	41.2	13.8	12.5	10	22.5	9 Peker	25.0
116	Zr-Ti-Ni-Cu-Be	Zr	Ti	Ni	Cu	Be	38.5	16.5	9.75	15.25	20	12LU	
117	Zr-Ti-Ni-Cu-Be	Zr	Ti	Ni	Cu	Be	39.88	15.12	9.98	13.77	21.25	12LU	

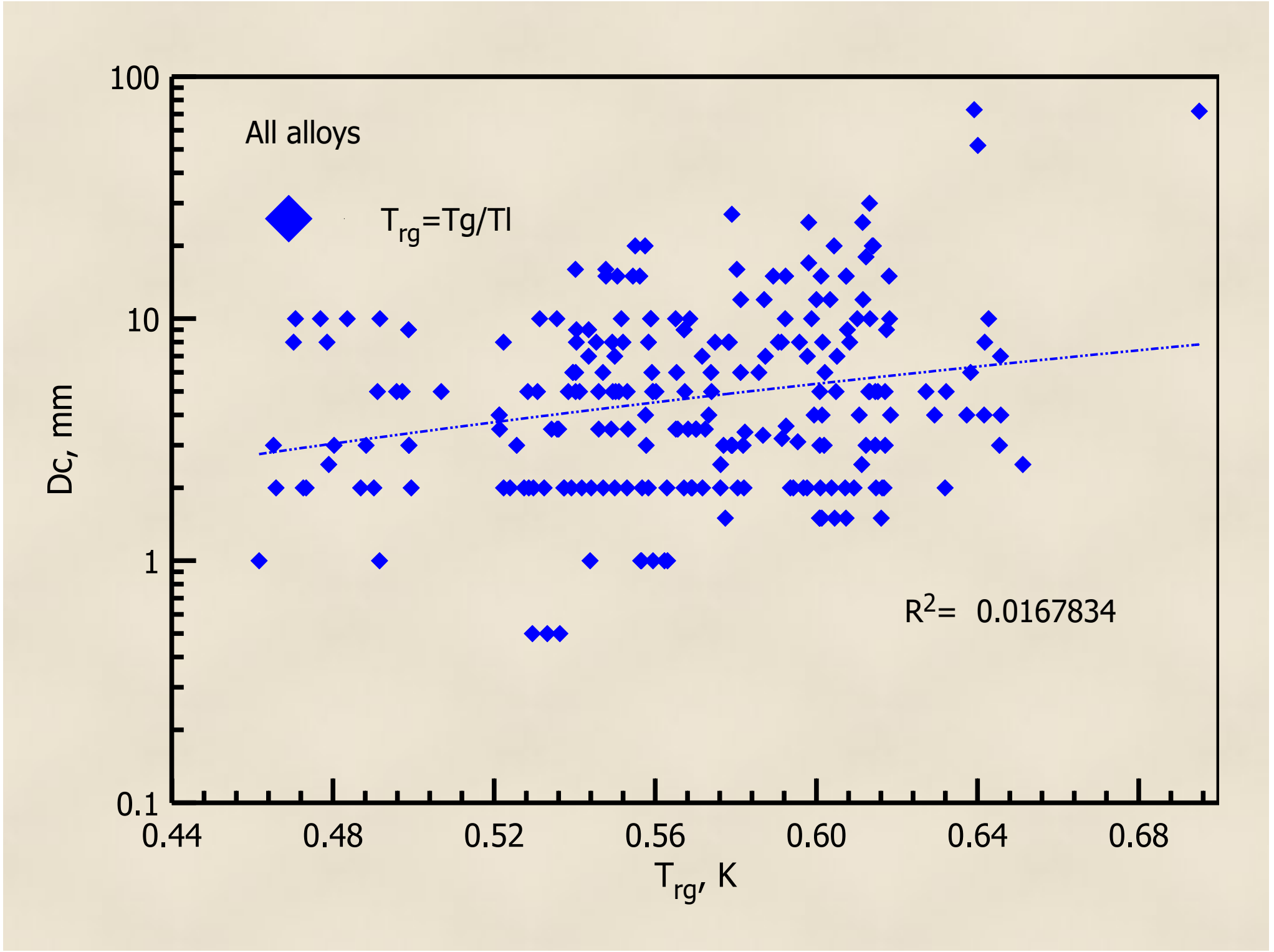
All alloys
T_{rg}=Tg/Tl
R^2= 0.0167834
Dc, mm
100
10
1
0.1
0.44
0.48
0.52
0.56
0.60
0.64
0.68
T_{rg}, K

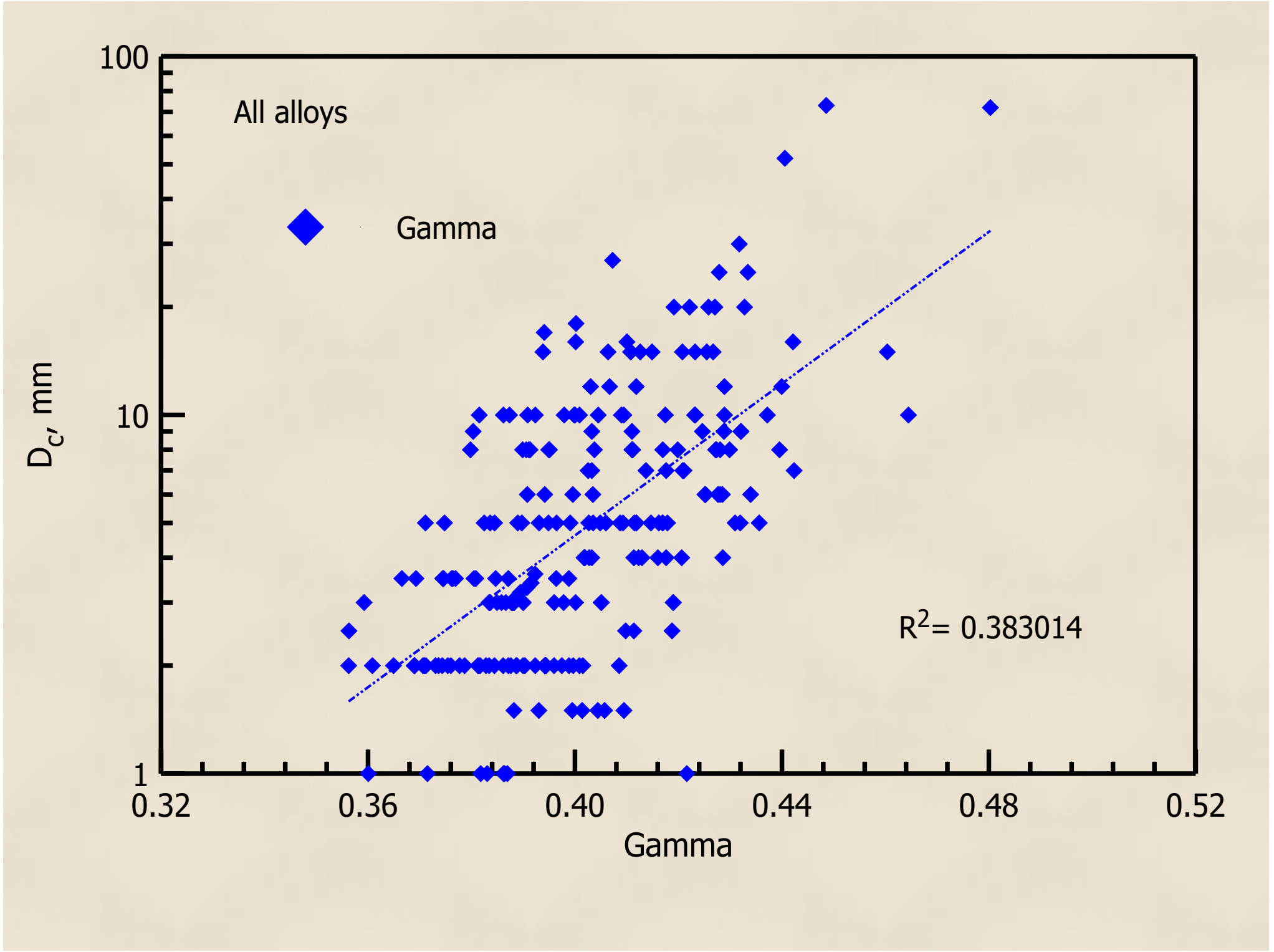
All alloys
Gamma
D_c, mm
100
10
1
0.32
0.36
0.40
0.44
0.48
0.52
Gamma
R^2= 0.383014

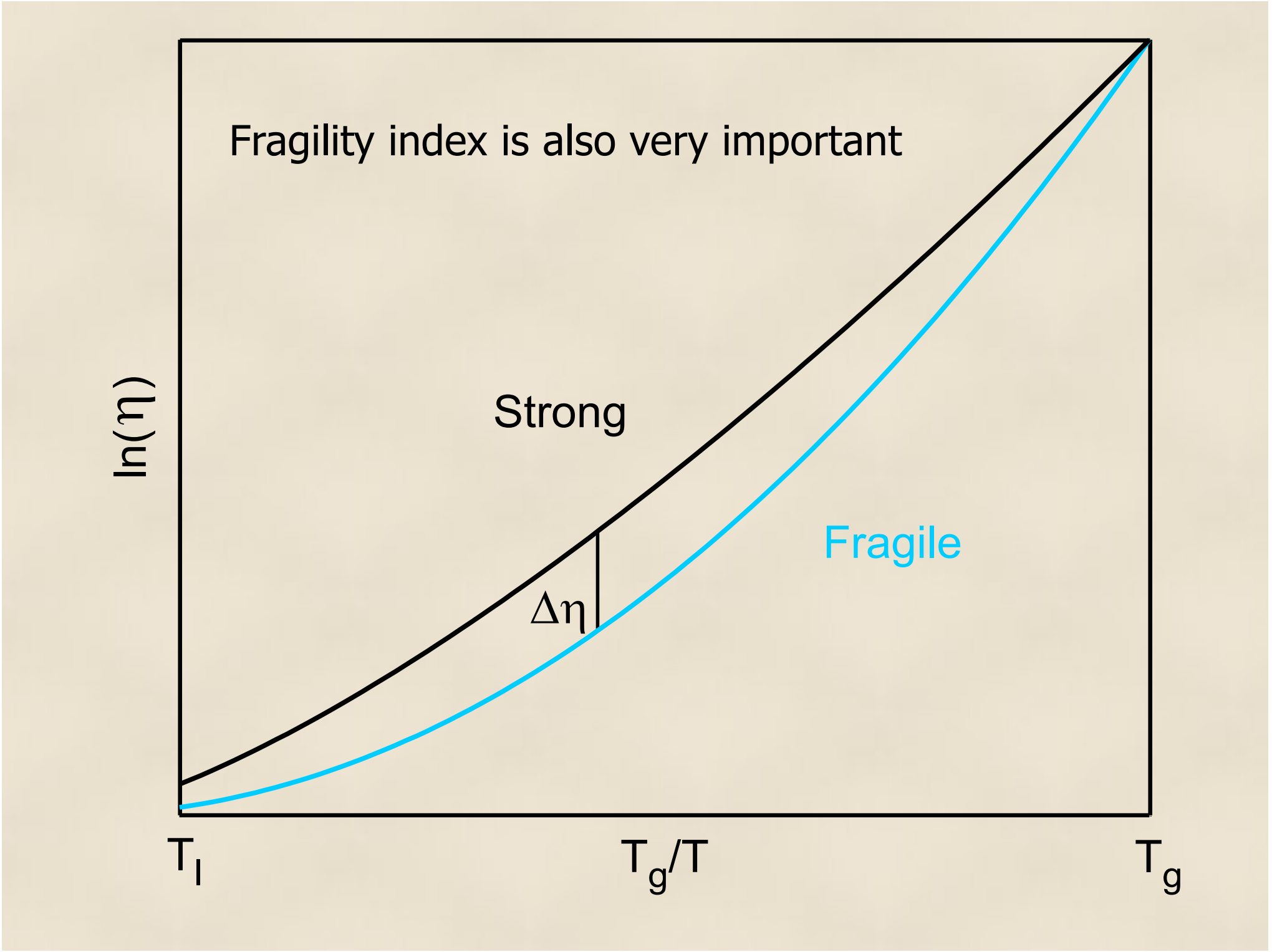
Fragility index is also very important
ln(η)
Strong
Fragile
Δη
T_l
T_g/T
T_g

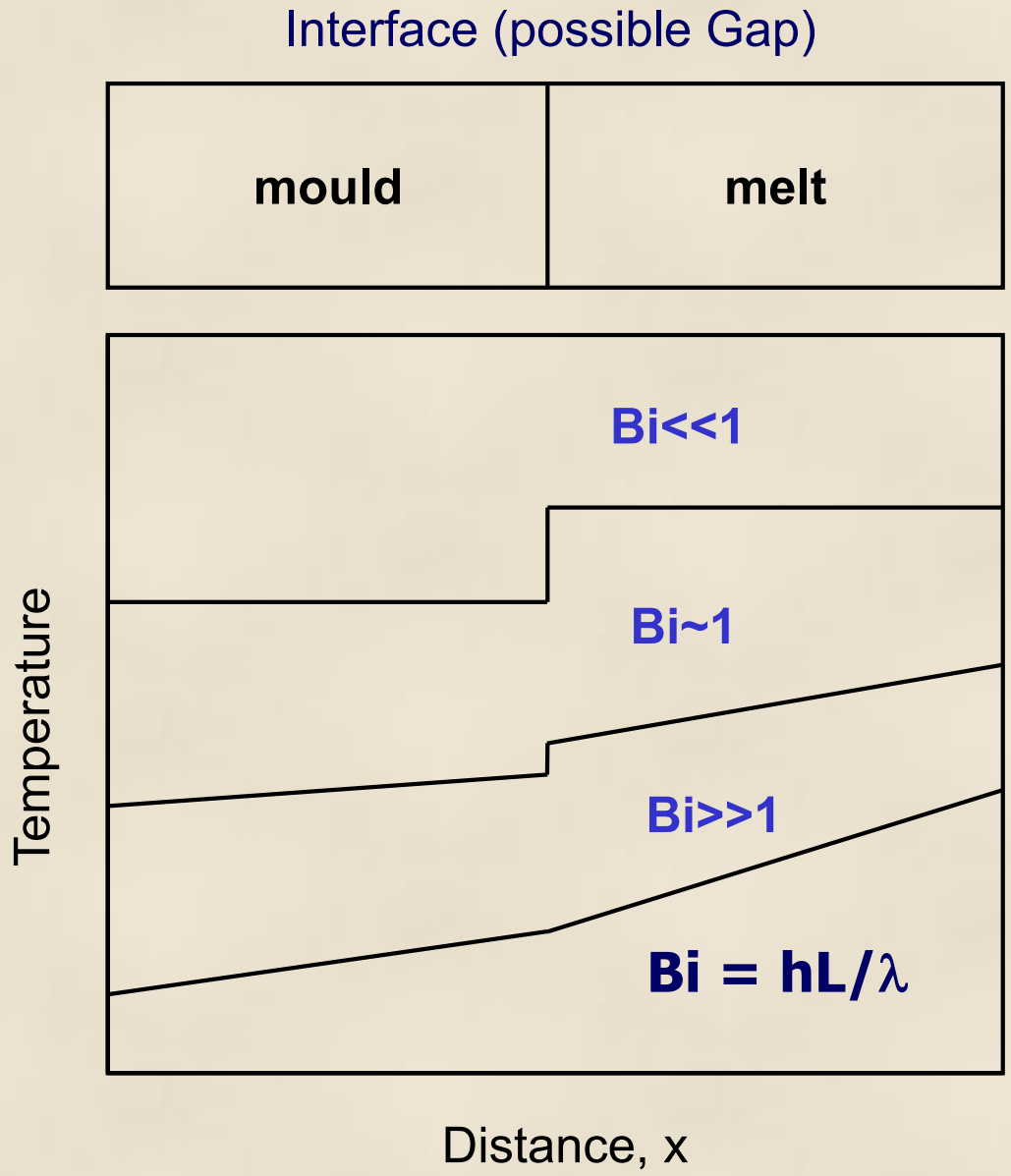

Within the melt

$$\frac{dQ}{dt} = -\lambda A \frac{dT}{dx}$$

Q is the heat flow, t is time,
λ is a thermal conductivity,
A is the transversal area,
dT/dx is the temperature gradient in the body through which the heat is passing.

At the interface

$$dQ/dt = h*A*\Delta T$$

h-heat transfer coefficient;
A - interfacial area

D. V. Louzguine-Luzgin, D. B. Miracle, A. Inoue "Intrinsic and extrinsic factors influencing the glass-forming ability of alloys" Advanced Engineering Materials, Vol. 10, N: 11, (2008) pp. 1008-1015

Influence of flux treatment. Flux B_2O_3

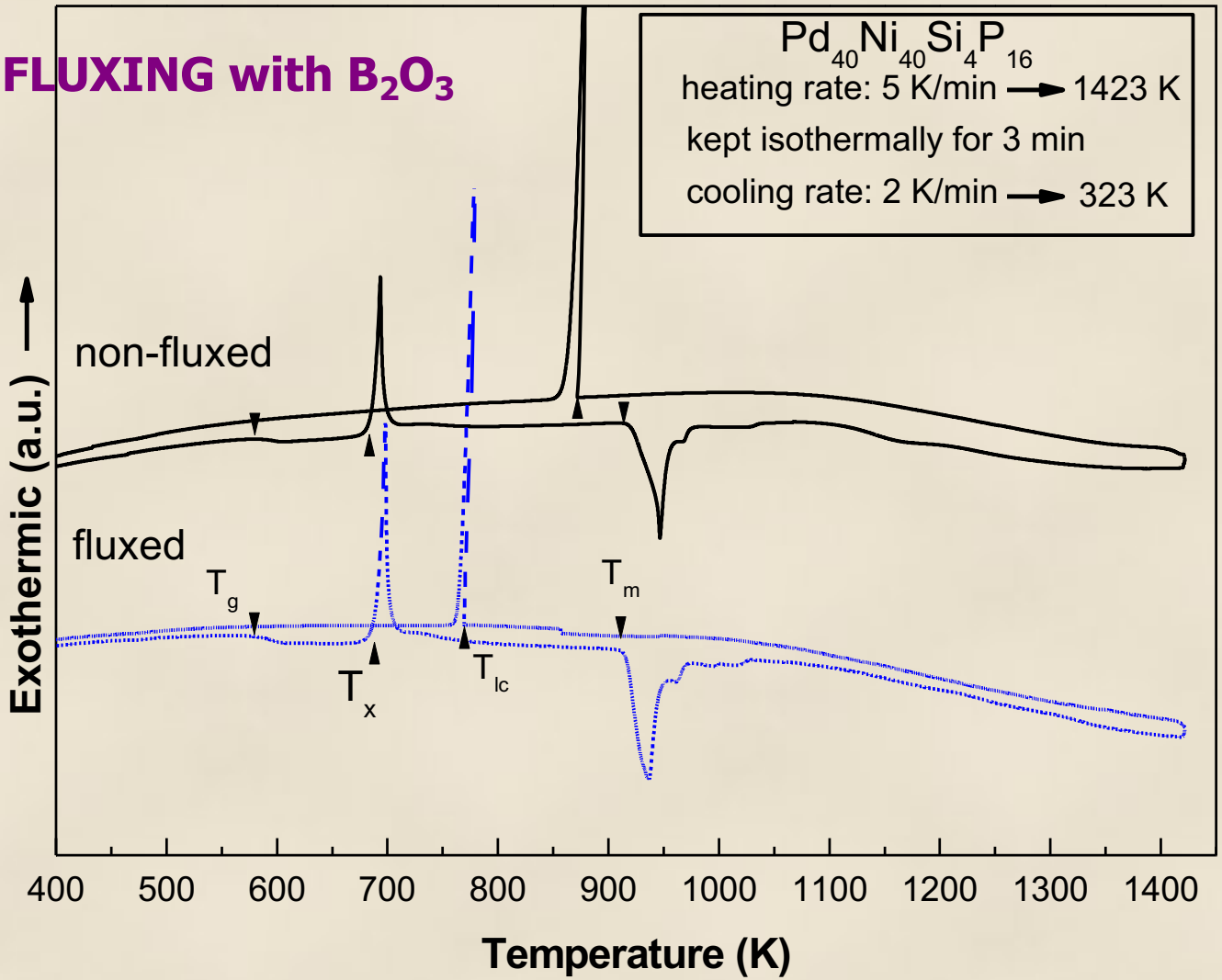

N. Chen, L. Gu, G. Q. Xie, D. V. Louzguine-Luzgin, A. R. Yavari, G. Vaughan, S. D. Imhoff, J. H. Perepezko, T. Abe and A. Inoue, "Flux-induced structural modification and phase transformations in a $Pd_{40}Ni_{40}Si_4P_{16}$ bulk-glassy alloy" Acta Materialia, Vol. 58, N: 18, (2010), pp. 5886-5897.

Groups of Purely Extrinsic Factors influencing the GFA are**:**

1. Modify **melt-mould heat transfer coefficient h(T,P…)** depending upon melting **temperature and pressure** as well as upon **chamber pressure and atmosphere**.

2. Cause **heterogeneous nucleation**

cleanness of the melt from contaminations (like Si, O, Cl), oxides and inclusions, which cause **heterogeneous nucleation**. For example, **flux treatment** causes a rather homogeneous nucleation instead of heterogeneous one or reduces the nucleation rate in case of heterogeneous nucleation as well as an external **alternating electromagnetic field** does, etc... Interfacial energy between the Cu mould and the melt - possibility of heterogeneous nucleation on the surface of Cu mould reduces the GFA.

It is likely that the observed GFA is mainly limited by extrinsic factors not intrinsic.

Very good plasticity of $Ni_{52.5}Zr_{15}Nb_{10}Ti_{15}Pt_{7.5}$ in SQL region

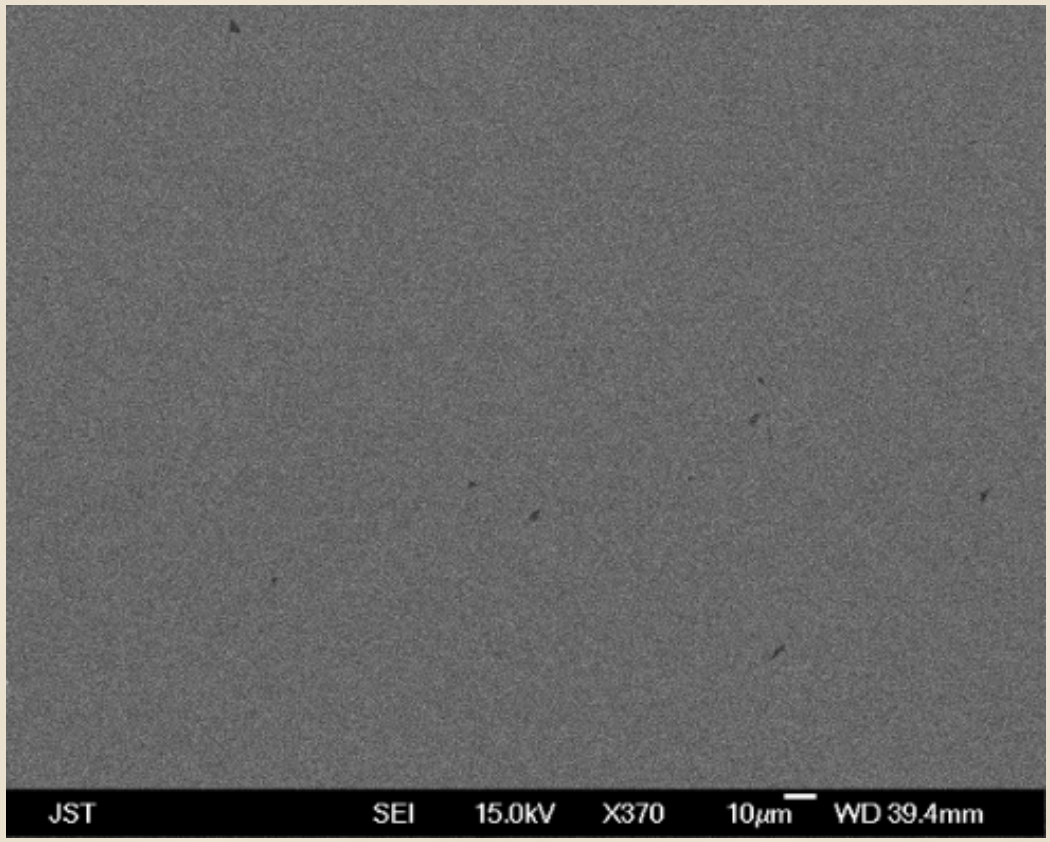

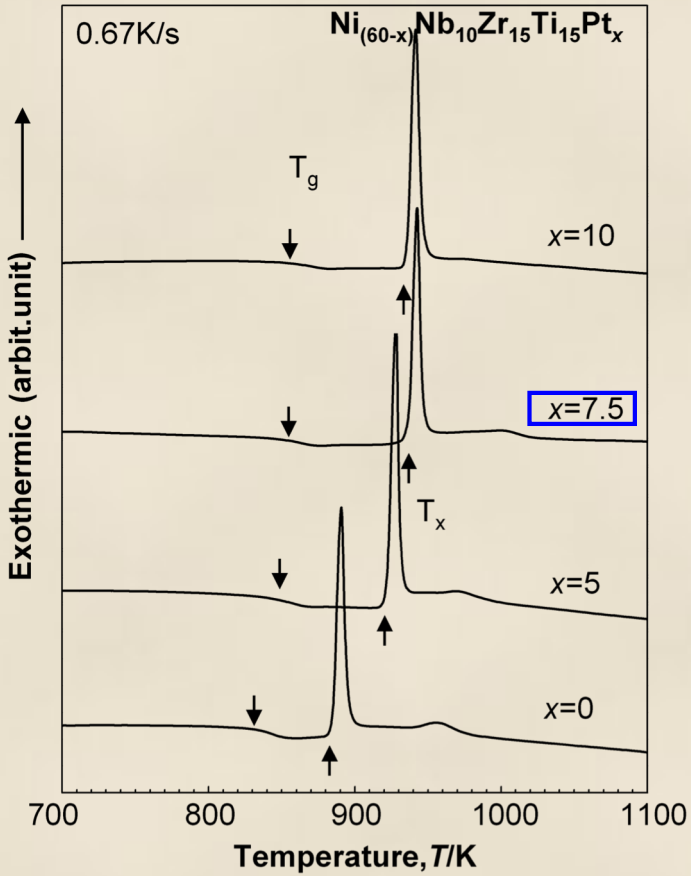

Spark plasma sintering at 773 K, >99.5 % density

G. Xie, D. V. Louzguine-Luzgin, H. M. Kimura and A. Inoue "Nearly full density $Ni_{52.5}Nb_{10}Zr_{15}Ti_{15}Pt_{7.5}$ bulk metallic glass obtained by spark plasma sintering of gas atomized powders" Applied Physics Letters, 90, (2007) 241902.

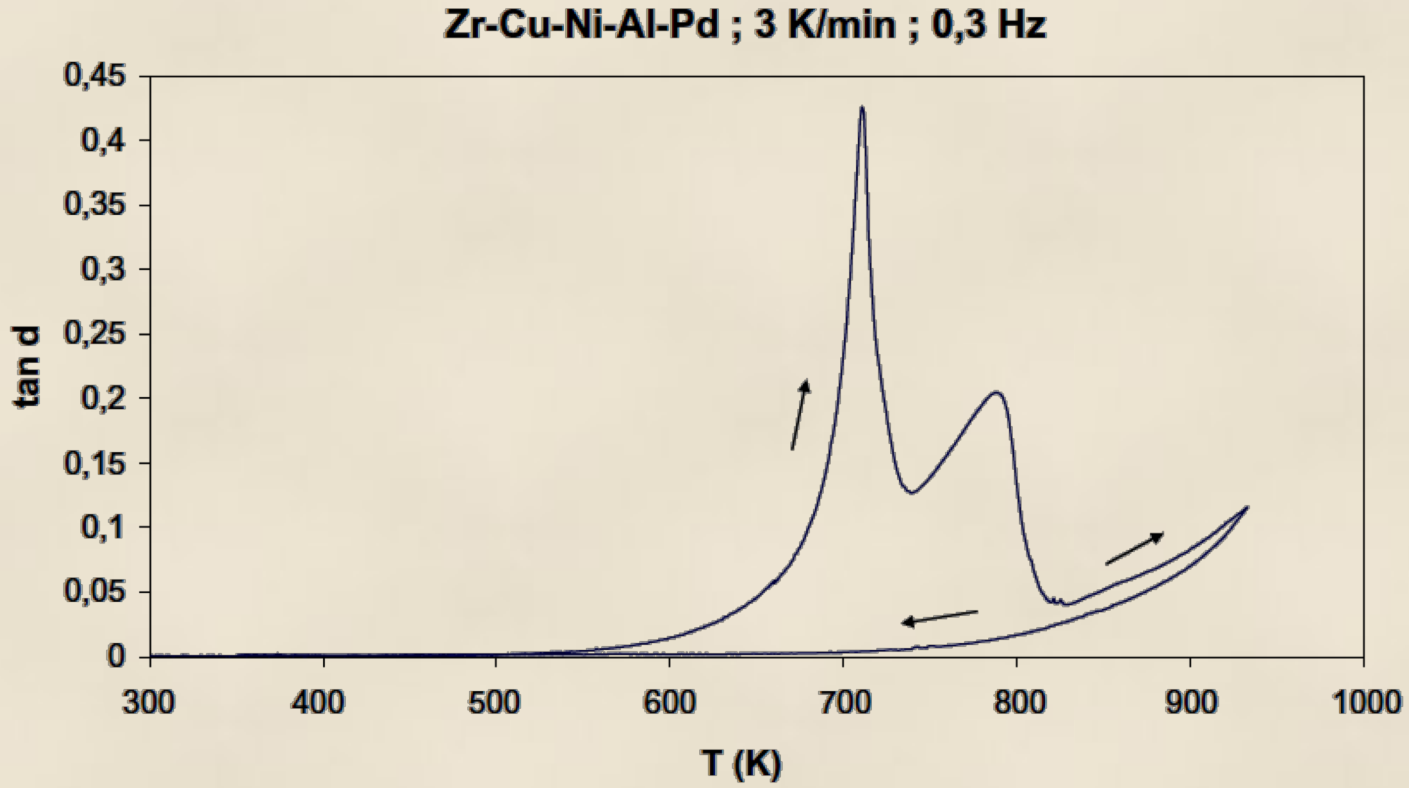

Relaxation: material response to an action with time

J.-M. Pelletier, D. V. Louzguine-Luzgin, S. Li and A. Inoue "Elastic and viscoelastic properties of glassy, quasicrystalline and crystalline phases in $Zr_{65}Cu_5Ni_{10}Al_{7.5}Pd_{12.5}$ alloys" Acta Materialia Vol. 59, N: 7, (2011), pp. 2797-2806.

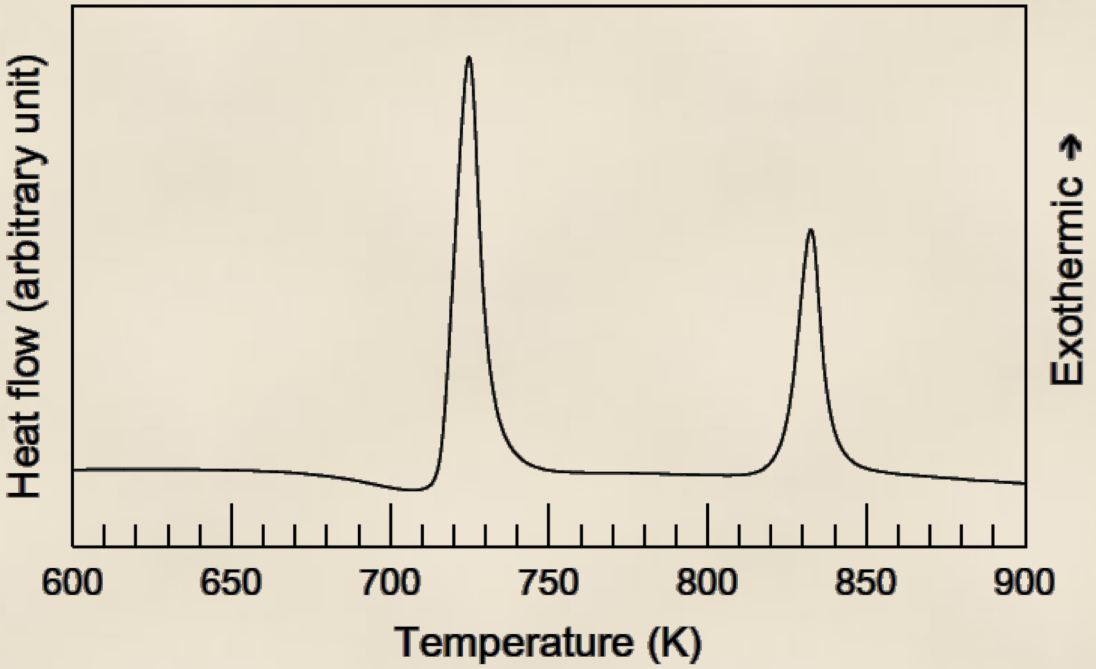

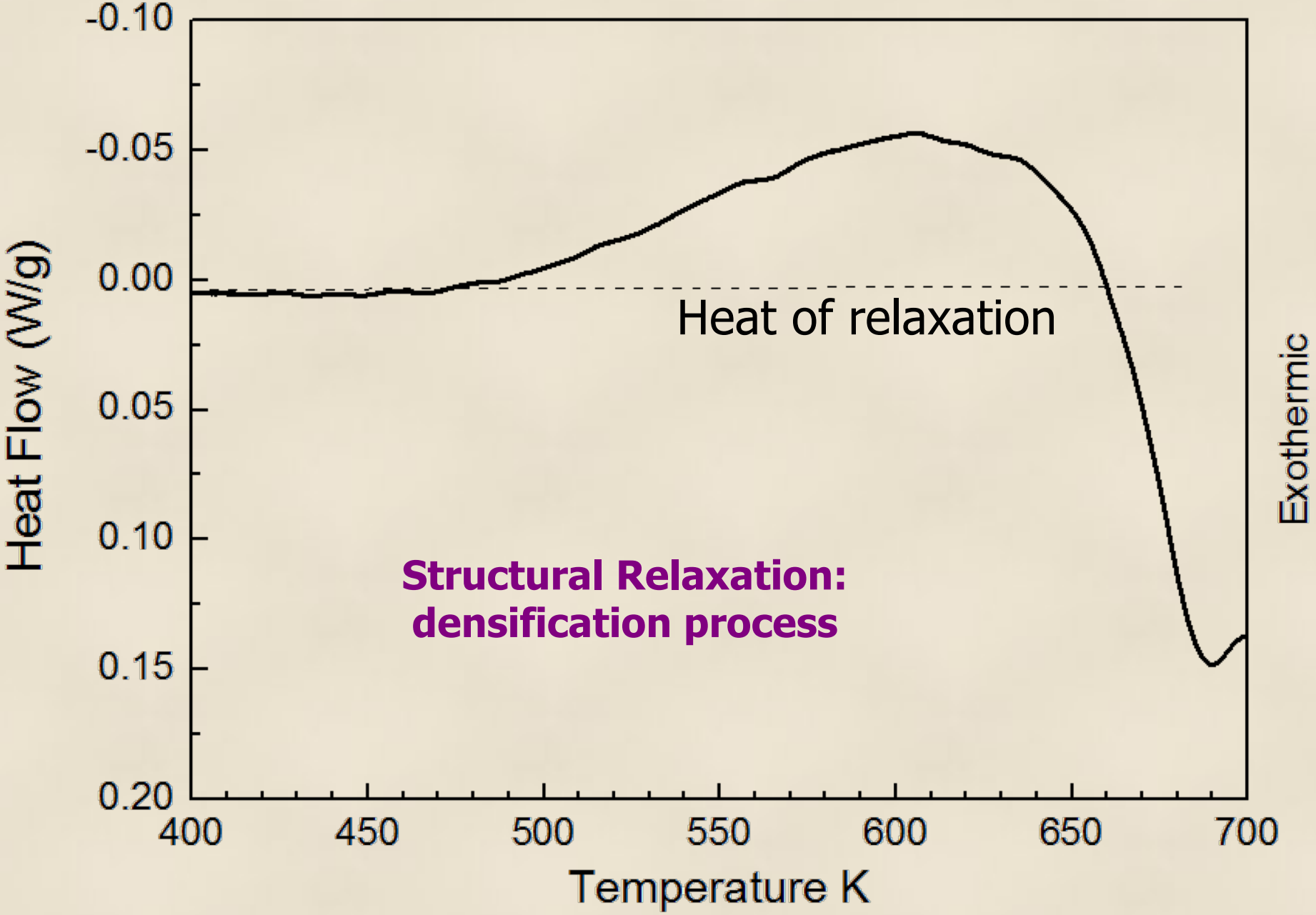
-0.10
-0.05
0.00
0.05
0.10
0.15
0.20
Heat Flow (W/g)
Exothermic
Heat of relaxation
Structural Relaxation:
densification process
400
450
500
550
600
650
700
Temperature K

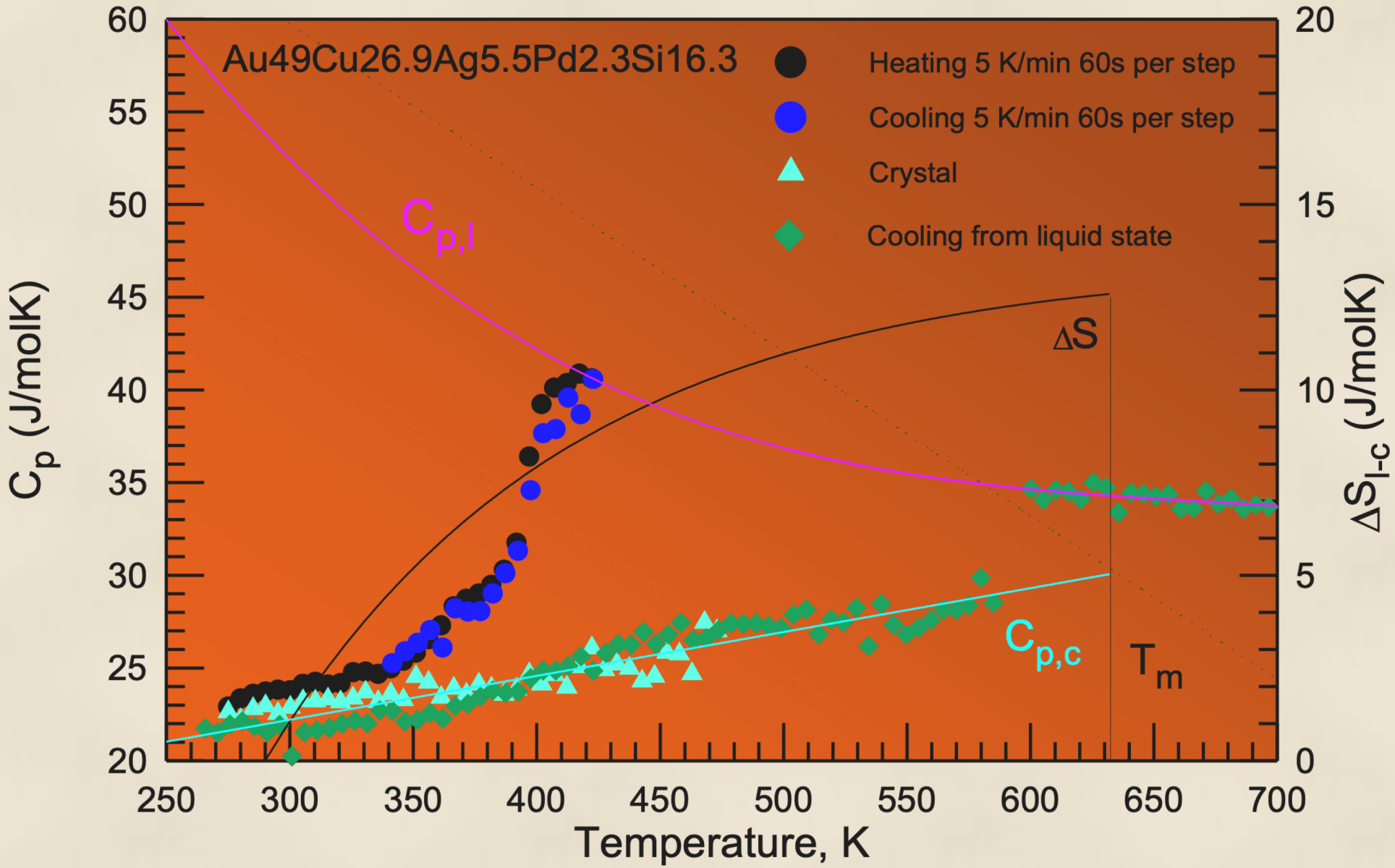

D. V. Louzguine-Luzgin, I. Seki, S. V. Ketov, L. V. Louzguina-Luzgina, V. I. Polkin, N. Chen, H. Fecht, A. N. Vasiliev, H. Kawaji, “Glass-transition process in an Au-based metallic glass”, Journal of Non-Crystalline Solids, Vol. 419, (2015), 12–15.

In order to minimize the kinetic effects associated with structural relaxation upon continuous heating, we measured the specific heat capacity in **a step scan mode.**
A double-stage transformation is observed

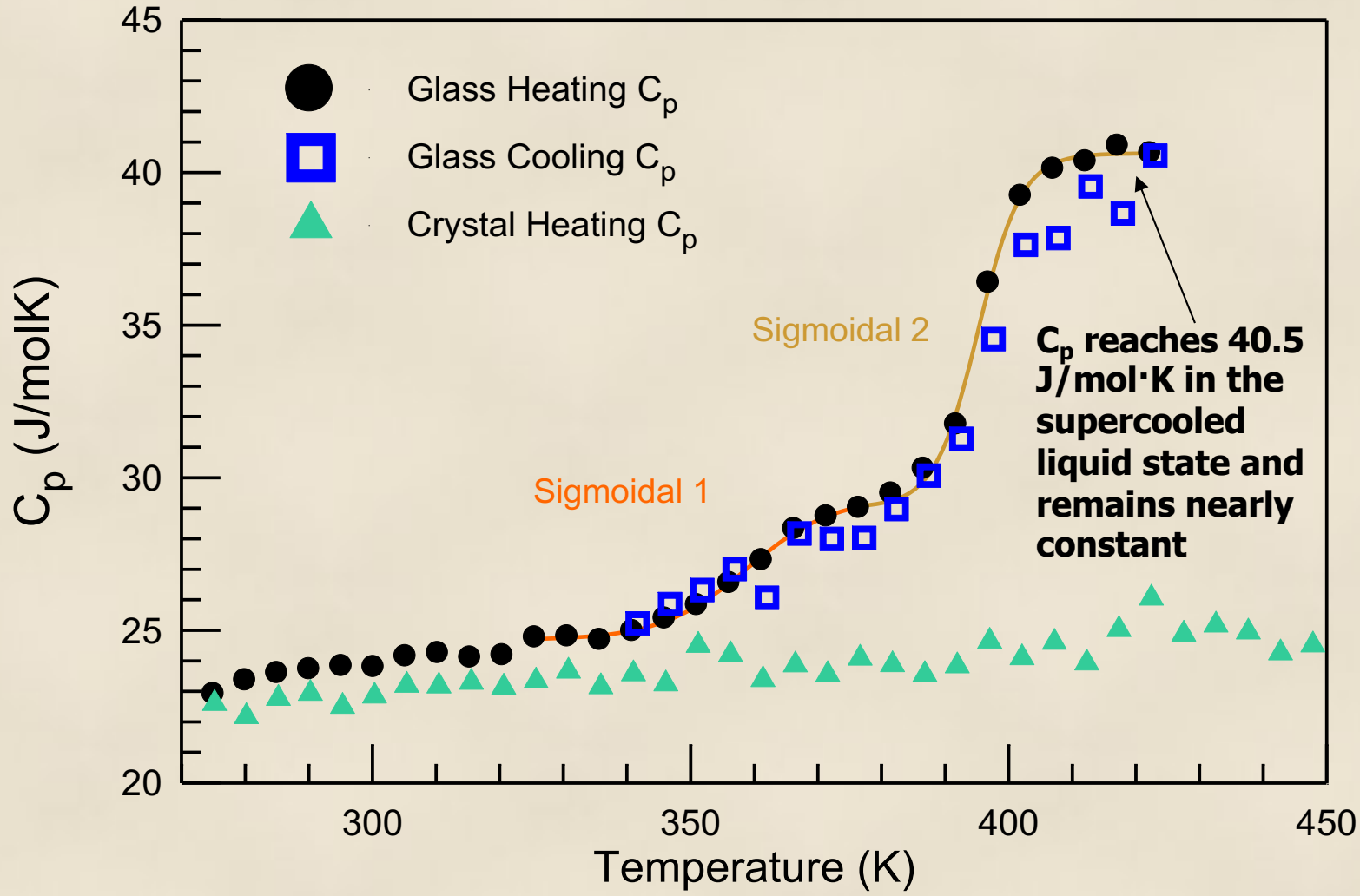

C_p of glassy and crystalline phases measured on heating and on cooling. The heating and cooling rates were 83 mK/s. The annealing time between each heating or cooling step was 60 s.

Devitrification

(**crystallization**)
of metallic glasses on heating

1. Primary
2. Eutectic
3. Polymorphous
4. Binodal or Spinodal

Takes place owing to
thermodynamical instability
of metallic glasses which posses higher free energy
compared to crystalline phase(s).
Driving force – free energy difference.

Some glasses devitrify even at room temperature.

Nucleation and Growth Rates as a F(T)
Undercooling/overheating

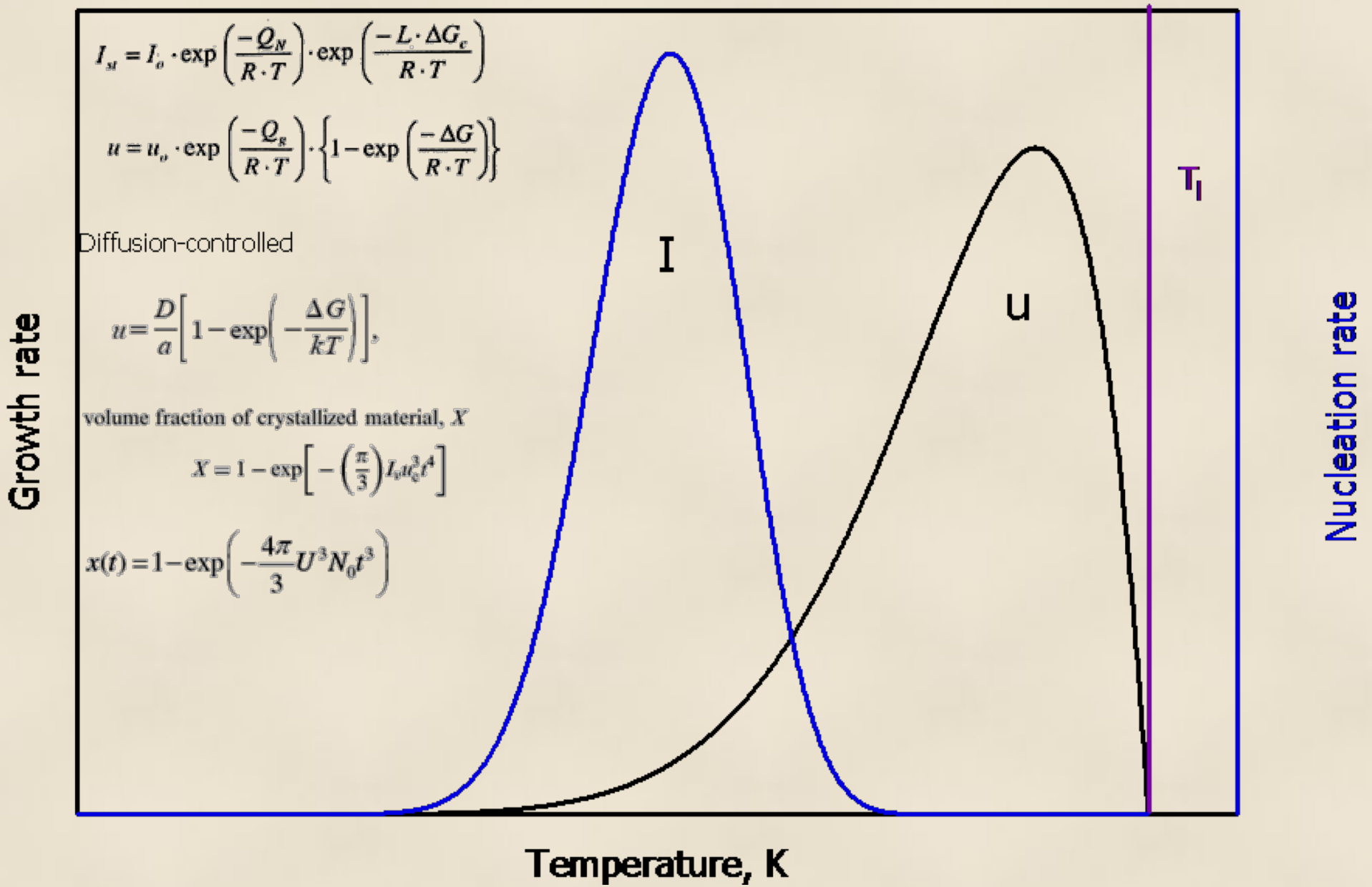

Primary crystallization

$Ti_{50}Ni_{20}Cu_{23}Sn_7$

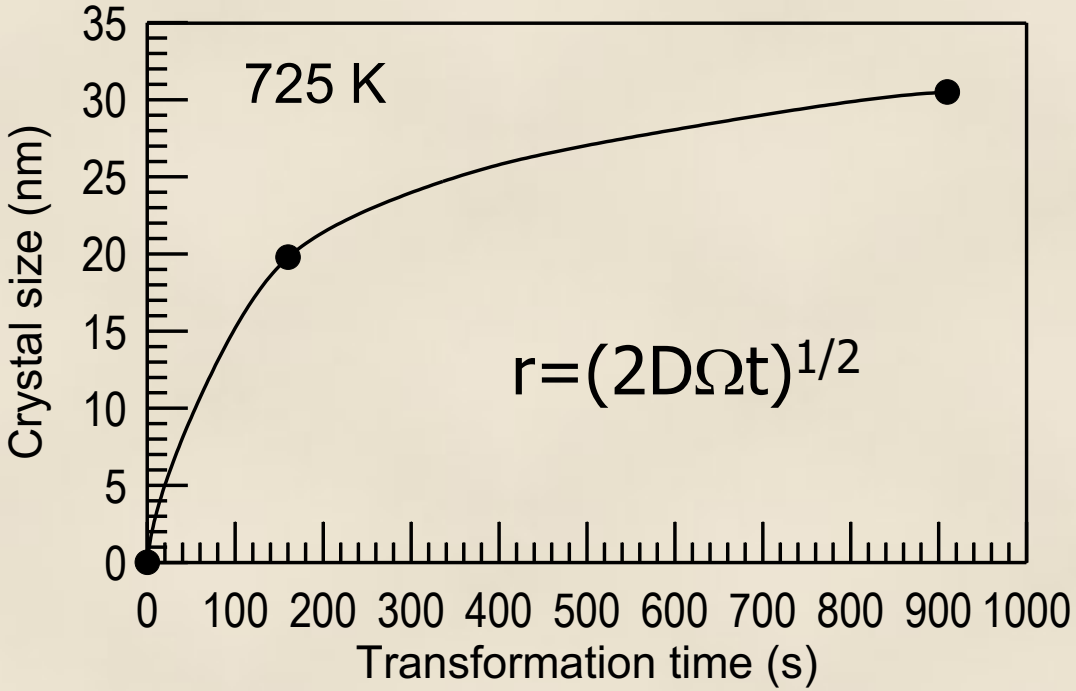

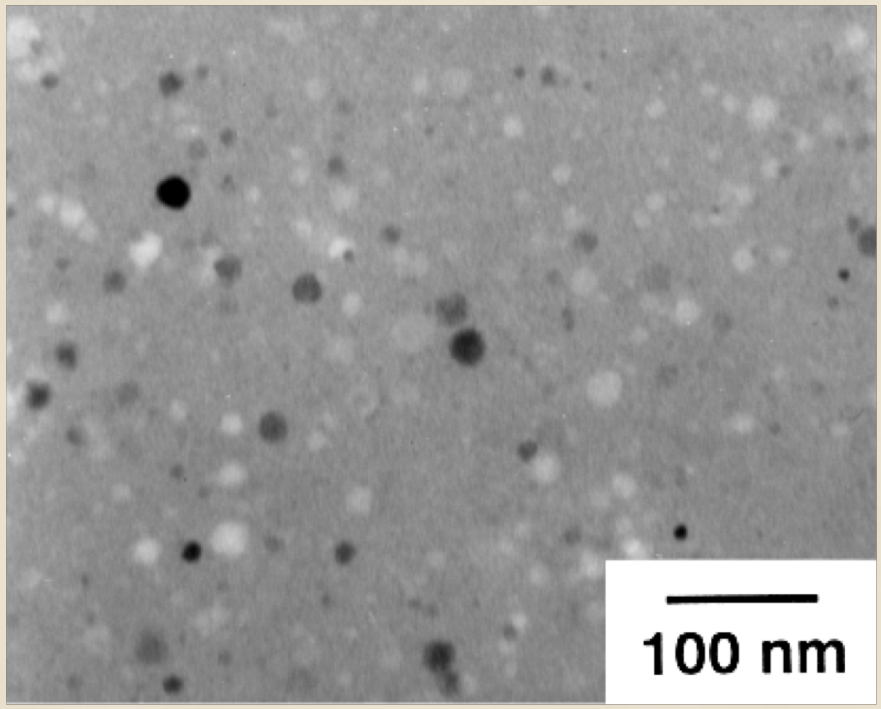

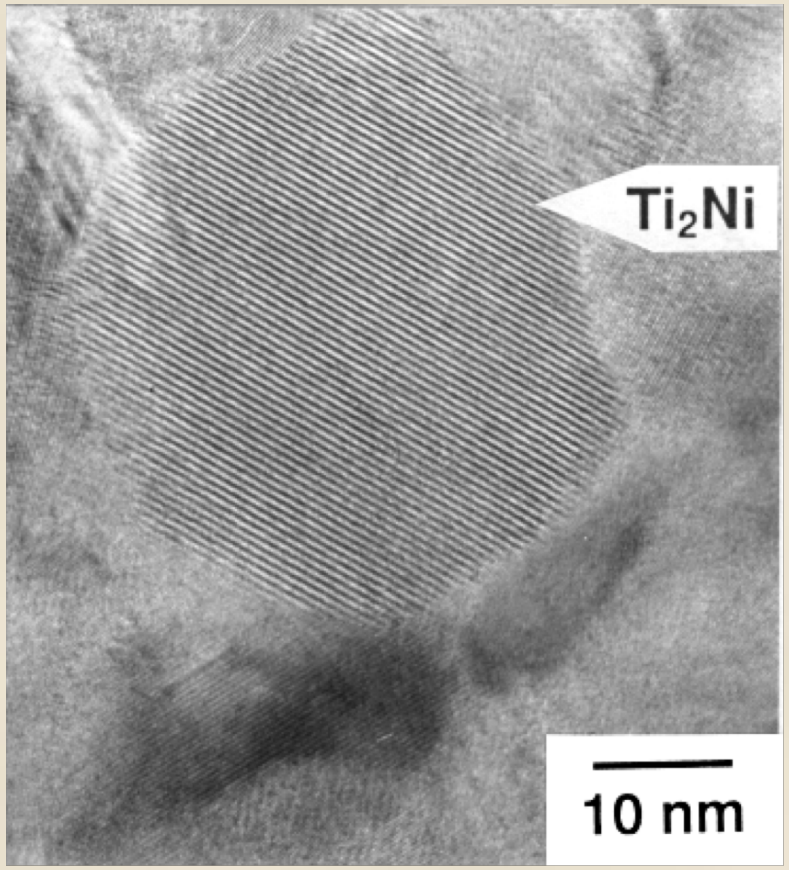

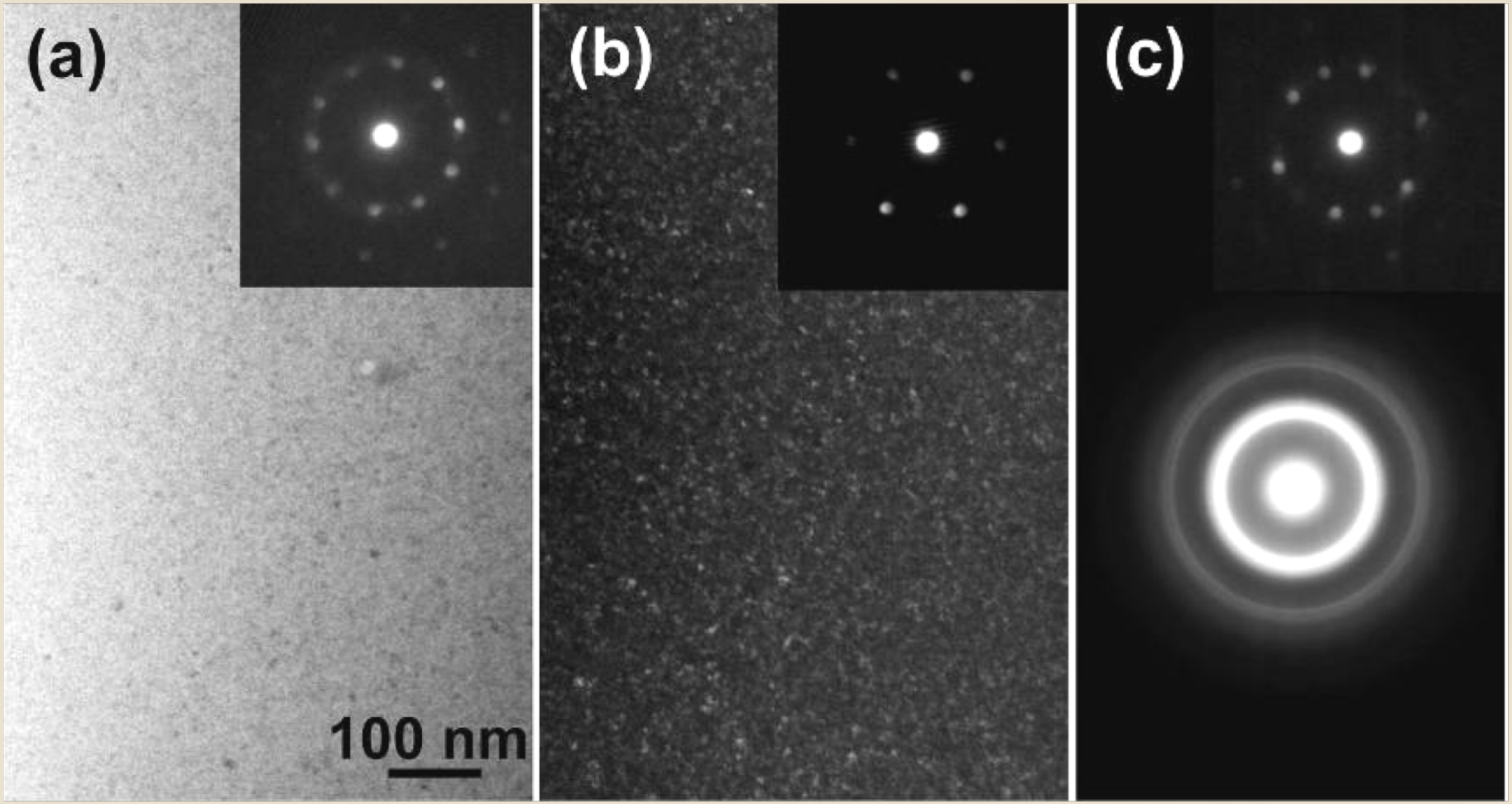

$Cu_{55}Zr_{30}Ti_{10}Pd_5$ alloy annealed for 2 ks at 750 K TEM

D. V. Louzguine and A. Inoue ”Nanoparticles with icosahedral symmetry in Cu-based bulk glass former induced by Pd addition” Scripta Materialia, 48, N: 9, (2003) 1325

$Cu_{55}Zr_{30}Ti_{10}Pd_5$

Differential isothermal calorimetry

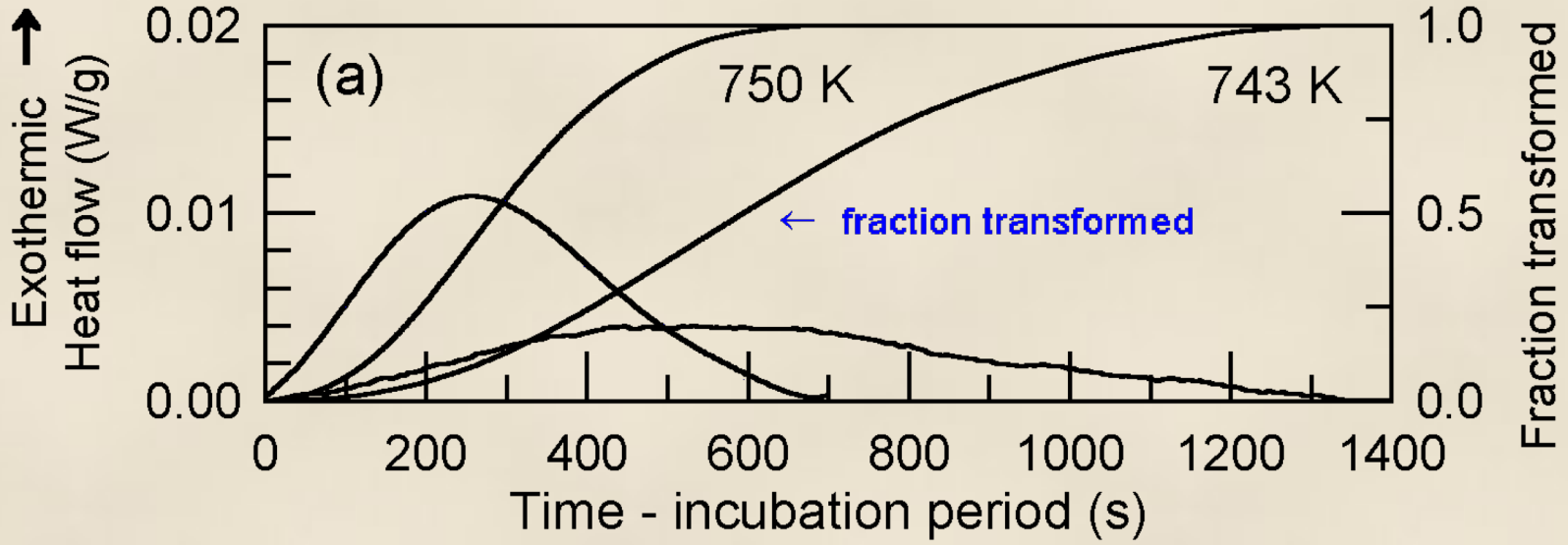

$x(t) = 1 - \exp[-Kt^n]$ $\ln[\ln(1/(1-x)] = \ln(K) + n\ln(t)$

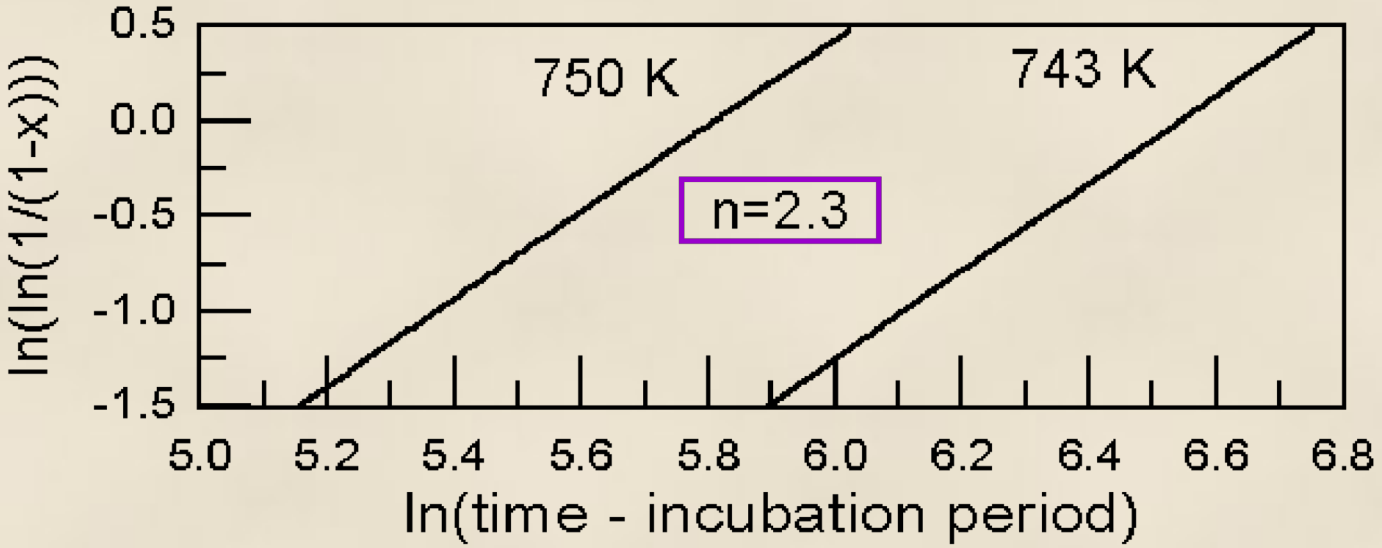

D. V. Louzguine-Luzgin, A. Inoue, D. Nagahama, and K. Hono "Composition and structure of Cu-based nanoicosahedral phase in Cu-Zr-Ti-Pd alloy" Applied Physics Letters Vol. 87, (2005) pp. 211918

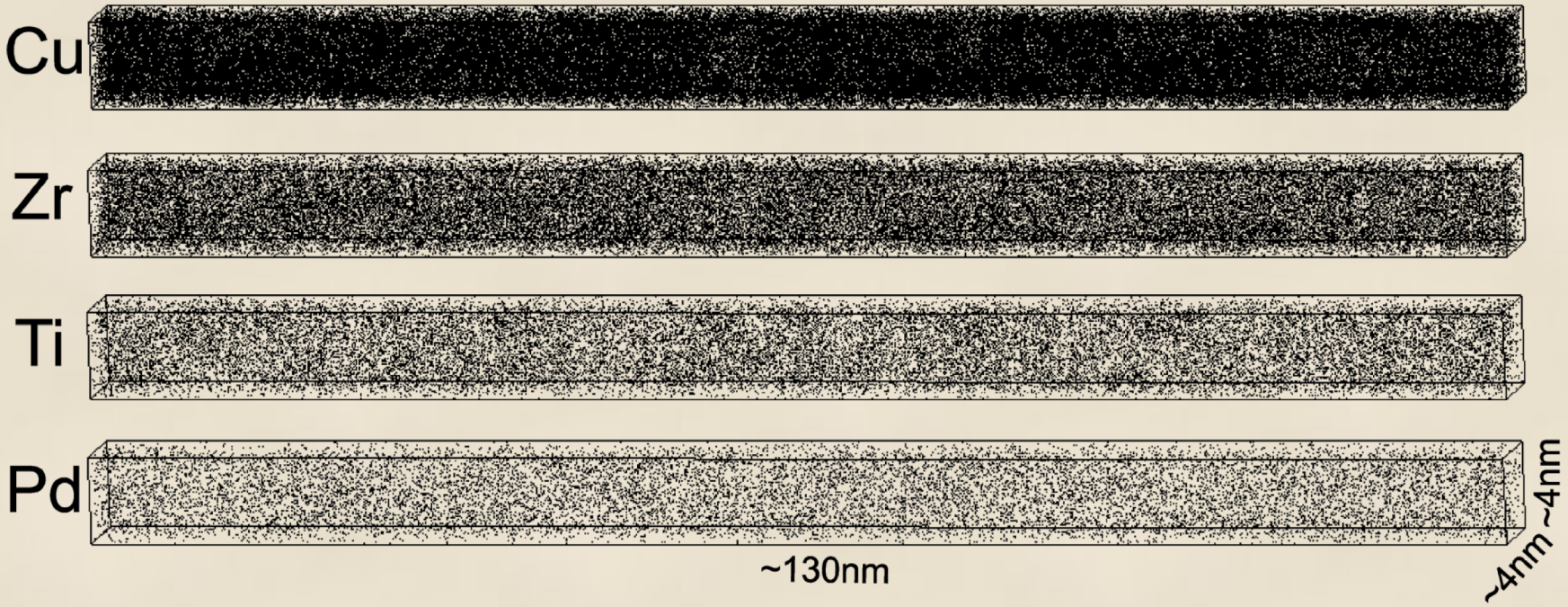

Atom map for the $\mathbf{Cu_{55}Zr_{30}Ti_{10}Pd_5}$ alloy sample after annealing at 785 K for 600 s.

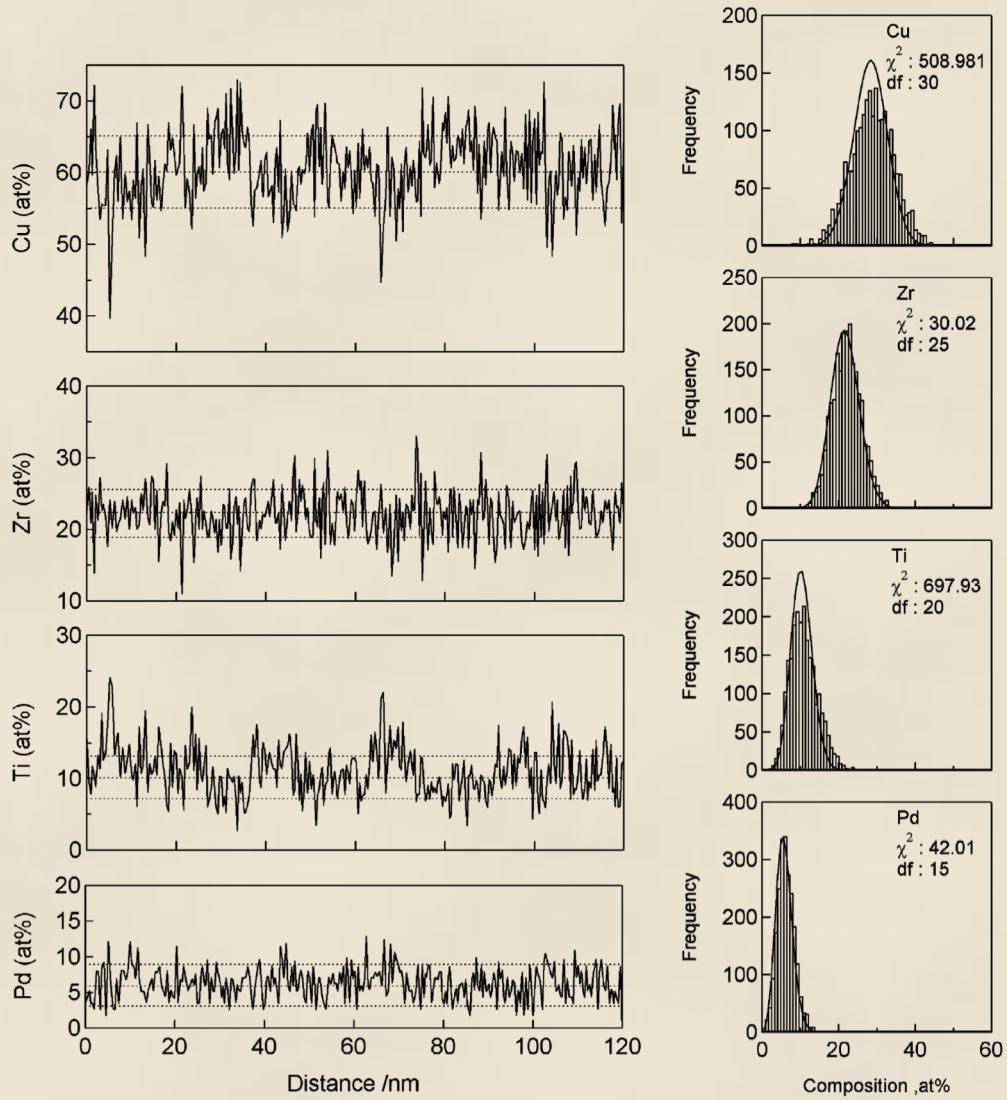

Atom probe concentration depth profiles for different alloying elements obtained from the **$Cu_{55}Zr_{30}Ti_{10}Pd_5$** sample after annealing at 785 K for 600 s and the concentration frequency distribution diagrams.

Polymorphous (rear case for BMGs) $Ti_{50}Ni_{25}Cu_{25}$ Ti(Ni,Cu)

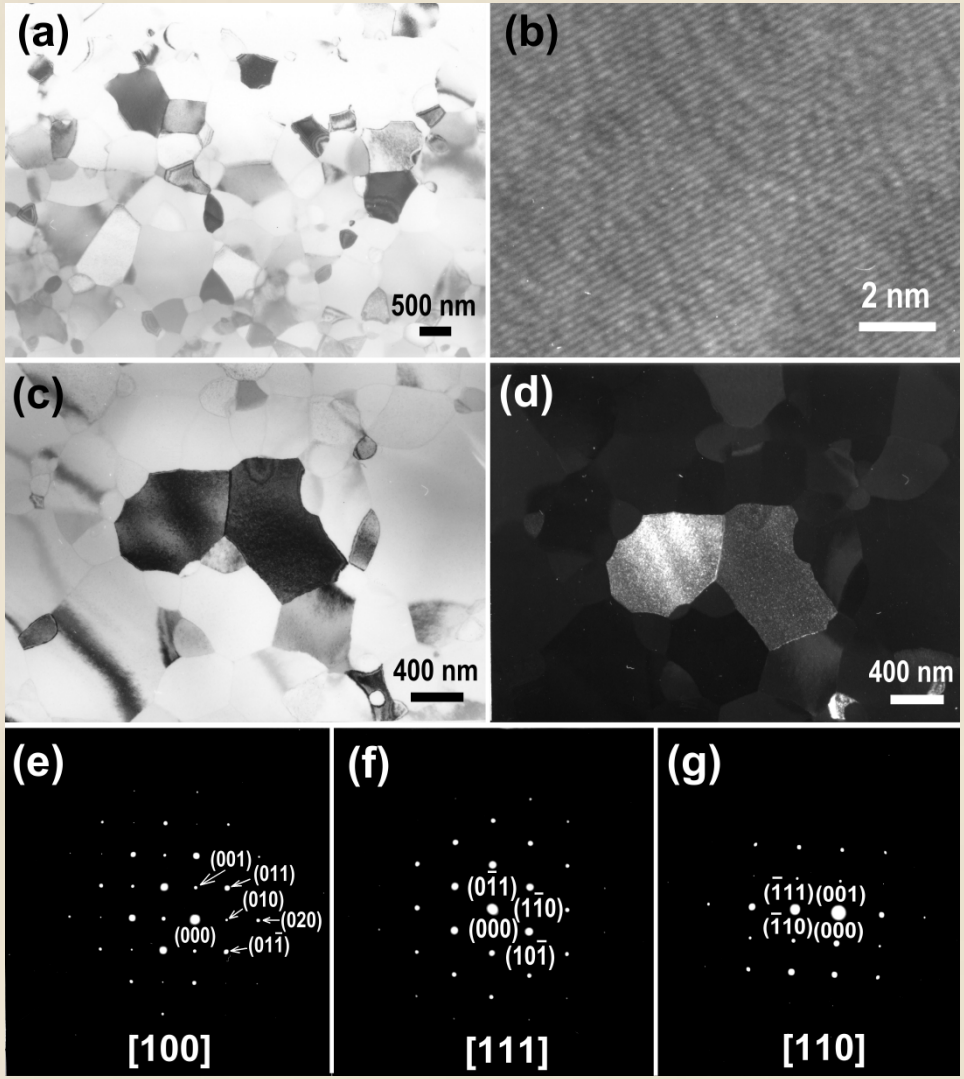

Linear growth
$r = M'\Omega t$

D. V. Louzguine and A. Inoue, "Crystallization behavior of $Ti_{50}Ni_{25}Cu_{25}$ amorphous alloy" Journal of Materials Science, Vol. 35, N: 16 (2000) pp. 4159-4164.

Eutectic

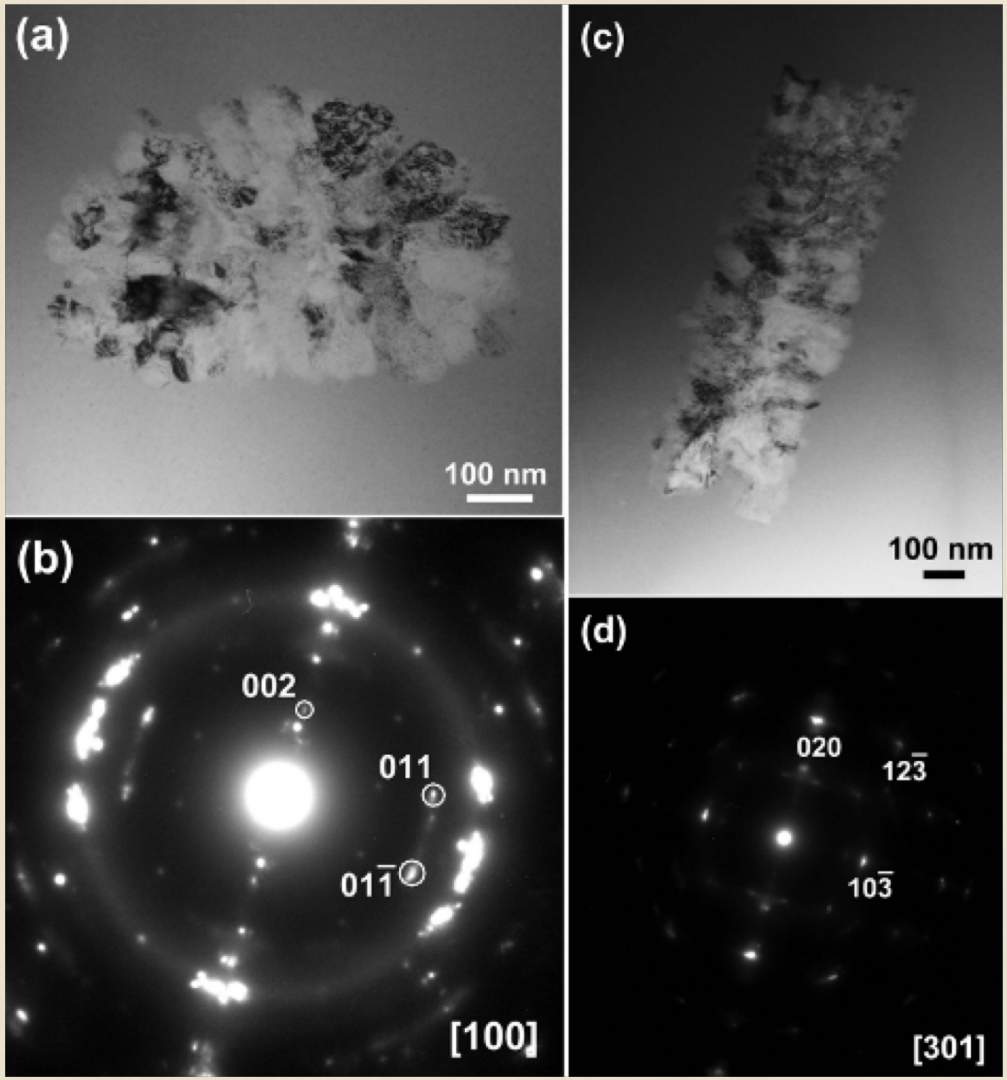

D. V. Louzguine-Luzgin, G. Xie, Q. Zhang and A. Inoue "Effect of Fe on the glass-forming ability, structure and devitrification behavior of Zr-Cu-Al bulk glass-forming alloys" Philosophical Magazine, Vol. 90, N: 14, (2010), pp. 1955–1968.

(a,c) Bright-field images and (b,d) corresponding selected-area electron diffraction patterns taken from the eutectic colonies (central objects in (a and b)) in $Zr_{62.5}Cu_{22.5}Al_{10}Fe_5$ glassy sample annealed at 713 K for 600 s, TEM. Selected reflections in (b) belong to Zr_2Cu phase Most of reflections in (d) belong to Zr_2Cu phase. Visible camera length in (b and d) is different.

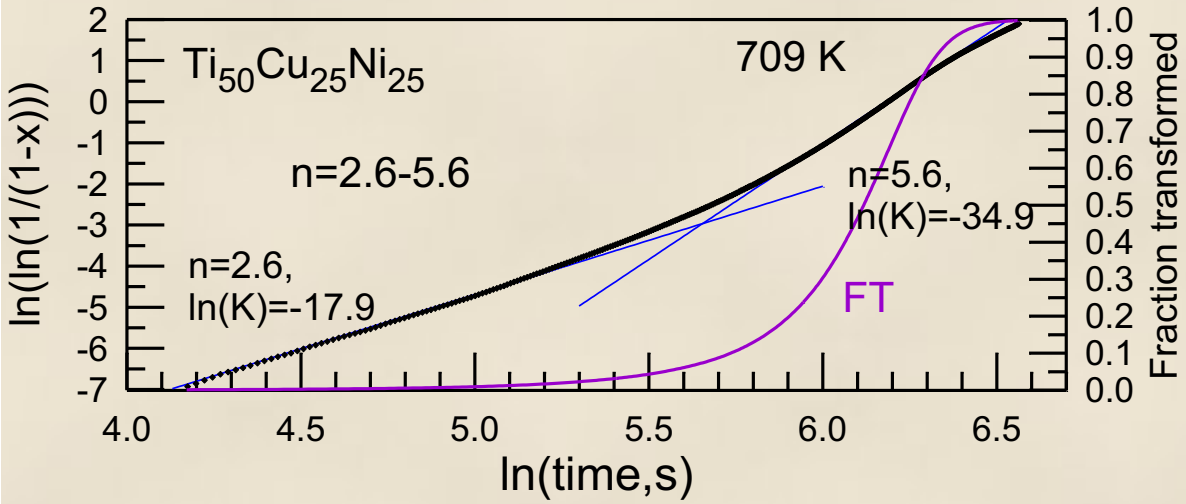

Surface and heterogeneous nucleation at the early stages. After that cite saturation

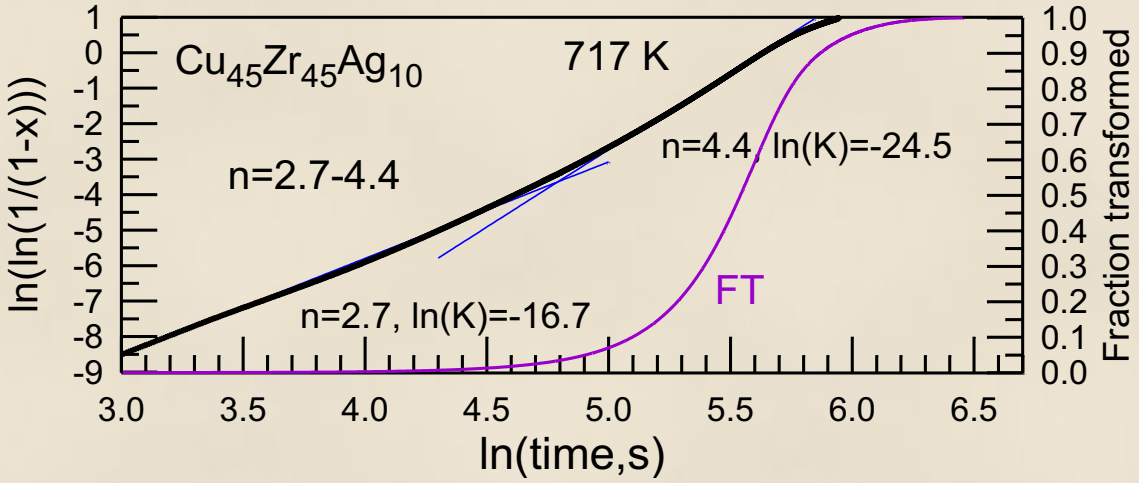

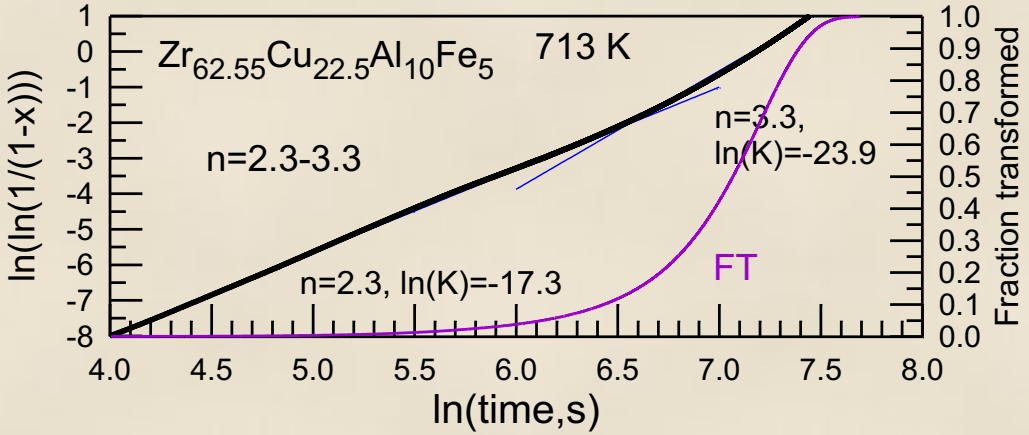

D. V. Louzguine-Luzgin, "Early stage crystallization kinetics in metallic glass-forming alloys", Journal of Alloys and Compounds Vol. 586, (2014), pp. 216–219.

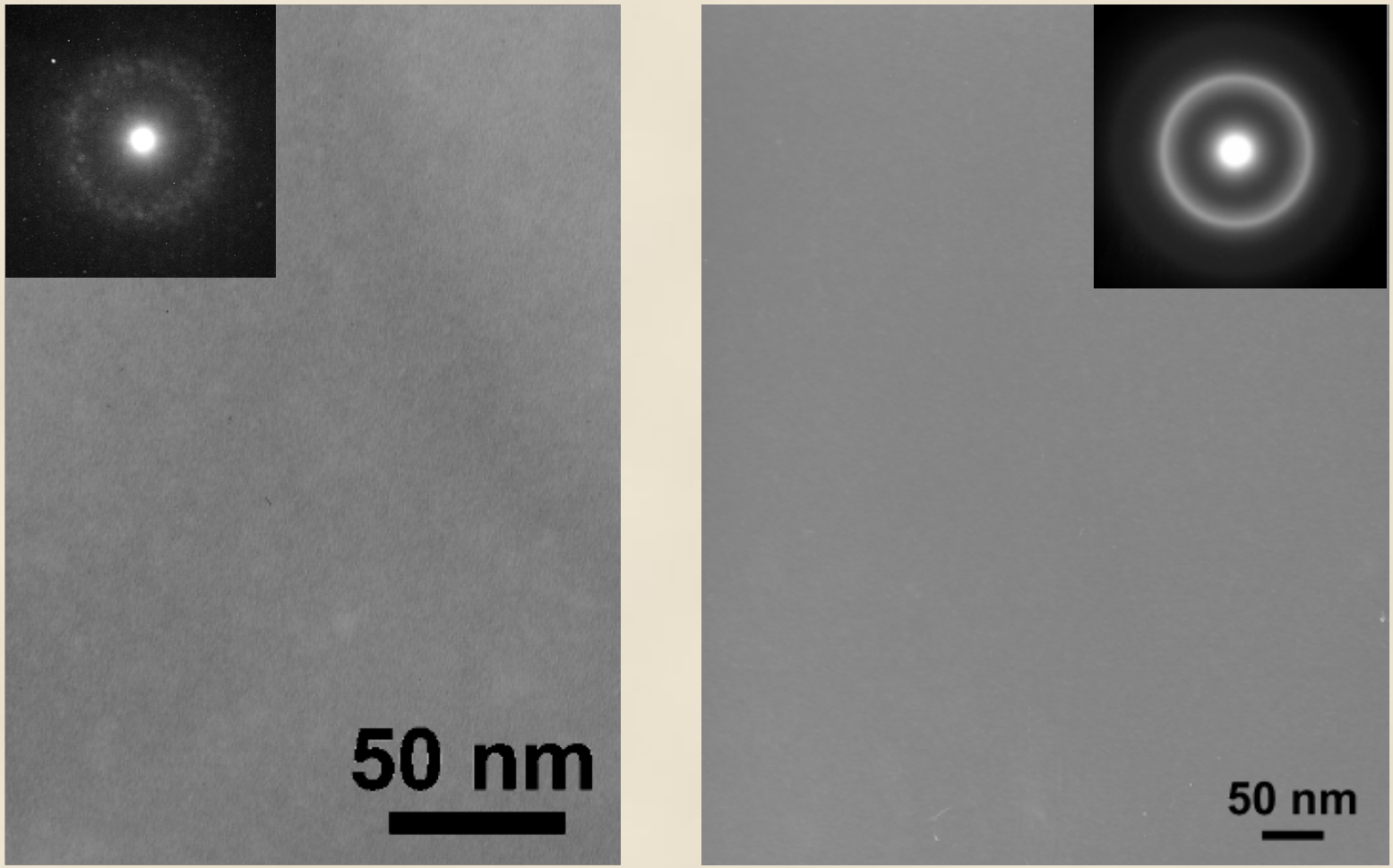

Bright (left) and dark-field (right) TEM images of the $Zr_{62.5}Cu_{22.5}Al_{10}Fe_5$ sample annealed using DIC at 713 K for 300 s as well as SAED and NBD patterns embedded.

D. V. Louzguine-Luzgin, G. Xie, Q. Zhang and A. Inoue "Effect of Fe on the glass-forming ability, structure and devitrification behavior of Zr-Cu-Al bulk glass-forming alloys" Philosophical Magazine, Vol. 90, N: 14, (2010), pp. 1955–1968.

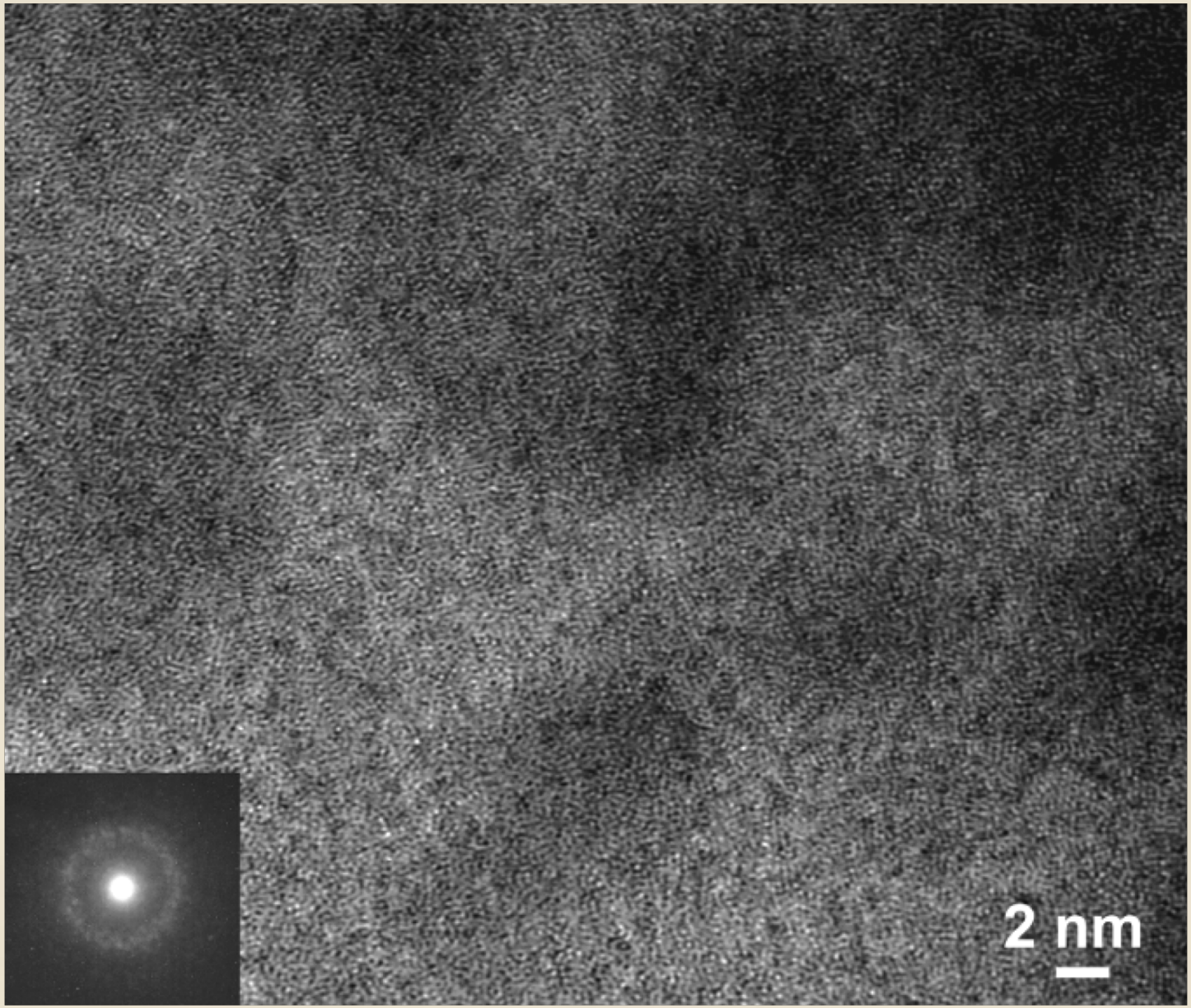

HRTEM image of the $Zr_{62.5}Cu_{22.5}Al_{10}Fe_5$ sample annealed using DIC at 713 K for 300 s. The insert – typical nanobeam diffraction (NBD) pattern (produced using a probe size of 3 nm) exhibiting a halo pattern. Contrast enhanced.

Binodal/Spinodal mechanism

Nanoscale phase separation

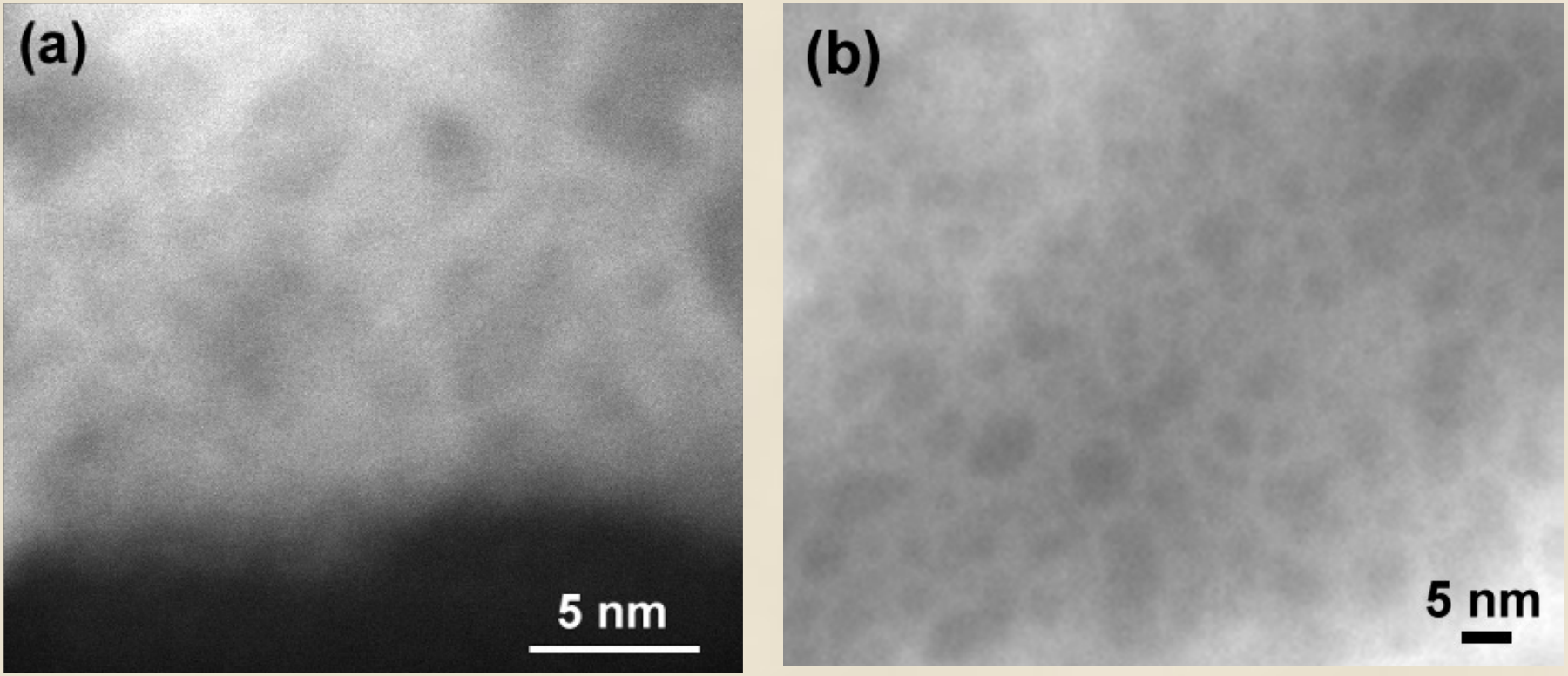

(a) HAADF (High Angle Annular Dark Field) image of the $Zr_{62.5}Cu_{22.5}Al_{10}Fe_5$ sample annealed using DIC at 713 K for 300 s (STEM TITAN). (b) Drift-corrected image.

D. V. Louzguine-Luzgin, G. Xie, Q. Zhang and A. Inoue "Effect of Fe on the glass-forming ability, structure and devitrification behavior of Zr-Cu-Al bulk glass-forming alloys" Philosophical Magazine, Vol. 90, N: 14, (2010), pp. 1955–1968.

Summary:

Glassy alloys were first developed by rapid solidification in 60th. Their applications were limited due to their small thickness of about tens of microns.

Bulk metallic glasses (> 1 mm size in every spatial dimension) have high tensile strength, hardness, surface quality, good corrosion resistance, reasonable fracture toughness, low internal friction and good processability.

Bulk metallic glasses are used in micro-machines, consumer electronic industries, sporting goods industries, etc.